

LA-UR-14-24271
June 2014
EP2014-0224

Sandia Wetland Performance Report, Baseline Conditions 2012–2014



Prepared by the Environmental Programs Directorate

Los Alamos National Laboratory, operated by Los Alamos National Security, LLC, for the U.S. Department of Energy under Contract No. DE-AC52-06NA25396, has prepared this document pursuant to the Compliance Order on Consent, signed March 1, 2005. The Compliance Order on Consent contains requirements for the investigation and cleanup, including corrective action, of contamination at Los Alamos National Laboratory. The U.S. government has rights to use, reproduce, and distribute this document. The public may copy and use this document without charge, provided that this notice and any statement of authorship are reproduced on all copies.

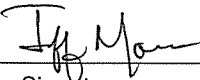
Sandia Wetland Performance Report, Baseline Conditions 2012–2014

June 2014

Responsible project manager:

| | | | | |
|--------------|---|--------------------|---------------------------|---------|
| Steve Veenis |  | Project Manager | Environmental Programs | 6-25-14 |
| Printed Name | Signature | Title | Organization | Date |

Responsible LANS representative:

| | | | | |
|---------------|---|-----------------------|---------------------------|---------|
| Jeff Mousseau |  | Associate Director | Environmental Programs | 6-25-14 |
| Printed Name | Signature | Title | Organization | Date |

Responsible DOE representative:

| | | | | |
|----------------|---|----------------------|--------------|-----------|
| Peter Maggiore |  | Assistant Manager | DOE-NA-LA | 6-30-2014 |
| Printed Name | Signature | Title | Organization | Date |

EXECUTIVE SUMMARY

The Sandia Wetland Performance Report, Baseline Conditions 2012–2014 is the first of ongoing annual reports that will assess the overall condition of the wetland at the head of Sandia Canyon and its ability to stabilize wetland sediments in the context of the newly installed grade-control structure at the terminus of the wetland and possible changes to Los Alamos National Laboratory operational practices that may affect outfall volumes and chemistry. This first report presents the results of monitoring conducted for surface water, alluvial groundwater, and geomorphology to establish a systematic assessment methodology and baseline condition for the wetland. Monitoring data include water levels and water chemistry from an array of 13 piezometers installed in the wetland, surface water and storm water data from 2 gaging stations located upstream, and 1 gaging station located downstream of the wetland, vegetation monitoring, and geomorphic/topographic cross-sections. Initial baseline monitoring results from November 2012 to March 2014 are presented herein as well as recommendations for key metrics to assess wetland performance in the future. Suggested changes to the monitoring plan are also proposed.

The baseline data indicate little to no evidence that any detrimental effects have occurred within the Sandia wetland to date from decreases in effluent volumes to the wetland. Changes in chemistry related to enhanced water treatment at the Sanitary Effluent Reclamation Facility are evident, particularly in surface water. However, these changes do not appear to have had an adverse effect in terms of contaminant mobilization.

CONTENTS

1.0 INTRODUCTION 1

1.1 Project Goals 2

1.2 Timeline 2

1.3 Design and Function of the Grade-Control Structure 2

1.4 Sandia Canyon Outfalls and SERF 3

1.5 Monitoring Plan 4

1.6 Conceptual Model for Assessing Wetland Performance 6

1.6.1 Hydrologic and Geochemical Status 6

1.6.2 Contamination in Wetland Sediment 8

1.6.3 Cr(III) Stability in the Sandia Wetland 9

1.6.4 Current State of the Sandia Wetland 11

2.0 SAMPLING AND ANALYSIS 11

3.0 MONITORING RESULTS 12

3.1 Analytical Results from Surface Water Gaging Stations E121, E122, and E123 12

3.2 Analytical Results from Piezometers 15

3.3 Water-Level Results from Piezometers 18

3.4 Geomorphic Survey Results 18

3.5 Vegetation Monitoring 18

4.0 RECOMMENDED WETLANDS PERFORMANCE METRICS 18

4.1 Spatial and Temporal Geochemical Patterns 18

4.2 Temporal and Spatial Trends in Water Levels 19

4.3 Performance of Grade-Control Structure 20

4.4 Total Wetland System Performance 20

4.5 Key Monitoring Locations and Proposed Performance Metrics 20

4.6 Lessons Learned and Changes to Monitoring Plan 21

5.0 CONCLUSIONS 22

6.0 REFERENCES 23

Figures

Figure 1.2-1 Sandia Canyon Wetland timeline 25

Figure 1.3-1 Locations of the Sandia GCS, NPDES outfalls, piezometers, alluvial wells, surface and storm water gaging stations, and reach S-2 26

Figure 1.3-2 GCS design plan view 27

Figure 1.4-1 Daily, monthly average, and yearly average effluent release volumes (expressed as Kgal/day) for Outfall 001 since 2006 and daily effluent releases for Outfalls 03A027 (SCC) and 03A199 (LDCC) from August 2007 to January 2010 and from November 2012 to March 2013 28

Figure 1.4-2 Updated process schematic for the power plant, SWWS, and SERF connections to Outfall 001 (current configuration) 29

| | | |
|--------------|--|----|
| Figure 1.4-3 | Daily water volumes from November 2012 to April 2014 for effluent released from Outfall 001, effluent from the SCC cooling towers, which release to Outfall 03A027, and makeup water sources (potable or SERF-blended water) used at the SCC cooling towers..... | 30 |
| Figure 1.5-1 | A drive point with 2-ft screen used in the study | 31 |
| Figure 1.5-2 | Photo of SCPZ-1 as installed in the field | 32 |
| Figure 1.5-3 | Schematic of piezometer transects and depths..... | 32 |

Tables

| | | |
|-------------|---|----|
| Table 1.5-1 | Completion Data for Alluvial Piezometers | 33 |
| Table 1.5-2 | Alluvial Groundwater Sampling and Analysis Plan for Sandia Wetland Stabilization Monitoring | 33 |
| Table 1.5-3 | 2012 and 2013 Storm Water Sampling Planned at Gage Stations E121, E122, and E123..... | 34 |
| Table 2.0-1 | Precipitation at RG121.9 and Storm Water Sampling at Gage Stations E121, E122, and E123..... | 35 |
| Table 2.0-2 | Types, Locations, and Period of Record for Data Used in This Report..... | 37 |
| Table 3.1-1 | NMWQCC Surface Water Standards..... | 38 |
| Table 3.1-2 | Maximum Detected Results by Station and Event above Comparison Values in Sandia Storm Water Samples Since 1999 | 39 |
| Table 4.5-1 | Efficacy of Locations for Monitoring Recent Hydrologic and Geochemical Forcing Function and Associated Impacts..... | 42 |
| Table 4.6-1 | Modified Sample Analytes and Preservation Requirements for Sandia Wetland..... | 42 |
| Table 4.6-2 | ISCO Bottle Configurations and Analytical Suites, Calendar Year 2013 Storm Water Sampling Plan, and ISCO Analytical Suites and Bottle Sequence..... | 43 |

Appendixes

| | |
|------------|---|
| Appendix A | Acronyms and Abbreviations, Metric Conversion Table, and Data Qualifier Definitions |
| Appendix B | Baseline Geomorphic Conditions and Vegetation Monitoring in Sandia Canyon Reach S2 |
| Appendix C | Geochemical and Hydrologic Trends |
| Appendix D | Analytical Data and Frequency of Detects Tables (on CD included with this document) |

1.0 INTRODUCTION

The Sandia Canyon wetland developed in the early 1950s in response to liquid effluent released by the Los Alamos National Laboratory (LANL or the Laboratory) at the head of Sandia Canyon. The wetland has been supported since then by continued effluent releases to the canyon. Contamination is present in wetland sediments because of historical releases from Laboratory operations (LANL 2009, 107453).

The Laboratory has prepared this “Sandia Wetland Performance Report, Baseline Conditions 2012–2014” in response to requirements set forth in the document “Work Plan and Final Design for Stabilization of the Sandia Canyon Wetland” (LANL 2011, 207053). In that document, the Laboratory proposed reporting of Sandia wetland monitoring data to the New Mexico Environment Department (NMED) by April 30 of each year. The requirement for design of a Sandia Wetland monitoring program was previously set forth in NMED’s “Approval with Modification, Interim Measures Work Plan for Stabilization of the Sandia Canyon Wetland” (NMED 2011, 203806) in response to the Laboratory’s “Interim Measures Work Plan for Stabilization of the Sandia Canyon Wetland” (LANL 2011, 203454). The monitoring plan was provided in the work plan (LANL 2011, 207053) and is summarized in section 1.5 of this report. The monitoring plan is designed to identify physical or chemical changes in the Sandia wetland related to (1) the installation of a grade-control structure (GCS) at the terminus of the wetland (LANL 2013, 251743) and (2) changes in outfall chemistry and discharge volumes related to the Sanitary Effluent Reclamation Facility (SERF) expansion (DOE 2010, 206433).

This report is the first of ongoing annual reports that will assess the overall condition of the wetland and its ability to stabilize wetland sediments in the context of the newly installed grade-control structure at the terminus of the wetland and possible changes to Laboratory operational practices that may affect outfall volumes and chemistry. This first report presents the results of monitoring conducted for surface water, alluvial groundwater, and geomorphology to establish a systematic assessment methodology and baseline condition for the wetland. Monitoring data include water levels and water chemistry from an array of 13 piezometers installed in the wetland, surface water and storm water data from 2 gaging stations located upstream and 1 gaging station located downstream of the wetland, vegetation monitoring, and geomorphic/ topographic cross-sections. Initial baseline monitoring results from November 2012 to March 2014 are presented herein as well as recommendations for key metrics to assess wetland performance in the future. Suggested changes to the monitoring plan are also proposed.

Hexavalent chromium [Cr(VI)] was historically released as part of liquid effluent from the Technical Area 03 (TA-03) power plant (TA-03-22) at the head of Sandia Canyon from 1956 to 1972. Some of the Cr(VI) made its way to the regional aquifer beneath Sandia and Mortandad Canyons, and Cr(VI) concentrations presently exceed NMED groundwater standards and U.S. Environmental Protection Agency maximum contaminant levels. The Sandia Canyon wetland performance monitoring is related to the overall chromium remediation project because a large portion of the original chromium inventory and other contaminants are currently sequestered in the wetland sediment, as described below. The results of characterization work conducted to date in Sandia Canyon are described in the “Investigation Report for Sandia Canyon” (hereafter, the Phase I IR) (LANL 2009, 107453), and in the “Phase II Investigation Report for Sandia Canyon” (hereafter, the Phase II IR) (LANL 2012, 228624).

Information on radioactive materials and radionuclides, including the results of sampling and analysis of radioactive constituents, is voluntarily provided to NMED in accordance with U.S. Department of Energy policy.

1.1 Project Goals

Geochemical reducing conditions within the Sandia wetland converted some of the Cr(VI) released from 1956 to 1972 to stable, relatively insoluble trivalent chromium [Cr(III)]. A significant inventory of chromium as Cr(III), possibly around 15,000 kg, remains in wetland sediment (LANL 2009, 107453). Although studies presented in the Phase I IR have shown that the trivalent form of chromium is unlikely to oxidize and convert to mobile hexavalent chromium (LANL 2009, 107453), maintaining the reducing condition is a prudent measure to ensure stability of the chromium inventory within the wetland sediment. The wetland also contains constituents adsorbed to sediment such as polychlorinated biphenyls (PCBs) that remain in situ as long as the wetland sediment remains physically stable with abundant vegetation.

The monitoring presented in this report is intended, in part, to assess the stabilizing impacts of the GCS on the eastern terminus of the wetland. Before the GCS was constructed, the terminus of the wetland had an active headcut (up to 3 m high). Installation of the GCS is expected to arrest the headcut, to facilitate physical stability, and to maintain hydrologic and geochemical function at the easternmost end of the wetland. Maintenance of physical and chemical stability will in turn help prevent potential physical mobilization of adsorbed contaminants associated with sediment and chemical mobilization of precipitated contaminants under changing geochemical conditions (LANL 2011, 203454; LANL 2011, 207053). The Sandia wetland has, however, concurrently experienced decreased liquid effluent volumes (both daily and annual) from National Pollutant Discharge Elimination System– (NPDES-) permitted Outfalls 001 and 03A027 as part of the SERF expansion project. As part of the SERF expansion, a portion of the effluent previously released to Sandia Canyon is now being rerouted to cooling towers at TA-03. Effluent releases to Sandia Canyon will be reduced further, although at levels sufficient to maintain the ecologic, hydrologic, and geochemical functioning of the wetland. It is anticipated that future effluent discharges will be subject to an adaptive management approach that will adjust to changing wetland conditions as necessary.

More detailed background on the GCS- and SERF-related outfall chemistry and discharge volume changes are provided in sections 1.3 and 1.4. The monitoring plan and associated rationale designed to identify physical and chemical changes in the wetland are presented in section 1.5.

1.2 Timeline

A graphical timeline showing changes related to outfall discharge and SERF chemistry as well as the construction of the GCS and the addition of piezometer monitoring locations is shown in Figure 1.2-1. The following sections refer to this timeline.

1.3 Design and Function of the Grade-Control Structure

A location map and plan view schematic of the GCS are shown in Figures 1.3-1 and 1.3-2. The overall objectives of the GCS were to arrest the headcut in the lower portion of the wetland and to maintain hydrologic and geochemical conditions to minimize contaminant migration. The GCS was designed to meet the following objectives:

- Provide an even grade to allow wetland expansion and further stabilization
- Be sufficiently impervious to prevent the draining of alluvial soils and promote a high water table
- Facilitate nonchannelized flow
- Minimize erosion during large flow events
- Support wetland function under potentially reduced effluent conditions

The GCS transitions the grade approximately 11 vertical feet from the elevation of the wetland just upgradient of the former headcut location to the natural stream bed just upstream of gage E123. To maintain grade and to reduce the overall fill and size of a single structure, a set of three steel-sheet-pile walls was installed with smaller elevation drops. Downstream of the third sheet-pile wall, a cascade pool was constructed of boulders and cobbles to transition to the final grade. The transition from the wetland above the GCS to the stream channel below is gradual, smooth, and stepped to prevent erosive flows that could scour and destabilize the stream reach below the structure (LANL 2013, 251743). Design features should also allow reduction of effluent in the canyon without compromising the physical and geochemical function of the wetland, particularly of the eastern terminus where the GCS controls wetland water levels. The area behind the GCS was backfilled and wetland vegetation was planted to allow expansion of the wetland area. These measures physically stabilize the wetland by reducing sediment and associated contaminant transport into the lower sections of the canyon and should also maintain reducing conditions within the sediment near the terminus of the wetland, thus contributing to the goal of reducing potential contaminant transport (LANL 2013, 251743).

A set of as-built drawings for the GCS can be found in Appendix C of the completion report for the construction of the GCS (LANL 2013, 251743). A plan view design diagram is shown in Figure 1.3-2.

Previous stabilization efforts involved the planting of cottonwood and willow stems in March and April 2007 to help stabilize contaminated sediment deposits, slow floodwaters, enhance the deposition of sediment and associated contaminants, and improve habitat (LANL 2009, 107453).

1.4 Sandia Canyon Outfalls and SERF

Outfalls have released liquid effluent to Sandia Canyon since development of TA-03 in the early 1950s. Currently, three NPDES outfalls release to upper Sandia Canyon upstream of the wetland, Outfalls 001, 03A027, and 03A199 (EPA 2007, 099009) (Figure 1.3-1). Effluent releases at these outfall discharge points are monitored in compliance with the Laboratory's industrial NPDES permit (Permit No. NM0028355). Information on the permitted water treatment chemicals can be found in the NPDES permit application (LANL 2014, 254864). Since the Laboratory's Chromium Investigation began in 2006 and until mid-2012, the releases to the canyon have been generally as follows. NPDES Outfall 001 has discharged liquid effluent, predominantly from the Laboratory's TA-46 Sanitary Waste Water System (SWWS) plant, the TA-03 steam plant boilers, and TA-03 power plant cooling towers. Figure 1.4-1 shows daily, monthly, and yearly average effluent volumes since 2006 for Outfall 001, which releases the greatest effluent volume to Sandia Canyon. From 2006 through 2011, average discharge ranged from approximately 230,000 to 300,000 gallons per day (gpd). NPDES Outfalls 03A027 and 03A199 (Figure 1.3-1) associated with facility cooling of the Strategic Computing Complex (SCC) and the Laboratory Data Communications Center (LDCC), also discharge to upper Sandia Canyon. Figure 1.4-1 shows daily releases from August 2007 to January 2010 and from November 2012 to March 2013 for these two outfalls. These two outfalls contributed approximately 50,000 to 100,000 gpd of cooling water effluent to the canyon between 2007 and 2010. The water source for both the SCC and LDCC cooling towers was potable water during that time period. Together these three outfalls (001, 03A027, and 03A199) have provided sufficient water to maintain the stability of the wetland.

In August 2012, the SERF expansion project enabled tertiary treatment of SWWS effluent so the water can be reused/recycled in Laboratory cooling towers. The upgrade allows for treatment of a maximum of 144,000 gpd, but the SERF expansion is not yet being used at full capacity. The treatment methods employed at SERF are chemical precipitation, flocculation, microfiltration, reverse osmosis (RO), and pH adjustment. Figure 1.4-2 shows a process schematic for water flow and treatment at the power plant, SWWS and SERF and their connections to Outfalls 001 and 03A027. The SERF RO product water is

extremely pure; the process removes metals, silica, organic compounds, and inorganic salts. Chloride concentrations, however, are high relative to other constituents. Ferric chloride and magnesium chloride are added for chemical precipitation in the first stage of treatment at SERF. This raises chloride concentrations enough that even after subsequent treatment through the SERF process, concentrations remain elevated in the SERF product water. The SERF product water is blended at an approximate 4:1 ratio with SWWS effluent (i.e., 4 parts SERF RO product to 1 part SWWS effluent) for reuse in the SCC cooling towers or to be released at Outfall 001. The use of the SERF-blended water has been phased in according to the following schedule and has resulted in the following changes to effluent volume and water quality released to the wetland, as depicted in Figure 1.2-1.

July 2012: SERF expansion began operation, treating SWWS effluent to meet PCB effluent standards. SERF RO to SWWS waters were blended at approximately a 4:1 ratio and released at Outfall 001. The resulting blended water chemistry has increased quality over previous effluent chemistry because constituent concentrations are approximately 20% of concentrations present in the SWWS effluent, with the exception of chloride, which is not affected by SERF treatment. Direct effluent from the power/steam plant is also released at Outfall 001. The July 2012 operational change had little, if any, effect on effluent volumes.

April 2013: The SCC cooling towers switched their water source from potable water to SERF-blended water. Between November 2012 and April 8, 2013, the SCC cooling towers underwent a trial period in which they transitioned from using potable water to using SERF-blended water that had been previously released at outfall 001 (Figure 1.4-3). On April 9, 2013, the transition was completed, and since then the cooling towers have almost exclusively used SERF-blended water as their cooling water source, resulting in lower effluent releases at both Outfalls 001 and 03A027. Figure 1.4-3 shows effluent volumes released at Outfall 001 and from the SCC cooling towers, which release to Outfall 03A027, from November 2012 to April 2014. The figure also shows the water sources used at the cooling towers. Overall, the transition has decreased effluent volume by approximately 50,000 to 60,000 gpd at Outfall 001. Daily variations in effluent flow have also decreased. The spike in effluent volume on September 13–14, 2013, corresponds to the large rain event (Figure 1.2-1) because the evaporation basins at SWWS took on many inches of rainwater that were routed up through the treatment system. The use of SERF-blended water in the SCC cooling towers has allowed for additional cycling of cooling water in the towers without buildup of precipitates from lower levels of silica in SERF-blended water as compared with potable water. With the additional cycles, effluent volumes at outfall 03A027 have dropped from approximately 50,000 gpd to 15,000 to 20,000 gpd. The water chemistry has changed as well, going from potable water with ~86 ppm silicon dioxide (SiO₂) to SERF-blended water with ~12–20 ppm SiO₂. However, sodium bisulfite is now added as a chlorine scavenger before release of the SCC cooling tower effluent; the bisulfite converts to sulfate once released to the environment. The LDCC cooling towers continue to use potable water at rates that have not changed with the SERF expansion.

Future: Future plans allow for the SERF to run at full capacity so that Laboratory computing facilities have access to larger amounts of SERF-blended water for cooling. The variability in effluent volumes and water chemistry that may be released to the wetland will depend on return flow from facilities to outfalls that release to the wetland.

1.5 Monitoring Plan

The detailed monitoring plan for the Sandia Wetland is found in Section 6.0 of the document “Work Plan and Final Design for Stabilization of the Sandia Canyon Wetland” (LANL 2011, 207053). A multiphase approach to monitoring is used to evaluate hydrologic and geochemical changes associated with either

the engineered controls described in this plan and/or those associated with the SERF expansion and subsequent effluent reduction:

- Evaluate changes in hydrology and key geochemical indicators to monitor the health of the wetland at 12 alluvial wells
- Evaluate transport of nutrients and metals and organic chemicals through the wetland by monitoring surface-water base flows and storm flows at three gage stations
- Monitor vegetation every 2 yr via photo surveys
- Conduct periodic geomorphic surveys to evaluate erosion and aggradation of sediments within the wetland.

Monitoring of alluvial chemistry was accomplished through a series of 13 drive-point piezometers arranged in 4 transects in the wetland (Figure 1.3-1) that were scheduled to be sampled quarterly. A drive-point is shown in Figure 1.5-1, and Figure 1.5-2 shows a piezometer as installed. Figure 1.5-3 is a schematic of piezometer transects and depths.

The piezometer transects are as follows.

- Piezometers SCPZ-1 to SCPZ-3 are located on a sand and gravel terrace near the active channel (c1 geomorphic unit) towards the western end of the wetland, which has experienced channel incision and dewatering relative to historical conditions. These piezometers are located on the c3 geomorphic unit away from the active channel and associated inset terrace (c2a geomorphic unit), which are locations of recent cattail expansion. Piezometer SCPZ-1 is screened towards the base of alluvial fill, while the top of the screens in piezometers SCPZ-2 and SCPZ-3 are approximately 6 and 3 ft bgs, respectively (see Table 1.5-1 and Figure 1.5-3). The ground surface is dry at this transect.
- Piezometers SCPZ-4 to SCPZ-6 form a transect in the widest portion of the wetland, and the tops of their screens are approximately 3 ft bgs. The wetland water level is at or very near the ground surface at this transect. It is at these shallowest depths that changes in water level and sediment oxidation state would be expected to manifest as a result of reduced effluent discharge. Similarly, the lateral margins of the wetland may dewater before the longitudinal axis of the wetland as a result of reduced effluent volumes. This effect could be most pronounced where the wetland is widest and water flux is most spread out. It is also at such locations that preferential flow paths within the alluvium might be expected to form.
- Piezometer transect SPCZ-7 to SCPZ-9 is located in a narrow part of the wetland closer to its distal (eastern) end. This set of piezometers includes two shallow piezometers and one piezometer screened slightly deeper (see Table 1.5-1 and Figure 1.5-3). The wetland water level is at or just below the ground surface at this transect. These piezometers provide indications of changes near the surface of the wetland and at depth in a narrow portion of the wetland where preferential flow paths are less likely to develop.
- The final transect of piezometers SCPZ-10 to SCPZ-12 is located next to alluvial well SCA-1-DP (and the previous location of SCA-1) and will monitor the effect of the GCS. The wetland water level is near the surface at SCPZ-10 and below the ground surface at SCPZ-11A/B and SCPZ-12. Water was routed around this area during the period of construction of the GCS.

The sampling and analysis plan for these piezometers is provided in Table 1.5-2. Most of the analyses were designed as indicators of redox changes and/or indicators of organic matter degradation associated with potential dewatering of the wetland. Where possible, piezometers were also instrumented with sondes for continuous monitoring of water levels, specific conductance, and temperature. The same analytical suite was monitored at least quarterly at surface water gaging stations E121, E122, and E123 (see Figure 1.3-1). Analyses of storm water samples collected in 2012 and 2013 were planned as presented in Table 1.5-3. The results are discussed in section 3.0 with data plots provided in Appendix C and analytical data available on CD (Appendix D).

A baseline series of topographic cross-sections were established to begin documenting possible geomorphic change in the wetland (Appendix B). A vegetation photo survey was conducted in May, 2014, at key locations: wetland margins where dewatering or wetland expansion is most likely to occur, at the head of the main cattail wetland where floods have the greatest impact, at the newly planted GCS, and along the inset channel to the west of the active wetland where rapid expansion of cattails is occurring. These photo locations are presented in Appendix B and are expected to be integrated with photo locations used for geomorphic monitoring in the future.

1.6 Conceptual Model for Assessing Wetland Performance

1.6.1 Hydrologic and Geochemical Status

The Sandia wetland is predominantly an effluent-supported cattail wetland. Organic-rich alluvial sediment, described as both alluvial and wetland sediment in this report, forms the wetland soil. Mapping of the wetland sediment shows thicknesses ranging generally from approximately 13 ft at the western end of the wetland to approximately 8 ft at the eastern end (Figure 7.1-1; LANL 2009, 107453). However, the wetland sediment was observed to be greater than 16 ft deep at piezometer SCPZ-1 (Table 1.5-1). Based on the presence of anthropogenically derived materials throughout the sediment deposits, much of the sediment has accumulated since 1942 as Laboratory development and operations in upper Sandia Canyon have occurred. Shallow alluvial groundwater, perched on Bandelier Tuff is present throughout the wetland and expresses as surface water in the middle and lower portions. The sediment is generally fully saturated at the eastern end of the wetland; these conditions extend westward, but near-surface sediment is unsaturated at the margins and at the western end of the wetland. Surface water from effluent discharges and storm water generally pass over the wetland with a short residence time, while groundwater within the shallow perched zone has a longer relative residence time (LANL 2009, 107453). The history of effluent discharges is discussed in section 1.4. Decreases of approximately 60,000 to 80,000 gpd in effluent volumes have recently occurred from the recycling of SERF water in cooling towers and could potentially lead to dewatering of portions of the wetland. The upper portion of the wetland is the most vulnerable in this regard, as the effects of the GCS to maintain saturated conditions are only expected to manifest in the lower, and possibly middle, portions of the wetland. Water inputs to the wetland are monitored at outfalls and at gaging stations E121 and E122. Water levels within the wetland are monitored in the piezometer array, and wetland outflows are monitored at gaging station E123 (see section 1.5).

The chemistry of effluent water entering the wetland has recently changed as a result of changes in blended ratios of SERF to SWWS water and with changes in cooling tower recycling (see section 1.4.2). Depending upon the amount of exchange between surface water and groundwater, “cleaner” input waters could potentially lead to desorption/dissolution of contaminants. Surface water measured under base-flow conditions at gage E121 is affected by the water chemistry of the effluent released at Outfalls 001 and 03A027. Water chemistry measured under base-flow conditions at gaging station E122 is affected by effluent chemistry from Outfall 03A199 (Figure 1.3-1). Outfall 001 discharges a much greater volume of

water than the other two outfalls, and SERF-related chemistry and discharge volume changes are limited to outfalls flowing to this location. Thus, base-flow water chemistry at gaging station E121 is used in this report as representing the best location to monitor changes in input water chemistry to the wetland. Changes to input chemistry will also be partially reflected in samples taken from the piezometer array and with base-flow samples at downstream gage E123, though concentrations are modified by wetland biogeochemical processes (plant uptake, chemical reduction in sediments, etc.). Storm water samples collected at these gaging stations represent a composite of water inputs including effluent sources, precipitation, some groundwater exchange, and runoff.

Surface water has a short residence time within the wetland with most of the flow occurring within the active stream channel. Water present within the alluvial/wetland sediment has much longer residence times. Much of the alluvial system is currently saturated, particularly in the downgradient half of the wetland. This saturation, along with significant amounts of solid organic matter (SOM) produced from wetland vegetation, results in reducing alluvial aquifer conditions as indicated by detectable concentrations of ammonia and sulfide, high dissolved iron and manganese concentrations, and low nitrate and sulfate in alluvial water (see section 3.0). Isotope studies of cattails also verify the strong reducing conditions in the wetland sediments. The $\delta^{15}\text{N}$ signature of the cattails is consistent with a predominantly sewage source of nitrogen (Heikoop et al. 2002, 107001; Fair and Heikoop 2006, 098045). The very high values in the roots/rhizomes of some samples indicate the occurrence of denitrification in the sediments surrounding the cattails. Denitrification results in residual nitrate enriched in the heavy isotope of nitrogen. These results demonstrate that the cattails actively take up treated sewage nitrogen and that the wetland constitutes an actively denitrifying environment. Both factors can lead to partial attenuation of nitrate released to the wetland.

Alluvial groundwater levels within the wetland alluvium are monitored in the piezometer array. Chemical changes (e.g. change in sediment redox) are also monitored within the piezometers. Alluvial wells SCA-1 and SCA-1 DP (Figure 1.3-1) provide longer term records of alluvial chemistry near the terminus of the wetland (see Appendix C). Base-flow chemistry at gage E123 integrates all chemical changes occurring in the wetland. Repeat surveys of geomorphic cross-sections will monitor for physical changes in alluvial geomorphology.

A water-balance analysis conducted during 2007 and 2008 is summarized in the Phase I Sandia Canyon IR (LANL 2009, 107453). That study showed little surface water loss (approximately 2% of both effluent and runoff) occurs through the wetland area. A direct-current (DC) electrical-resistivity–based geophysical survey was conducted as part of the Phase II Sandia Canyon investigation to provide a model of electrical properties of subsurface materials of the region beneath and adjacent to the wetland in upper Sandia Canyon (LANL 2012, 228624). The DC resistivity survey found that large continuous areas of the wetland are underlain by highly resistive welded tuffs (Qbt2 of the Tshirege Member of the Bandelier Tuff) that probably represent a significant barrier to the infiltration of surface and alluvial water into the subsurface. A very conductive layer extending from the surface to 20 to 25 ft bgs (6.1 to 7.6 m bgs) correlates well with an alluvial aquifer perched on a welded tuff unit. In several areas, the survey also identified subvertical conductive zones that penetrate the upper bedrock units and in some cases appear to correlate with mapped fault and/or fracture zones. These subvertical conductive zones are noted because they may represent present-day or historical infiltration pathways. However, the DC resistivity data do not differentiate between conductive zones that contain higher water content (possibly representing active infiltration) and wetted clay-rich fracture fill that may hinder infiltration.

Storm water–induced flooding can cause erosion and, most importantly, headcutting at the terminus of the wetland. As such, sediment stability is key to wetland performance and was one of the major

objectives for construction of the GCS. Storm water is monitored at locations E121, E122, and E123. Storm-water data are compared with screening levels and are discussed in section 3.1.

The wetland vegetation community is important in mitigating storm water–related mobilization of contaminants through root binding and physical trapping of suspended sediments in storm flow. In addition, organic inputs from each year's cattail growth produce fresh SOM inputs that help maintain reducing conditions in the alluvial groundwater. Wetland vegetation may also directly uptake certain contaminants (LANL 2009, 107453). In many ways, the vegetation community can be seen as a surrogate for the depth of the water table in the wetland. For example, if the water table rises and persistently saturates soils around ponderosa pines located along the margin of the wetland, they will likely die. Conversely, when the water table lowers, wetland vegetation is replaced by upland species. Healthy cattail wetlands require a high water table. Vegetation is being monitored through photo surveys along key margins where dewatering or wetland expansion would most likely occur: at the head of the main cattail wetland where floods have the greatest impact, at the newly planted GCS, and along the inset channel and floodplain to the west of the active wetland where rapid expansion of cattails is occurring (Appendix B).

The GCS is designed to prevent the formation of nick points and headcutting at the terminus of the wetland (particularly during floods). It should also keep the downgradient portion of the wetland saturated which will promote physical and geochemical stability. Physical stability is monitored by geomorphic and vegetation surveys. Saturation and chemical stability are monitored in the piezometers.

1.6.2 Contamination in Wetland Sediment

Detailed sediment mapping was performed during the Phase I investigation of Sandia Canyon (LANL 2009, 107453). Sediment Reach S-2, which contains the Sandia wetland, is the most important reach in Sandia Canyon in the context of sediment contamination. It contains the highest concentrations and proportion of the contaminant inventory because of the proximity to contaminant sources, the large volume of sediment deposited during the period of active contaminant releases, the presence of high concentrations of organic matter in the wetland, and the presence of large amounts of silt and clay. Contaminants commonly adsorb to, or are precipitated in association with, sediment particles or organic matter. The fine-grained sediment in the wetland reach has a higher silt and clay content than the other reaches, contributing to higher contaminant concentrations (average of 60% silt and clay in S-2 fine-grained sediments, compared with averages of 30% to 43% in other investigation reaches in the western part of Sandia Canyon).

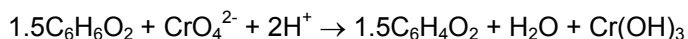
Chromium is the major inorganic contaminant that could be affected by both redox changes in the wetland and physical destabilization. Arsenic differs from chromium and other oxyanions in that it can be mobile under reduced conditions. Arsenic was seen in leachates from all drying/leaching experiments conducted as part of the Phase I Sandia Canyon investigation, with a maximum of 0.0425 ppm (see section 1.6.3) (LANL 2009, 107453). However, whereas average Sandia Canyon sediment arsenic concentrations are highest in reach S-2 (which includes the wetland) and decrease downgradient in the middle part of the canyon, in alluvial groundwater the lowest average concentrations occur within the wetland (~2 µg/L at well SCA-1; compared with other Sandia alluvial wells). The two organic contaminants, PCBs and polycyclic aromatic hydrocarbon (PAHs), are primarily subject to physical transport in floods because of low solubilities and a strong affinity for organic material and sediment particles. Important source areas for these contaminants are the former outfall for the power plant cooling towers in upper Sandia Canyon (chromium), a former transformer storage area along the south fork of Sandia Canyon (PCBs), and the former asphalt batch along the north fork of Sandia Canyon (PAHs)(LANL 2009, 107453).

1.6.3 Cr(III) Stability in the Sandia Wetland

Dewatering could reduce the physical stability of alluvial sediments and could lead to physical contaminant mobilization. It is feasible, although unlikely, that the existing chromium inventory within the wetland could be oxidized to its mobile Cr(VI) state through oxidation of Cr(III) to Cr(VI). Oxidation by atmospheric oxygen at environmental temperatures is not a known mechanism based on review of the relevant literature. Direct oxidation of Cr(III) to Cr(VI) by atmospheric oxygen has only been associated with high-temperature forest fires and burning of organic matter to produce alkaline vegetation ash (Panichev et al. 2008, 256734). Oxidation by manganese oxides under aqueous conditions is the primary mechanism responsible for oxidation of Cr(III) to Cr(VI) (Eary and Rai 1989, 256733).

A critical topic to address regarding Cr(III) stability in the Sandia wetland is the presence and reactivity of chemical reductants including Fe(II) and SOM to prevent or limit oxidation of Cr(III) to Cr(VI) (discussed in more detail in Appendix J of the Phase I IR [LANL 2009, 107453]). Mass balance calculations were performed to quantify the reducing capacity of the Sandia wetland by measuring sediment concentrations of one of the reductants, Fe(II), and an important oxidant, Mn(IV), to determine if there are excess concentrations of Fe(II) to keep Cr(III) stable within the wetland. Complete oxidation of Cr(III) to Cr(VI) is likely to take place if the molar concentrations of Mn(IV) exceed those of Fe(II), Cr(III), and organic carbon. This situation, however, is rare within the active Sandia wetland because concentrations of total iron, consisting mainly of Fe(II), and SOM are present at much higher weight percent concentrations than Mn(IV), which is usually present in the ppm range. During wetland drying and oxidation, however, Fe(II) can oxidize to Fe(III) and Mn(II) can oxidize to Mn(IV), making Mn(IV) available to oxidize Cr(III) to Cr(VI).

Under baseline conditions, concentrations of Fe(II) typically exceeded those of Mn(IV) and most of the Cr(III) in the wetland should remain reduced. SOM present in organic-rich portions of the Sandia wetland is considered to be the dominant reductant for immobilizing chromium. One reaction describing the reduction of Cr(VI) to Cr(III) in the presence of SOM containing hydroquinone (C₆H₆O₂), which provides the reduction capacity (McBride 1994, 058947), is



SOM was not included as a reductant in the mass balance calculation presented in the Phase I IR. Thus, those calculations underestimate the reducing capacity of the wetland; Cr(III) is likely to be more stable than indicated by consideration of Fe(II) and Mn(IV) concentrations alone.

Two hypotheses are proposed for the geochemical attenuation of chromium in the SOM-rich samples:

1. Aqueous species of Cr(III) in the forms of CrOH₂⁺ and Cr(OH)₂⁺ either adsorb onto negatively charged surfaces present on hydrous ferrous oxides (HFO), or on negatively-charged sites present in SOM, mainly consisting of deprotonated carboxylates (R-COO⁻) above pH 4.5 (Langmuir 1997, 056037), and
2. Cr(III) has precipitated from solution as Fe_xCr_{1-x}(OH)₃ and/or amorphous Cr(OH)₃. It is also likely that adsorption of Cr(III) onto SOM occurs before precipitation of Fe_xCr_{1-x}(OH)₃ and amorphous Cr(OH)₃.

Experiments were conducted on several Sandia wetland samples to quantify the potential release of chromium during dewatering and drying of the wetland material (LANL 2009, 107453). Dried samples were leached both with deionized and SWWS water. Total chromium concentrations in the SWWS effluent ranged from 1.4 ppb to 5 ppb in samples collected from February 2001 to June 2009. Most of the dissolved chromium in the wetland leachates occurred as Cr(III). Cr(VI) ranged from 0.06 ppb to

14.49 ppb in the leachates. With the exception of one sample from the SOM-poor gravel and sand bank of the already dewatered upper portion of wetland, Cr(VI) concentrations in leachates were less than 1 ppb. During drying, Cr(III) in most samples appears to remain stable, suggesting that insufficient Mn(IV) is produced to oxidize appreciable amounts of Cr(VI).

Most of the measured Eh values in the leachate samples are consistent with the stability of Cr(III) aqueous species and amorphous Cr(OH)₃. Elevated dissolved concentration of iron [presumably as Fe(II)] and manganese [presumably as Mn(II)] in leachates from active parts of the cattail wetland are consistent with Cr(III) stability related to reducing conditions. High dissolved iron concentrations are likely associated with dissolution of HFO, so absorption of Cr(III) and Cr(VI) may be less important than precipitation of Cr(III). Reductive dissolution of HFO also enhances desorption of arsenic, resulting in relatively high concentrations of this trace element within wetland pore water and leachates. These relatively high concentrations of dissolved arsenic suggest that soluble As(III) is the stable form of this trace element in water-saturated samples.

High concentrations of total dissolved (filtered at 0.22 μm) chromium in some leachates, mainly in the form of Cr(III), indicate that colloidal amorphous Cr(OH)₃ is likely to be present in the leachate samples. This may explain the presence of low but detectable concentrations of Cr(VI) measured in surface water east of the Sandia wetland. This explanation is supported by analytical results for surface water collected downstream of the wetland at gage E123 that were filtered through 0.45-, 0.22-, and 0.02-μm membranes before acidification and analyses for chromium. Concentrations of total chromium decreased dramatically in the 0.45 μm aliquot, suggesting that colloidal chromium, possibly stable as amorphous Cr(OH)₃ or Fe_xCr_{1-x}(OH)₃ and/or as chromium species adsorbed onto clay minerals and HFO, occurs at the eastern end of the Sandia wetland.

Other mechanisms that could account for the low-level mobilization of chromium from the wetland include the following:

- Cations concentrated in the SWWS treated effluent—including calcium, sodium, and magnesium—may enhance desorption of Cr(III) from wetland sediment through cation exchange reactions.
- Sulfate, phosphate, and total carbonate alkalinity are competing anions for Cr(VI), which limits adsorption of Cr(VI) onto iron (oxy)hydroxides at circumneutral pH. This effect could also influence arsenic concentrations.
- Complexing of Cr(III) with dissolved organic carbon, in the forms of humate and fulvate ligands (anions), may also enhance desorption of Cr(III) from the organic-rich solids concentrated within the wetland.

Note that improvement in outfall water quality associated with increased blending of SERF water would tend to decrease the first two of these mechanisms.

Some evidence from the leaching experiments indicates that atmospheric oxygen may be an important component for enhancing the leaching of chromium from the wetland samples. In some cases, higher leached concentrations of Cr(VI) were seen in samples that were oven or air dried versus samples that were vacuum dried. This likely does not represent direct oxidation of Cr(III) to Cr(VI) but rather oxidation of Mn(II) to Mn(IV), which was then available to oxidize Cr(III) in the leaching experiments.

1.6.4 Current State of the Sandia Wetland

Data from geochemical studies presented in the Phase I IR (LANL 2009, 107453) indicate that chromium in wetland sediments is predominantly geochemically stable as Cr(III) and that the proportionally high chromium inventory in the wetland is not likely to become a future source of chromium contamination in groundwater, especially if saturated conditions can be maintained within the wetland.

With installation of the GCS, the downgradient portion of the wetland should remain both physically and geochemically stable. Ongoing monitoring will determine the ultimate efficacy of the GCS in maintaining wetland stability. Monitoring will also help determine wetland response to changing outfall chemistry and discharge volumes.

2.0 SAMPLING AND ANALYSIS

Various factors led to challenges in implementing the monitoring plan as presented in the “Work Plan and Final Design for Stabilization of the Sandia Canyon Wetland” (LANL, 2011, 207053). Drive-point piezometers were installed in July 2012 and sampling began in November 2012. The period of record for data for this report included the sampling conducted between November 2012 and March 2014. During this period, there should have been a minimum of six sampling rounds, although only five samples were collected (November 2012, March 2013, July 2013, November 2013, and March 2014). The lapse of federal appropriations in October 2013 affected the monitoring schedule, and sampling was generally not feasible in winter months for safety concerns and from ice within the piezometers. In addition, construction of the GCS prevented sampling of piezometers in the lower wetland area. From May to November 2013, water was diverted into a basin located upstream of the easternmost piezometer array (SCPZ-10 to SCPZ-12), resulting in dry conditions at these piezometers. SCPZ-10 was inadvertently buried with dirt being staged along the wetland margin, and the entire eastern-most array had to be reinstalled following completion of the GCS. Gaging station E123 was also affected as water from the construction pond was returned to the stream channel below the gage during this period. The multiparameter sondes were not installed in piezometers SCPZ-7, SCPZ-10, SCPZ-11A/B, and SCPZ-12 because rapid siltation had occurred in these piezometers. Sondes in SCPZ-5 and SCPZ-9 were lost in the flood event that occurred on September 13, 2013, such that data going back to July 2013 could not be retrieved. Alluvial well SCA-1 was also lost in the September 2013 flood.

During several rounds, some piezometers were purged dry after 3 casing volumes and did not recover by the next day for sampling. This was particularly true in the easternmost transect (piezometers SCPZ-10 to SCPZ-12) and to a lesser extent in the transect in the narrow portion of the wetland (piezometers SCPZ-7 to SCPZ-9). The upper two piezometer transects were more amenable to sampling because of their location in the more transmissive substrate. For the March 2014 round, water from the easternmost set of piezometers (SCPZ-10 to SCPZ-12) was collected regardless of purge volume and as such may not be directly comparable with previously collected data. These piezometers were also cleaned and relocated a few days before sampling. In most cases, the analytical suite collected corresponds with that outlined in Table 1.5-2; however, in several cases, a piezometer purged dry and only volume sufficient to analyze for prioritized constituents was collected. With only two exceptions (see section 3.1), the piezometers yielded insufficient nitrate for isotopic analysis. Some ammonia and sulfide samples exceeded holding times and are therefore assessed in terms of their presence or absence rather than absolute values to determine if reducing conditions were present. Similarly, some ammonium isotope samples had preservation/holding time issues so more weight is put on recent data where samples were kept continuously frozen after collection and before analysis.

Field parameter data were collected during some sampling rounds for piezometers that did not purge dry. However, overall the data are not sufficient to assess temporal or spatial trends.

In 2012 and 2013, automated sampling systems attempted to collect storm water samples when discharge at the gage station was greater than 10 cubic feet per second (cfs) and resulted from precipitation. Storm water analyses in 2012 and 2013 were conducted according to the analyses listed in Table 1.5-3. The sampler at E123 was turned off for the winter shutdown on December 17, 2012, removed during GCS construction in June 2013, and reinstalled on May 21, 2014. Second ISCO samplers containing a 24-bottle carousel were installed at E121 on June 6, 2014; at E122 on May 24, 2014; and at E123 on May 21, 2014. Table 2.0-1 presents total precipitation at rain gage RG121.9 on days when discharge at E121, E122, or E123 was greater than 10 cfs.

Discharge at E121 with a contribution from precipitation exceeded 10 cfs 10 times during 2012 and 2013. Samples were collected from six of these discharge events. Discharge at E122 exceeded 10 cfs on two occasions; samples were not collected during these events, but discharge from a third smaller event on September 12, 2013, was collected. The sampler at E123 collected one of three potential events during 2012 before it was deactivated for the winter on December 17, 2012, and during GCS construction activities in 2013. Table 2.0-2 includes data types, dates, and locations for data collected from the wetland.

The “Work Plan and Final Design for Stabilization of the Sandia Canyon Wetland” (LANL, 2011, 207053) specified semiannual vegetation photo monitoring to occur every 2 yr beginning in 2012. Initially photo surveys provided by the Environmental Protection (ENV) Division seemed to be adequate to fulfill this requirement. However, upon review of these photos, it was determined that they did not sufficiently capture wetland margins essential for detecting early changes in vegetation. In May 2014, a set of 10 new photo locations was surveyed and is presented in Appendix B. Future integration of these photo locations with photo locations set up for geomorphic monitoring is covered in section 4.6.

Problems with sampling and recommendations for improving future sampling are discussed further in section 4.6.

3.0 MONITORING RESULTS

3.1 Analytical Results from Surface Water Gaging Stations E121, E122, and E123

Time-series plots of surface water base-flow chemistry for key parameters are presented in Figures C-1.0-1 to C-1.0-11 in Appendix C. Results from gage E121, which monitors most of the surface water flow into the head of the wetland, and gage E123, which monitors flow out of the wetland, are plotted together to show changes in surface water from upgradient to downgradient of the wetland. Results for arsenic and chromium from gage E122 are also discussed but are not shown graphically.

Similar chemistry between upgradient and downgradient locations would indicate relatively short residence times for surface water and possibly little interaction (exchange) with alluvial groundwater. Furthermore, similarity between chemistry at gages E123 and E121 suggests little alluvial groundwater discharge out of the wetland. That is, base flow at gage E123 does not contain a significant component of alluvial water, suggesting that discharge rates from the alluvium back to the surface are low, at least in the downstream portion of the wetland. Analytes chosen for plotting include major cations (sodium, calcium, and magnesium), a conservative anion (chloride), a trace metal (zinc), redox-sensitive species (iron, manganese, sulfate, and nitrate), and contaminants (chromium and arsenic) as well as a species that reflect changes in outfall chemistry (SiO_2 ; see section 1.4-2 and Figure C-1.0-12). Data are

summarized in frequency of detects tables organized by data from off-site and on-site laboratories (Appendix D, on CD).

No strong surface water temporal concentration trends exist for filtered arsenic, chloride, iron, or nitrate plus nitrite (Figures C-1.0-1, C-1.0-2, C-1.0-6, and C-1.0-11). While chloride does not show an overall concentration trend, variation post-SERF expansion is somewhat similar to that observed in outfall discharge (Figure C-1.0-2). Filtered chromium concentrations appear to increase at E123 following SERF expansion (Figure C-1.0-3). It should be noted, however, that this likely represents Cr(III) colloids smaller than 0.45 μm . Cr(VI) measurements taken at E121 and E123 in March 2013 were < 1 $\mu\text{g/L}$ and nondetect respectively (Figure C-1.0-3). The increase in colloidal transport of Cr(III) from the wetland may be related to construction activities associated with the GCS and/or flooding. Decreases in filtered magnesium, SiO_2 , sodium, and zinc associated with improvement in water quality discharge following the SERF upgrade are clearly evident (Figures C-1.0-4, C-1.0-7, C-1.0-8, and C-1.0-10). Surface water SiO_2 concentrations are plotted along with outfall total dissolved solids (TDS) to emphasize this signal (Figure C-1.0-12). Manganese may be showing slight water quality improvements through time, although this trend is obscured by a recent spike in concentrations in the case of gaging station E123 (Figure C-1.0-5). As the vast majority of the wetland is still saturated (section 3.3), it is unlikely that trends in manganese concentrations at downstream gage E123 reflect changes in redox conditions within the wetland. Further monitoring should help clarify the cause of the apparent decrease through time. It is unclear whether dissolved manganese is in the form of Mn(II) or colloidal Mn(IV). Sulfate in surface water at gages E121 and E123 increases post-SERF expansion (Figure C-1.0-9). This may reflect increased use of sodium sulfate for dechlorination of SCC cooling water.

For a given constituent, most of the time-series have similar concentration values and trends at gaging stations E121 and E123, suggesting surface water moves rapidly through the wetland and most constituents have little interaction with alluvial sediments. This does not preclude any mixing of surface water into the alluvium (see section 3.2). There is also little evidence for release of contaminants or other species from the wetland as part of base flow, either in the form of alluvial waters surfacing and mixing with base flow or advecting directly from the wetland. One exception to this observation is for manganese (Figure C-1.0-5). Dissolved concentrations of manganese are consistently higher at E123 because alluvial waters in the wetland have high manganese levels, probably as Mn(II) (see section 3.2). The manganese detected at E123 may be present partially as Mn(II) because of relatively slow oxidation kinetics, although speciation would need to be done to confirm this hypothesis. Mn(IV) colloids are also a distinct possibility. Iron mimics manganese in terms of higher values at gage E123 relative to gage E121 (Figure C-1.0-6). Sulfate may be slightly higher at E123 than at E121 (Figure C-1.0-9), perhaps as a result of the oxidation of sulfides known to occur in the alluvial system (see section 3.2). Zinc is actually lower at gage E123 than at gage E121, suggesting sorption as surface water passes through the wetland (Figure C-1.0-10). Relative differences between nitrate and nitrite at the two gages are not consistent through time, though in some periods nitrate plus nitrite does appear to be lower at E123, suggesting plant uptake and/or denitrification occurring in the wetland. A seasonal signal is not readily apparent (Figure C-1.0-11).

At gage E122, filtered arsenic in base flow may show a decreasing trend, although further monitoring will be required to verify (Figure C-1.0-1). Similarly, sulfate may show an increasing trend with time. Other constituents analyzed show little to no temporal trends but rather occasional concentration spikes.

Sulfide was not measured in surface waters as part of this monitoring program. Ammonium concentrations at gage E121 are often nondetect and are generally less than 0.3 mg/L (NH_4 as N). Recent concentrations at gage E123 have shown detects in two out of six samples with maximum

concentrations of approximately 0.7 mg/L. Low ammonia concentrations in the surface water system are consistent with the oxidizing environment and plant uptake.

Nitrogen isotope results from surface water are shown in Figure C-1.0-13. As only two piezometer samples yielded sufficient nitrate for isotopic analysis those results are also considered in this report. Nitrate at gage E122 has an isotopic signature consistent with background nitrate, whereas at gages E121 and E123, the nitrate isotopes show a very strong sewage signature (LANL 2012, 228624). The slopes of the linear trends between the nitrogen and oxygen isotopes at gages E121 and E123 are consistent with denitrification and presumably reflect variations in treatment efficiency associated with SWWS. The trend at gage E123 appears to be offset slightly to lower $\delta^{15}\text{N}$ values. This likely reflects a mixture of a background component from gage E122 and from any lateral surface flows or runoff into the wetland. The two piezometer values appear to be a mixture of sewage and background nitrate. It is interesting that these points fall at the lower end of the trend seen at gage E123. It is possible that alluvial water with this signature rises to the surface at some point in the wetland and mixes with surface flow dominated by a sewage signature, resulting at least partially in the observed linear trend.

While the focus of this report is the geochemical and physical function of the wetland, a frequency of detects table is provided in Appendix D for completeness. This table has been separated into results from the off-site laboratory and results run in the Earth and Environmental Sciences (EES) in-house laboratory. Of the contaminants highlighted in this performance report, only PCBs at gage E123 (in 2 out of 2 samples) and arsenic at gage E122 (1 out of 38 filtered samples) exceed applicable standards in surface water base flow. Other constituents that exceeded applicable comparison values in base flow from at least 1 of the 3 surface water locations above and below the wetland include total cyanide, aluminum, copper, selenium, silver, thallium, and zinc.

Paired storm water time-series from surface water gaging stations E121 and E123 are presented in Figures C-1.0-14, C-1.0-15, and C-1.0-17 to C-1.0-20 for key wetland contaminant species (chromium, arsenic; insufficient PCB data are available for time-series analysis) along with a plot of suspended sediment concentration (SSC) and total suspended sediments (TSS) (Figure C-1.0-16). Data are presented both as raw concentrations and concentrations normalized to SSC. By comparing storm water values upgradient and downgradient of the wetland it is possible to see if contaminants from the wetland are being entrained during flooding. Annual comparisons of data from E123 will also help determine if wetland stability aided by the GCS is improving storm-water quality. No clear temporal trend is seen for dissolved chromium, although concentrations at gage E123 are slightly higher than at gage E121 (Figure C-1.0-14). Dissolved concentrations are near background levels for Laboratory groundwater and may contain a colloidal component smaller than 0.45 μm as discussed previously in this section. Unfiltered chromium concentrations at gages E121 and E123 similarly show no compelling temporal trend (Figure C-1.0-15). Higher concentrations at gage E123 likely reflect colloidal transport. SSC/TSS concentrations are somewhat higher on average at gage E123 versus E121, reflecting some entrainment of sediment from the wetland (Figure C-1.0-16). Unfiltered chromium concentrations normalized to SSC show no temporal trends, although concentrations are higher at gage E123, which is consistent with incorporation of colloidal Cr(III) as storm water passes through the wetland (Figure C-1.0-17). Filtered arsenic concentrations show many nondetects (Figure C-1.0-18). Where detected, arsenic could be present as a true dissolved phase or as a colloidal component. The low dissolved concentrations of arsenic suggest there is no significant transport from the alluvial system during floods (see section 3.2). There may be a decreasing trend through time in unfiltered arsenic concentrations in storm water at E123 (Figure C-1.0-19). During some periods arsenic concentrations appear to be higher at gage E123 than at E121, while at other times the opposite seems to be true. When normalized to SSC, however, arsenic is clearly transported from the wetlands though the speciation is unknown (Figure C-1.0-20).

Very little storm-water data exist for the period following construction of the CGS, so continued monitoring is necessary to further evaluate temporal trends and the efficacy of the GCS as an interim measure.

The GCS was not installed with the objective of reducing concentrations of storm water to specific target levels. However, annual evaluations of storm water data will help determine if wetland stability provided by the GCS is effective at mitigating contaminant transport in floods. Existing storm water data are presented to provide some historical perspective for use in future reports. Analytical results are therefore not compared with water-quality standards or other criteria for the purpose of evaluating compliance with regulatory requirements. The New Mexico Water Quality Control Commission (NMWQCC) Standards for Interstate and Intrastate Surface Waters (New Mexico Administrative Code 20.6.4) establish surface water standards for New Mexico. The NMWQCC classifies all surface water within the Laboratory boundary with segment-specific designated uses. This Sandia stream segment is classified as perennial, with designated uses of limited aquatic life, livestock watering, wildlife habitat, and secondary contact. Some of the standards are for total concentrations, which are compared with data from unfiltered surface water samples. Other standards are for dissolved concentrations, which are compared with data from filtered samples. The NMWQCC standards, presented in Table 3.1-1, are used as numeric values for comparison with monitoring results as a frame of reference. When chemicals have comparison values for multiple designated uses, the smallest value was selected to compare with analytical results. Table 3.1-2 presents results of this comparison for storm water analyses conducted at E121, E122, and E123 since 1999.

Hydrographs from gaging stations E121, E122, and E123 are provided in Figure C-1.0-21.

3.2 Analytical Results from Piezometers

Analytical results for water chemistry from the piezometer array are presented in Figures C-2.0-1 to C-2.0-24. All data shown represent filtered samples. The plots are presented in the relative spatial distribution of the piezometers (i.e., upper graphs are from the western transect ordered from south to north, the next downgradient transect is in the middle, again ordered from south to north, and so on). Because of insufficient data, the easternmost transect is not shown. Because of the difficulties with sampling discussed in sections 2.0 and 4.6 and the relatively short periods of record, less emphasis is placed on temporal trends, although ranges in data from alluvial wells SCA-1 and SCA-1-DP from 2006 to 2011 are included to provide a longer baseline context. For some constituents, the complete long-term record (SCA-1/SCA-1DP plus the piezometers) is provided to emphasize possible temporal trends. It is recognized that with little piezometer data from the easternmost transect and with no temporal overlap between piezometer data (all piezometer data are post-SERF upgrade) and data from wells SCA-1 and SCA-1-DP, such comparisons must be made with caution. More emphasis is placed on spatial relationships that might indicate preferential flow paths within the wetland sediment, redox domains, and/or areas subject to dewatering. In addition, the data are compared with recent base-flow data from gaging station E121. Differences between base-flow data from E121 and alluvial water may indicate subsurface processes (e.g., reduction) and provide information about residence times in the alluvial system. Most importantly, data are assessed in terms of potential as alluvial redox indicators. Key analytes plotted include major cations (calcium, magnesium, and sodium), a major conservative anion (chloride), redox-sensitive species (iron, manganese, sulfate, and ammonium), key contaminants [chromium, including as Cr(VI), arsenic, and molybdenum] as well as a species that reflect changes in outfall chemistry (SiO_2 ; see section 1.4-2).

Field parameter data for temperature and specific conductivity recorded by the sondes are presented in Figure C-2.0-25. Sonde data for SCPZ-1 appear to record an instrument malfunction as shown by the wide variability in recorded values. Temperatures of alluvial water within the wetland range from around

4°C to near 20°C and show seasonality with higher temperatures recorded in the summer. A cooling trend is observed within the alluvial aquifer from west to east across the wetland. Specific conductance values range from 400 $\mu\text{S}/\text{cm}$ to 600 $\mu\text{S}/\text{cm}$ with locations on the southern side of the wetland generally showing much greater variability than other locations. Piezometers SCPZ-1 through SCPZ-3 show the greatest response of conductance to the September flood event. This response is likely because of their location at the head of the wetland where they tap highly transmissive sands and gravels as compared with the finer silt and clay that occurs within the wetland proper.

Calcium concentrations as measured in the piezometers are within the range of historical data from alluvial wells SCA-1 and SCA-1-DP and show no consistent temporal trends or significant spatial variation between sites (Figure C-2.0-1). Calcium is not a redox-sensitive species but does appear to be concentrated in alluvial water versus surface water, probably because of longer alluvial residence times and sediment-water interactions. Magnesium shows similar patterns to calcium, except that concentrations in the upper two transects are lower than the historical range at SCA-1/SCA-1-DP, which are located near the end of the wetland (Figure C-2.0-2). To the extent that this comparison is valid, it may reflect improvements in outfall water quality related to the SERF expansion. If so, this would indicate some degree of surface water/alluvial water interaction that had not yet propagated to the transect containing piezometers SCPZ-7 to SCPZ-9 perhaps because this part of the wetland is more clay- and organic-rich with lower hydraulic connectivity to surface water. Sodium concentrations also show no clear and compelling spatial and temporal trends (Figures C-2.0-3 and C-2.0-4). The relationship between surface water and alluvial water sodium concentrations is unclear. As with magnesium, some alluvial sodium concentrations are lower than the historical range found in SCA-1/SCA-1-DP, although the same caveats apply. This same trend is apparent for chloride (Figures C-2.0-5 and C-2.0-6), which as a conservative species is expected to show surface-water influences sooner. Surface water and alluvial chloride concentrations are relatively similar and show no significant temporal or spatial patterns. Longer piezometer time series may help address the degree to which changes in outfall chemistry have influenced alluvial chemistry.

Sulfate concentrations are low and are generally lower than surface water concentrations, consistent with reducing conditions in the wetland (Figure C-2.0-7). Locations SCPZ-1, SCPZ-5, SCPZ-6 and SCPZ-8 appear to be particularly reducing based on lower sulfate concentrations relative to other locations. Location SCPZ-1 may be reducing because of its depth (Table 1.5-1), though it is likely completed in sands and gravels. SCPZ-6 is sited in a very stagnant location based on observations of limited standing water with no apparent flow. Piezometers SCPZ-5 and SCPZ-8 are in or next to the central surface water flow path in the wetland but may be completed in tighter, more reducing sediments. Sulfide was detected periodically at locations SCPZ-1 through SCPZ-9 (see Appendix D; the highest detected sulfide concentration was 0.45 mg/L at location SCPZ-7). SO_4 concentrations are within historic ranges at SCA-1 and SCA-1-DP and show no temporal trends.

Arsenic concentrations are within historical ranges, except at locations SCPZ-5 and SCPZ-6 where concentrations are higher (Figures C-2.0-8 and C-2.0-9). Arsenic may also be slightly elevated at location SCPZ-1. These locations also had anomalously low sulfate, suggesting a redox control on arsenic concentrations. A plot of arsenic versus sulfate is shown in Figure C-2.0-10. There is an inverse correlation with locations SCPZ-5, SCPZ-6 and SCPZ-8 having lower sulfate and higher arsenic concentrations, consistent with more reducing conditions at these locations. As stated in section 1.6.2, arsenic can exist as As(III) and be relatively mobile under reducing conditions. The ratio of As(III) to As(V) (possibly present as colloids $<0.45 \mu\text{m}$) in these samples is not known. Some evidence suggests that arsenic concentrations may be decreasing at a number of piezometer locations, but longer time series will be required for verification.

Dissolved chromium concentrations in the wetland alluvial system are quite high (Figure C-2.0-11) but likely predominantly reflect colloidal Cr(III). Cr(VI) concentrations measured in the March 2013 round were all nondetects, reflecting the strong reducing conditions in the wetland. Most locations show concentrations within the historic range of SCA-1 and SCA-1 DP (Figure C-2.0-12). No obvious temporal or spatial trends are seen. Alluvial concentrations are higher than surface water concentrations, presumably because of the abundance of Cr(III) colloids in the subsurface.

Piezometer iron concentrations are higher than in surface water, presumably reflecting dissolved Fe(II) present under reducing conditions (Figure C-2.0-13). Locations SCPZ-5 and SCPZ-1 have the highest concentrations of iron as well as higher SO₄ and lower arsenic concentrations. No consistent temporal trends are observed. Some measured iron concentrations are higher than in the historical record from SCA-1 and SCA-1-DP, although the validity of this comparison is questionable. Similarly, manganese concentrations are sometimes higher than the historical record (Figures C-2.0-14 and C-2.0-15). Like iron, manganese concentrations are higher in alluvial water than in surface water, again reflecting reducing conditions. Consistent temporal trends are not obvious. As with some of the other redox-sensitive species, manganese is higher at locations SCPZ-1, SCPZ-5, SCPZ-6, and SCPZ-8, suggesting these locations may be more reducing at the depth of screen completion. Location SCPZ-7 also appears to be moderately reducing. Locations SCPZ-2 and SCPZ-3 have lower manganese concentrations consistent with their shallow completion depths in sands and gravels. Interestingly, location SCPZ-4 also has low manganese. In May 2014, no surface water was present at this location. A plot of iron versus manganese is shown in Figure C-2.0-16. While the observed correlation is not that strong, the lower manganese and iron concentrations at locations SCPZ-2, SCPZ-3, and SCPZ-4 are clear.

Molybdenum values are within historical ranges at SCA-1 and SCA-1-DP and show no clear temporal trends, although there is some indication of overall decreases with time at several locations (a longer time-series will be needed to verify this) (Figure C-2.0-17). Alluvial concentrations are higher than in surface water and are spatially variable. Molybdenum occurs as a redox sensitive oxyanion similar to chromium, but molybdenum was used as a corrosion inhibitor from 1993 to 2001, well after potassium dichromate, and therefore has a very different release history (LANL 2006, 094431).

Dissolved silicon dioxide concentrations are clearly lower than historical values at SCA-1 and SCA-1DP and may show early evidence of decreasing trends (Figures C-2.0-18 and C-2.0-19). This pattern is likely related to improvements in outfall water quality following the SERF upgrade and indicates some degree of infiltration and mixing of surface water with alluvial water. A plot of silicon dioxide versus chloride is shown in Figure C-2.0-20. The apparent inverse trend is consistent with water treatment associated with the SERF expansion where silicon dioxide is removed but chloride concentrations have increased. The SERF adjusts chloride depending on the composition of water coming from the SWWS and other waters that are being released to Outfall 001. Chloride concentrations will continue to be affected by waters processed through the SERF as it expands its capacity. Lower alluvial concentrations are seen in all three transects, which tends to suggest that this signal is propagated rapidly throughout the wetland alluvial system, likely via surface water infiltration rather than alluvial advection. Silicon dioxide is not a redox-sensitive species. Spatial trends are generally absent, although concentrations are lowest at location SCPZ-6 for reasons that are unclear. Silicon dioxide concentrations are generally higher in alluvial water than in surface water, likely reflecting longer residence times in the alluvial system and water-sediment interaction.

Nitrate values were generally nondetect, consistent with reducing conditions in the wetland (see Appendix D). Ammonium, however, was detected periodically at most piezometers (Figure C-2.0-21; the highest ammonia concentration was 2.9 mg/L at location SCPZ-10). Ammonium is higher in alluvial water than in surface water because it is stable under reducing conditions in the wetland and likely derives from mineralization of organic matter (e.g., dead cattail fronds). High concentrations of ammonium are not

necessarily expected in the subsurface, however, because of potential nutritive uptake by wetland plants. Ammonium nitrogen isotope values varied between 5.8‰ and 12.7‰ (see Appendix D). The relatively high $\delta^{15}\text{N}$ values for ammonium likely results from decay of plants with high $\delta^{15}\text{N}$ related in turn to inputs of sewage-related nitrate with high $\delta^{15}\text{N}$ into the wetland and subsequent denitrification (see section 1.6.1).

Time series for oxygen isotopes are shown in Figure C-2.0-22. There is an overall decline in $\delta^{18}\text{O}$ versus time. In Figure C-2.0-23, oxygen isotopes are plotted versus deuterium isotopes with respect to the local meteoric water line. Typical values for summer and winter precipitation and for the regional aquifer are shown. The data appear to represent a mixture of summer precipitation versus winter precipitation/regional aquifer water. The data broadly fall along the local meteoric water line but in total have a slope of 5, characteristic of an evaporative component to the isotopic signal (evaporation leaves residual water enriched in heavy isotopes). There is no significant variation between locations. The observed temporal trend may reflect less evaporation through time. It is possible that the GCS slows down surface water flow through the wetland, allowing for enhanced interaction of surface water with alluvial groundwater.

3.3 Water-Level Results from Piezometers

Water-level data were continuously recorded in several piezometers throughout the wetland (Figure 1.3-1) using Aqua TROLL Sondes between April 2013 and November 2013. The sondes were removed during the winter months to avoid detrimental impacts to the instruments from freezing temperatures. Water-level data collected at the piezometers are presented in Figure C-3.0-1. The plots are arranged within the figure to represent the spatial distribution of the piezometers throughout the wetland. Daily flows at gage E121 are plotted along with the piezometer water-level data. The E121 data reflect inputs from Outfalls 001 and 03A027, as well as surface water flow from precipitation and runoff.

3.4 Geomorphic Survey Results

Geomorphic survey results are presented in Appendix B. As these are baseline results with resurveying to be done after the summer 2014 monsoon season and in subsequent years, these results are not considered further herein.

3.5 Vegetation Monitoring

Baseline photos from the wetland taken in May 2014 are presented in Appendix B. Suggested frequency and timing of future photo surveys are discussed in section 4.6. Photos are from key margins in the wetland (see sections 1.5 and 1.6), including the GCS proper.

4.0 RECOMMENDED WETLANDS PERFORMANCE METRICS

4.1 Spatial and Temporal Geochemical Patterns

Several surface water analytes (e.g., chloride, magnesium, SiO_2 , sodium, and zinc) show evidence for improved water quality associated with the SERF expansion. The overall similarity between surface water geochemistry at gaging stations E121 and E123 suggests a short residence time for surface water in the wetland. Based on silicon dioxide and chloride concentrations and $\delta^{18}\text{O}$ of alluvial water, however, it appears that while the alluvial system has a longer residence time there is gradual infiltration of and replacement/mixing by surface water. The geochemical similarity of the water between gages E121 and

E123 also suggests little alluvial water discharges from the wetland, although manganese and iron may either discharge to the surface from the alluvium at the end of the wetland, or surface and mix with base flow at some point upgradient within the wetland (with construction of the GCS, alluvial water discharge from the end of the wetland is no longer a factor). There do not appear to be many surface water concentration trends with time that cannot be directly related to water-quality improvements associated with the treatment at SERF. Longer time-series from the piezometers will be necessary to meaningfully assess temporal alluvial concentration trends.

Several analytes clearly reflect reducing conditions in the wetland (sulfate, arsenic, iron, manganese, nitrate, ammonium, and sulfide). Piezometer locations SCPZ-1, SPCZ-5, SCPZ-6 and SCPZ-8 seem to be the most reducing locations (based on alluvial arsenic, iron, manganese, and sulfate concentrations) while locations SCPZ-2, SCPZ-3, and perhaps SCPZ-4 are more oxidizing (based on alluvial manganese concentrations). While no preferential flow paths were identified in the alluvium, there do appear to be distinct geochemical domains in terms of redox conditions.

There is clearly some contaminant transport from the wetland. In the case of chromium, it is likely that most of the mass transported from the wetland in base flow or storm water flows is in the form of colloidal Cr(III). Arsenic also appears to be transported from the wetland by storm water, although the form (dissolved, colloidal) and speciation are not known. PCBs in both base flow and storm water exceed applicable standards at gage E123. Manganese and iron are also released from the wetland. These elements are associated with the reducing conditions in the wetland alluvium.

4.2 Temporal and Spatial Trends in Water Levels

The following groundwater-level observations were made at each piezometer transect based on the data presented in Figure C-3.0-1:

- SCPZ-1 to SCPZ-3: The SCPZ-1 sonde recorded apparent fluctuations of up to 25 ft in groundwater elevation. These results are thought to be caused by an instrument malfunction because temperature data for this sonde are also unreliable. The more reliable results for the first transect from piezometers SCPZ-2 and SCPZ-3 show that groundwater levels almost immediately respond to changes in flow recorded at gage E121. This suggests that the aquifer material in this narrow transect is relatively highly transmissive. The water level at this transect is about 1 to 2 ft bgs. The water level fluctuation is typically less than a foot and highly responsive to variations in surface flow. The water level rose close to 2 ft in SCPZ-2 and SCPZ-3 following the heavy rains of September 2013 and remained over 0.5 ft higher into November 2013.
- SCPZ-4 to SCPZ-6: Water levels at the second transect (SCPZ-4, SCPZ-5, and SCPZ-6) also respond almost immediately to flow at gage E121; however, the variations are generally a few tenths of a foot. The smaller water-level fluctuations are attributed to the following factors at this transect. First, the wetland is much broader and is well vegetated. Surface flow has spread across the wetland because of the low topographic gradient, and interaction with cattails and other wetland vegetation. Second, the water table is very near or at the surface here, so the piezometers are measuring filling of a small depth of nearly saturated wetland sediment probably accompanied by changes in the water level of ponded surface water. The alluvial material in this area is more fine grained and has a lower hydraulic conductivity so it probably neither drains nor fills rapidly, causing a small subsurface response. The water level rose only slightly (~0.1 ft) following the heavy rains of September 2013.

- SCPZ-8 and SCPZ-9: The water level elevation results from SCPZ-9 depict a gradual decline in water-level elevation over the period the sonde was recording. This could be the result of impacts from the construction of the GCS. The water level at this piezometer will be monitored further to determine the longer-term trends following GCS construction. SCPZ-8, which is also in the third transect, did not record a similar decline in water level throughout the monitoring period. SCPZ-8 is located next to the channel and shows water-level response to flow at gage E121, similar to those observed at SCPZ-2 and SCPZ-3 in the first transect. There is a small time lag in the water level response because this transect is so much farther down the wetland than the gage or the other transects. The water level rose close to 2 ft in SCPZ-8 following the September 2013 storm and remained 0.2 to 0.3 ft higher through November 2013.

Monitoring of water levels will continue as a means to determine how operational effluent releases affect the overall wetland hydrology. A longer period of record that follows completion of the GCS will be helpful at establishing baseline conditions.

4.3 Performance of Grade-Control Structure

The GCS was completed in August 2013 before the September 13, 2013, flood that occurred across the Laboratory, including in Sandia Canyon. Minor geomorphic response was manifest as relatively thin new deposits at the head of the cattail section in the upper one-third of the wetland. No evidence of erosion or headcutting was found at the GCS.

It is too soon after completion of the GCS to fully evaluate its effectiveness in terms of helping to maintain wetland geochemical and physical stability. Further monitoring will be useful in assessing performance.

4.4 Total Wetland System Performance

Thus far, there is no evidence for significant dewatering of the wetland related to the SERF expansion. For example, water-level data suggest that the alluvial system remains saturated. Little overall change to water levels was observed in the two westernmost transects, other than an apparent wetting of the upgradient sediment in response to the September 2013 flooding. More data are needed from the two easternmost transects to evaluate the effect of the GCS as little data are available for those two locations, and construction of the GCS caused significant change to the channel. Water-quality changes associated with the SERF upgrade have been seen in surface water and alluvial water. However, thus far, no adverse effects of changing water chemistry have been noted. The wetland appears to remain strongly reducing, with some portions of the wetland being more reducing than others. The storm water data post-GCS are not sufficient to assess the effectiveness of the GCS in maintaining physical stability of the wetland. No significant increases in base-flow contaminant concentrations have been noted at downgradient gaging station E123. As a whole, the wetland appears to continue to represent a relatively stable environment for the contaminants present in wetland sediment.

4.5 Key Monitoring Locations and Proposed Performance Metrics

Based on initial monitoring results (section 3), the following locations and metrics are seen as key to assessing future Sandia wetland performance in relation to the GCS and changes in outfall flow volumes and chemistry.

Gaging station E121 is a good location to monitor the integrated impacts of changing input chemistry and decreasing effluent volumes from Outfalls 001 and 03A027 in base flow. Gaging station E122 will

continue to provide information on inputs to the northern side of the wetland but does not reflect any of the changes related to the SERF expansion.

Gaging station E123 is the key integrating location of total wetland performance. Monitoring of storm water at E123 will reveal if anomalously high levels of sediment and contaminants are mobilized during floods resulting from a reduction in chemical and/or physical stability in the wetland. Monitoring during base-flow conditions will indicate changes in outfall chemistry and changes associated with wetland biogeochemistry and function.

The piezometer array provides valuable water-level and alluvial water chemistry data. These locations monitor potential changes associated with potential changes in outfall volumes, changing hydrogeomorphology, distribution of reducing zones, and outfall chemistry (in the case of more conservative constituents).

Table 4.5-1 details how these locations will be effective at monitoring various factors that could affect wetland stability and their related impacts.

The existing geomorphic transect locations are ideal for assessing hydrogeomorphic changes and physical stability in the system (see Appendix B).

Different metrics will be important to monitor at each of these locations. Significant metrics can be thought of as early warning indicators of detrimental changes in physical or chemical stability occurring in the wetland. For example, at gage E123, key metrics will be concentrations of total chromium in storm water and dissolved chromium (as evidenced by microfiltration with 0.02- μm filters) in base flow. In addition, monitoring of PCBs and PAHs in storm water will provide useful information on wetland stability. Hydrographs from this location will continue to be key to understanding the hydrology of the wetland and the effects of the GCS in terms of flood attenuation.

At gage E121, measurements of dissolved silica and major cation concentrations, which have been shown to reflect improvements in outfall water quality associated with SERF water treatment, along with hydrographs reflecting base flow and storm water will be important for understanding wetland inputs

In the wetland proper, measurements of water levels and significant contaminant and redox parameters will be of paramount importance for indicating signs of dewatering and changing geochemistry with respect to contaminants in the sediment. Key chemical species include chromium and arsenic (as primary contaminants) and iron, manganese, sulfate, sulfide, nitrate, and ammonia as important redox-sensitive indicator species. Microfiltration will be useful in determining the redox state of these metals and to quantify dissolved concentrations.

Over time, assuming the wetland stays relatively stable, geochemical control charts could be developed to place boundaries on the expected ranges of concentrations and other geochemical parameters. Deviations outside these boundaries would be suggestive of system changes.

4.6 Lessons Learned and Changes to Monitoring Plan

As a result of monitoring activities in the Sandia wetland, it has become apparent that the drive points used for sampling present challenges for long-term sampling, particularly in the very fine-grained, organic-rich sediments in downgradient portion of the wetland. The piezometers are prone to clogging of screens and filling with silt making it difficult to purge and sample after reasonable recovery periods. While it would be feasible to clean and reposition drive-point piezometers each round, this could present

inconsistencies between data from quarterly monitoring events. As such, the Laboratory proposes several changes to the monitoring approach.

The Laboratory proposes to pilot the use of more robust permanent alluvial wells for sampling within the wetland. Well design will occur in consultation with NMED but could include such options as prepacked wells, wells with a sand filter pack, or wells that are augured out within a casing and back-filled with native materials, followed by pulling of the casing. The Laboratory proposes to have the pilot testing phase last for 3 to 5 mo. Sampling of existing piezometers will be conducted while efforts to install better wells are implemented.

A revised sampling suite is provided in Table 4.6-1. The main changes are (1) that $\delta^{15}\text{N}/\delta^{18}\text{O}$ of nitrate has been removed as piezometer concentrations of nitrate have consistently been lower than required for isotopic analysis, and (2) the metals suite will include microfiltration to understand the effect of colloids on “dissolved” concentrations.

Base-flow and piezometer sampling will continue to occur quarterly in conjunction with monitoring of the rest of the chromium monitoring group as proposed in the current Interim Facility-Wide Groundwater Monitoring Plan (LANL 2013, 241962).

The overall scheme for storm water sampling will not change, although the analyte suite has been modified slightly to meet the needs of other projects, including environmental surveillance reporting. The modified suite is shown in Table 4.6-2.

Vegetation photo surveys will continue to occur (see section 3.6) but may be combined with photo surveys that are done as part of the geomorphic monitoring (Appendix B). This survey should take place on an annual basis during the summer when vegetation is at its peak. In addition, geomorphic monitoring fulfills the requirement for “other means” of vegetation monitoring specified in the work plan by documenting locations of willows and cattails along a number of north-to-south transects. It is further proposed that no other vegetation monitoring occur as part of this monitoring plan, but rather that those activities default to monitoring normally carried out ENV Division (e.g., wetland delineation) to meet requirements for performance monitoring of the GCS as outlined in the Corps of Engineers Dredge and Fill Permit (USACE 2013, 251704).

5.0 CONCLUSIONS

There is little to no evidence that any detrimental effects have occurred within the Sandia wetland to date as a result of installation of the GCS or of decreases in effluent volumes to the Sandia wetland. Changes in chemistry related to enhanced water treatment at SERF are evident, particularly in surface water. However, these changes do not appear to have had an adverse effect in terms of contaminant mobilization. It is too early to assess the efficacy of the GCS, though it likely prevented potentially significant erosion during the September 13, 2013 flood.

Ongoing monitoring will continue to allow the Laboratory to assess changes, either positive or negative, within the Sandia wetland related to the GCS, changes in effluent chemistry, and to decreases in effluent volumes and discharge rates. The Laboratory will respond with an adaptive management strategy should adverse changes be noted.

6.0 REFERENCES

The following list includes all documents cited in this report. Parenthetical information following each reference provides the author(s), publication date, and ER ID. This information is also included in text citations. ER IDs are assigned by the Environmental Programs Directorate's Records Processing Facility (RPF) and are used to locate the document at the RPF and, where applicable, in the master reference set.

Copies of the master reference set are maintained at the NMED Hazardous Waste Bureau and the Directorate. The set was developed to ensure that the administrative authority has all material needed to review this document, and it is updated with every document submitted to the administrative authority. Documents previously submitted to the administrative authority are not included.

DOE (U.S. Department of Energy), August 24, 2010. "Final Environmental Assessment for the Expansion of the Sanitary Effluent Reclamation Facility and Environmental Restoration of Reach S-2 of Sandia Canyon at Los Alamos National Laboratory, Los Alamos, New Mexico," U.S. Department of Energy document DOE/EA-1736, Los Alamos Site Office, Los Alamos, New Mexico. (DOE 2010, 206433)

Eary, L.E., and D. Rai, February 1989. "Kinetics of Chromate Reduction by Ferrous Ions Derived from Hematite and Biotite at 25°C," *American Journal of Science*, Vol. 289, pp. 180–213. (Eary and Rai 1989, 256733)

EPA (U.S. Environmental Protection Agency), June 8, 2007. "Authorization to Discharge under the National Pollutant Discharge Elimination System, NPDES Permit No. NM 0028355," Region 6, Dallas, Texas. (EPA 2007, 099009)

Fair, J.M., and J.M. Heikoop, 2006. "Stable Isotope Dynamics of Nitrogen Sewage Effluent Uptake in a Semi-Arid Wetland," *Environmental Pollution*, Vol. 140, pp. 500-505. (Fair and Heikoop 2006, 098045)

Heikoop, J.M., D.D. Hickmott, D. Katzman, P. Longmire, and R.S. Beers, 2002. "N-15 Signals of Nitrogen Source and Fate in a Semiarid Wetland," *Wetlands and Remediation II, Proceedings of the Second International Conference on Wetlands and Remediation, September 5–6, 2001, Burlington, Vermont*, pp. 355–362. (Heikoop et al. 2002, 107001)

Langmuir, D., 1997. *Aqueous Environmental Geochemistry*, Prentice Hall, Inc., Upper Saddle River, New Jersey. (Langmuir 1997, 056037)

LANL (Los Alamos National Laboratory), November 2006. "Interim Measures Investigation Report for Chromium Contamination in Groundwater," Los Alamos National Laboratory document LA-UR-06-8372, Los Alamos, New Mexico. (LANL 2006, 094431)

LANL (Los Alamos National Laboratory), October 2009. "Investigation Report for Sandia Canyon," Los Alamos National Laboratory document LA-UR-09-6450, Los Alamos, New Mexico. (LANL 2009, 107453)

LANL (Los Alamos National Laboratory), May 2011. "Interim Measures Work Plan for Stabilization of the Sandia Canyon Wetland," Los Alamos National Laboratory document LA-UR-11-2186, Los Alamos, New Mexico. (LANL 2011, 203454)

- LANL (Los Alamos National Laboratory), September 2011. "Work Plan and Final Design for Stabilization of the Sandia Canyon Wetland," Los Alamos National Laboratory document LA-UR-11-5337, Los Alamos, New Mexico. (LANL 2011, 207053)
- LANL (Los Alamos National Laboratory), September 2012. "Phase II Investigation Report for Sandia Canyon," Los Alamos National Laboratory document LA-UR-12-24593, Los Alamos, New Mexico. (LANL 2012, 228624)
- LANL (Los Alamos National Laboratory), May 2013. "Interim Facility-Wide Groundwater Monitoring Plan for the 2014 Monitoring Year, October 2013–September 2014," Los Alamos National Laboratory document LA-UR-13-23479, Los Alamos, New Mexico. (LANL 2013, 241962)
- LANL (Los Alamos National Laboratory), December 2013. "Completion Report for Sandia Canyon Grade-Control Structure," Los Alamos National Laboratory document LA-UR-13-29285, Los Alamos, New Mexico. (LANL 2013, 251743)
- LANL (Los Alamos National Laboratory), March 2014. "Los Alamos National Laboratory Renewal Application for NPDES Permit Number NM0030759, Individual Permit for Storm Water Discharges from Solid Waste Management Units and Areas of Concern," Los Alamos National Laboratory document LA-UR-14-21861, Los Alamos, New Mexico. (LANL 2014, 254864)
- McBride, M., January 1, 1994. "Trace and Toxic Elements in Soils," in *Environmental Chemistry of Soils*, Oxford University Press, New York, New York. (McBride 1994, 058947)
- NMED (New Mexico Environment Department), June 9, 2011. "Approval with Modification, Interim Measures Work Plan for Stabilization of the Sandia Canyon Wetland," New Mexico Environment Department letter to G.J. Rael (DOE-LASO) and M.J. Graham (LANL) from J.E. Kielling (NMED-HWB), Santa Fe, New Mexico. (NMED 2011, 203806)
- Panichev, N., W. Mabasa, P. Ngobeni, K. Mandiwana, and S. Panicheva, May 2008. "The Oxidation of Cr(III) to Cr(VI) in the Environment by Atmospheric Oxygen during the Bush Fires," *Journal of Hazardous Materials*, Vol. 153, No. 3, pp. 937–941. (Panichev et al. 2008, 256734)
- USACE (U.S. Army Corps of Engineers), March 27, 2013. "Action No. SPA-2012-00050-ABQ, McCann, LANL, Sandia Canyon, Wetland, Los Alamos County, NM," USACE letter to J. McCann (LANL) from W. Oberle (USACE), Albuquerque, New Mexico. (USACE 2013, 251704)

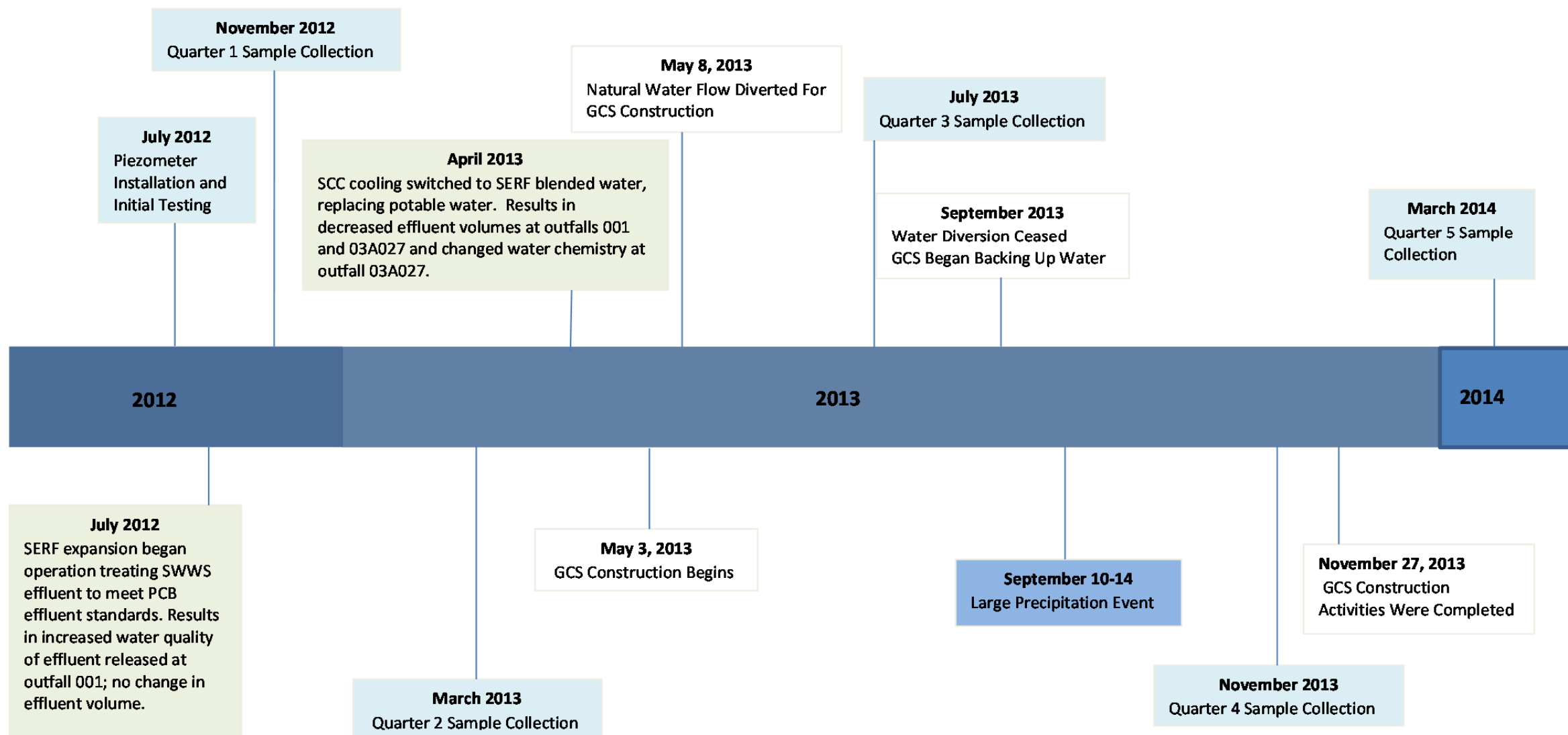


Figure 1.2-1 Sandia Canyon Wetland timeline

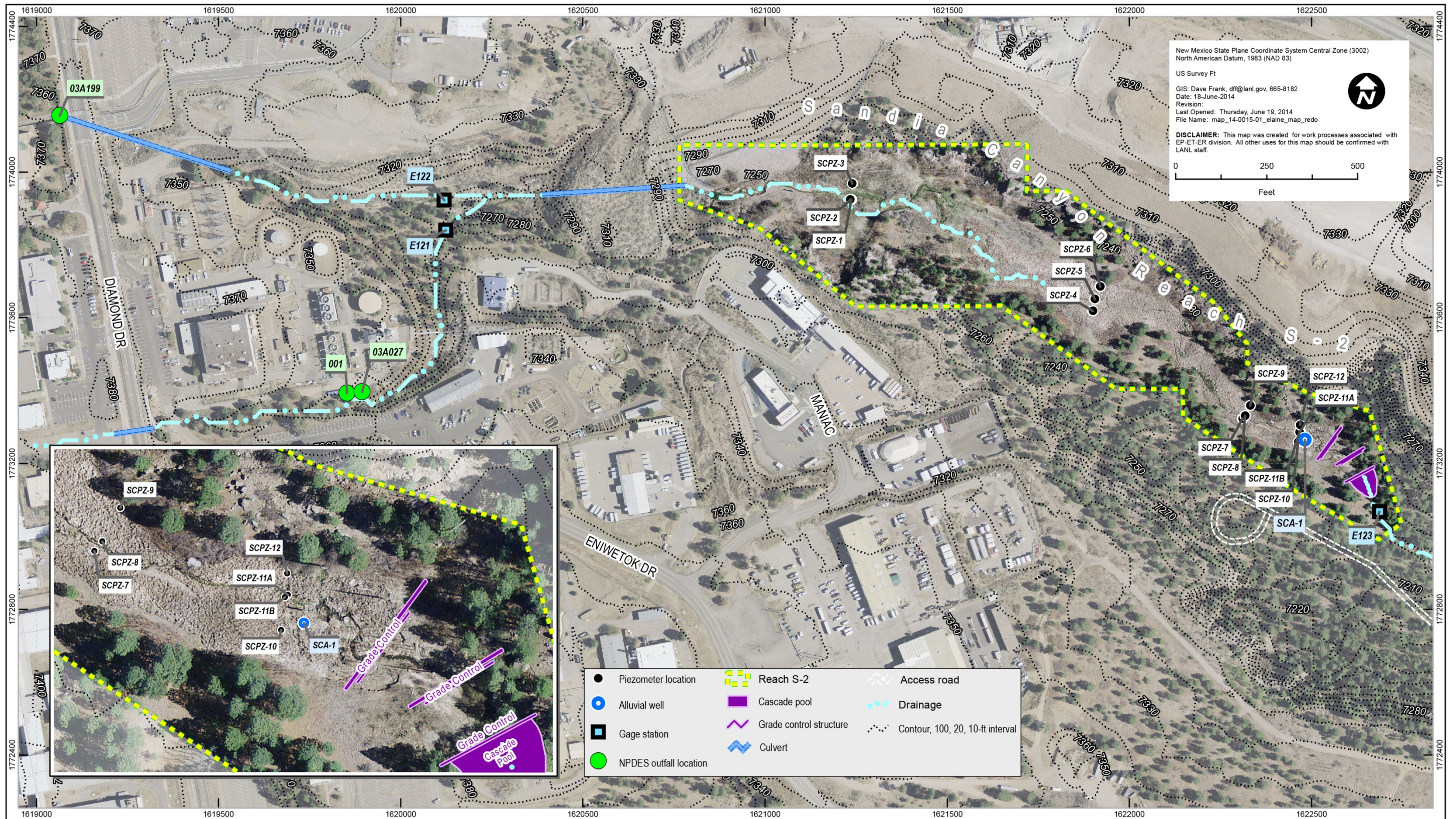


Figure 1.3-1 Locations of the Sandia GCS, NPDES outfalls, piezometers, alluvial wells, surface and storm water gaging stations, and reach S-2

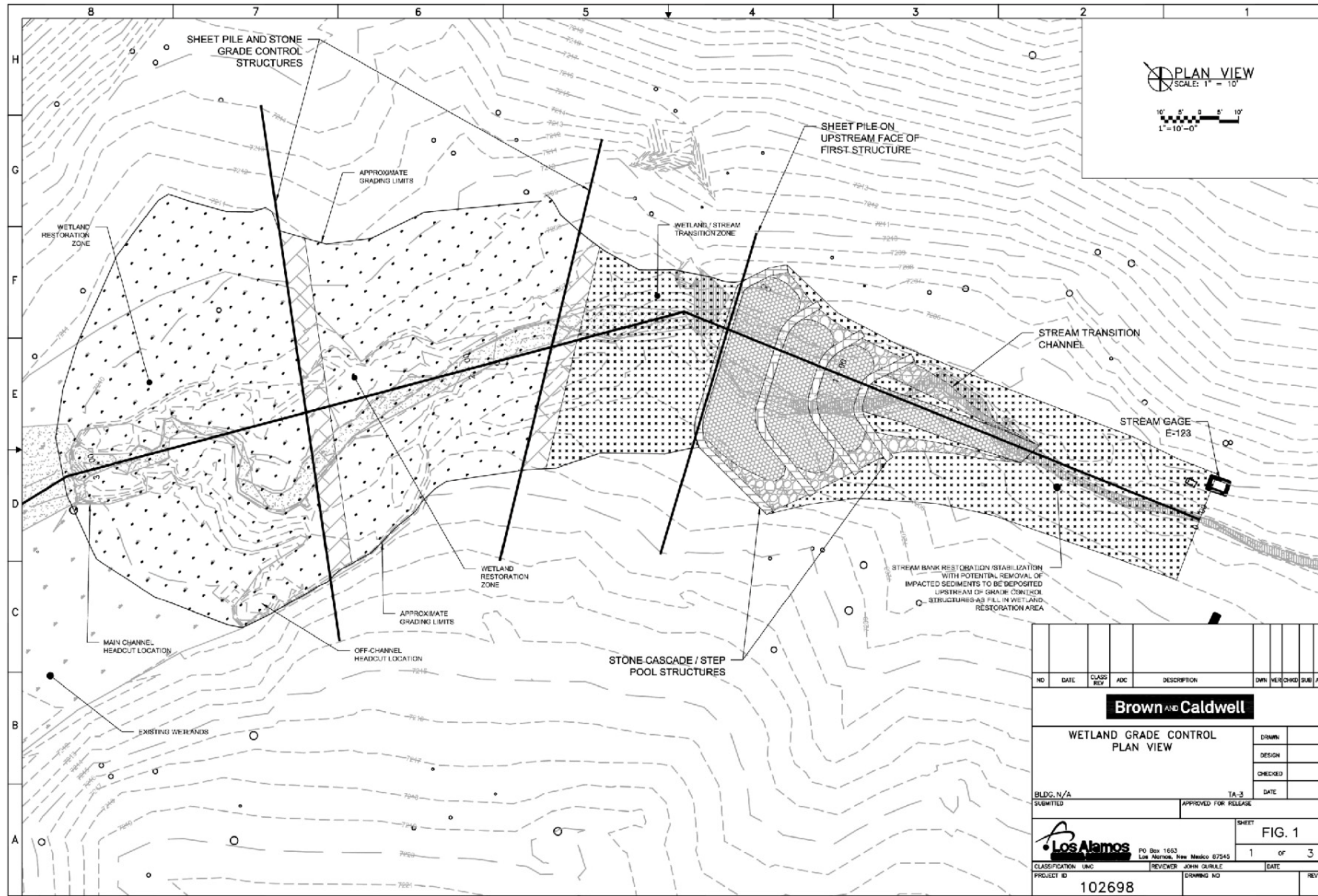


Figure 1.3-2 GCS design plan view

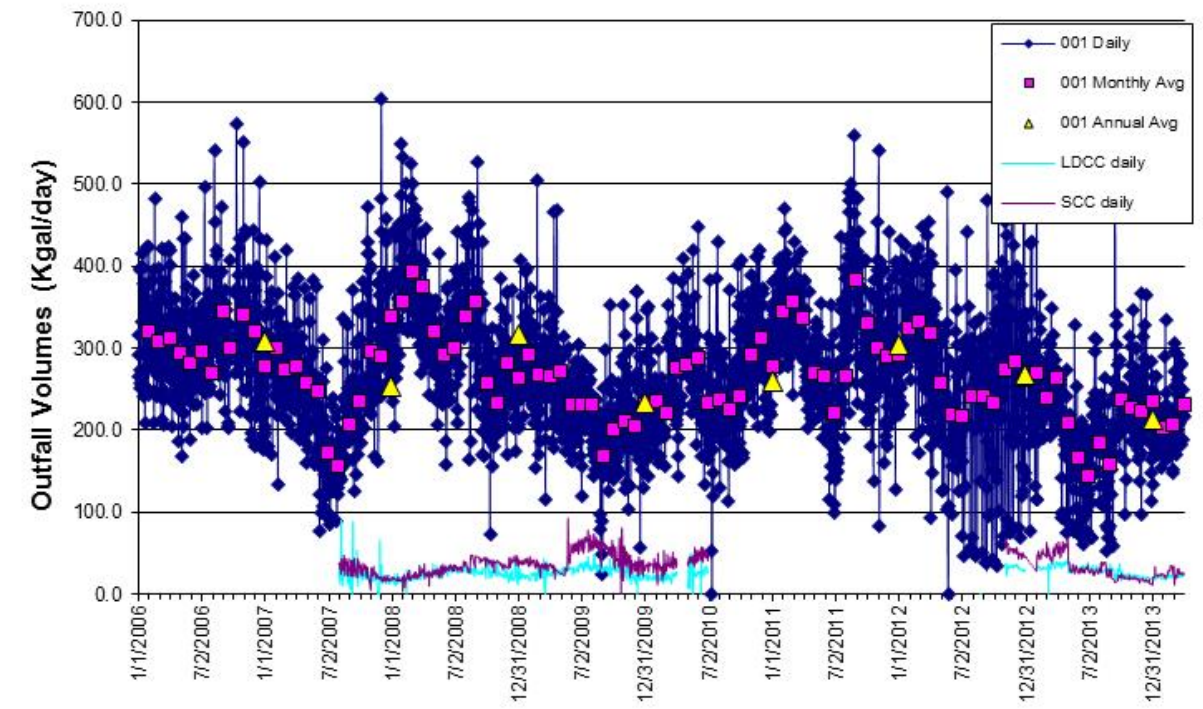


Figure 1.4-1 Daily, monthly average, and yearly average effluent release volumes (expressed as Kgal/day) for Outfall 001 since 2006 and daily effluent releases for Outfalls 03A027 (SCC) and 03A199 (LDCC) from August 2007 to January 2010 and from November 2012 to March 2013

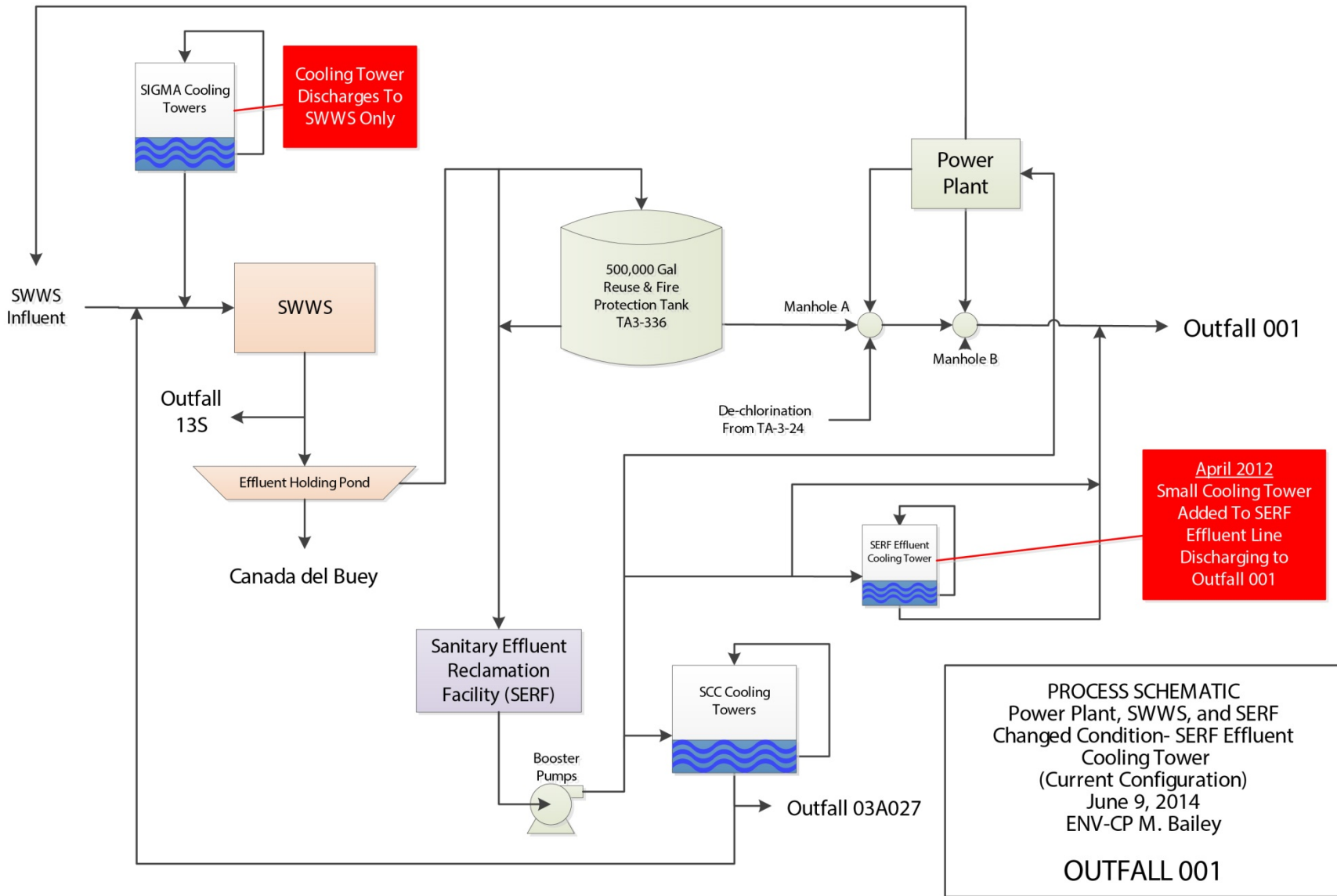


Figure 1.4-2 Updated process schematic for the power plant, SWWS, and SERF connections to Outfall 001 (current configuration)

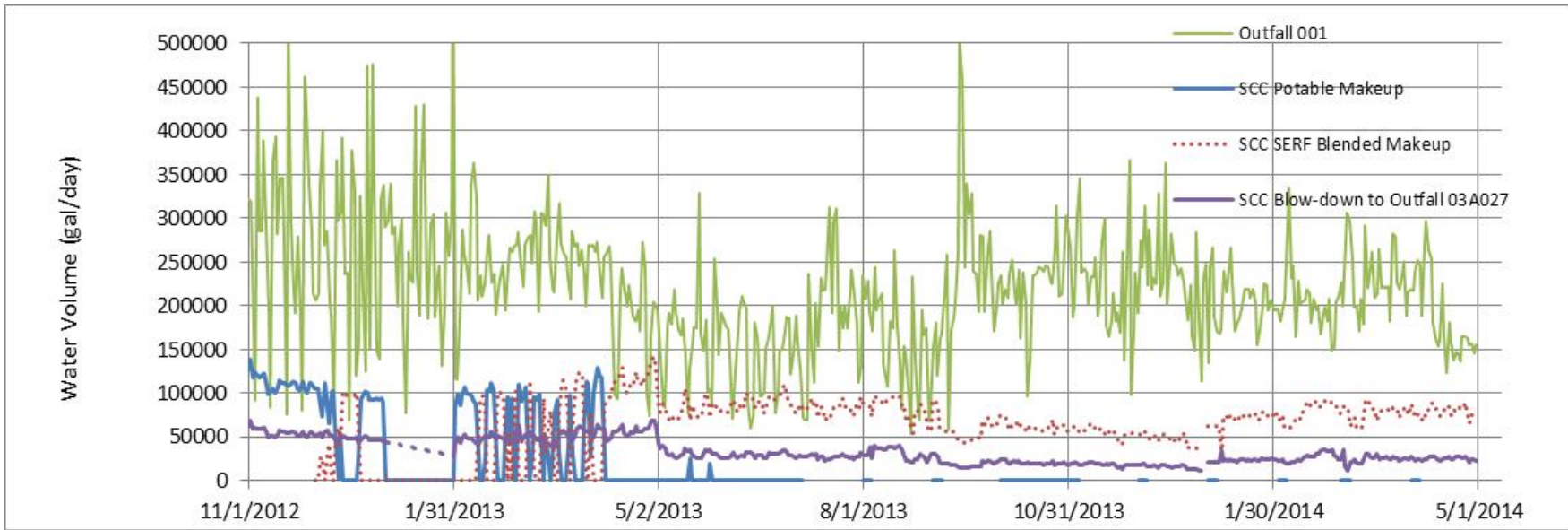


Figure 1.4-3 Daily water volumes from November 2012 to April 2014 for effluent released from Outfall 001, effluent from the SCC cooling towers, which release to Outfall 03A027, and makeup water sources (potable or SERF-blended water) used at the SCC cooling towers



Figure 1.5-1 A drive point with 2-ft screen used in the study



Figure 1.5-2 Photo of SCPZ-1 as installed in the field

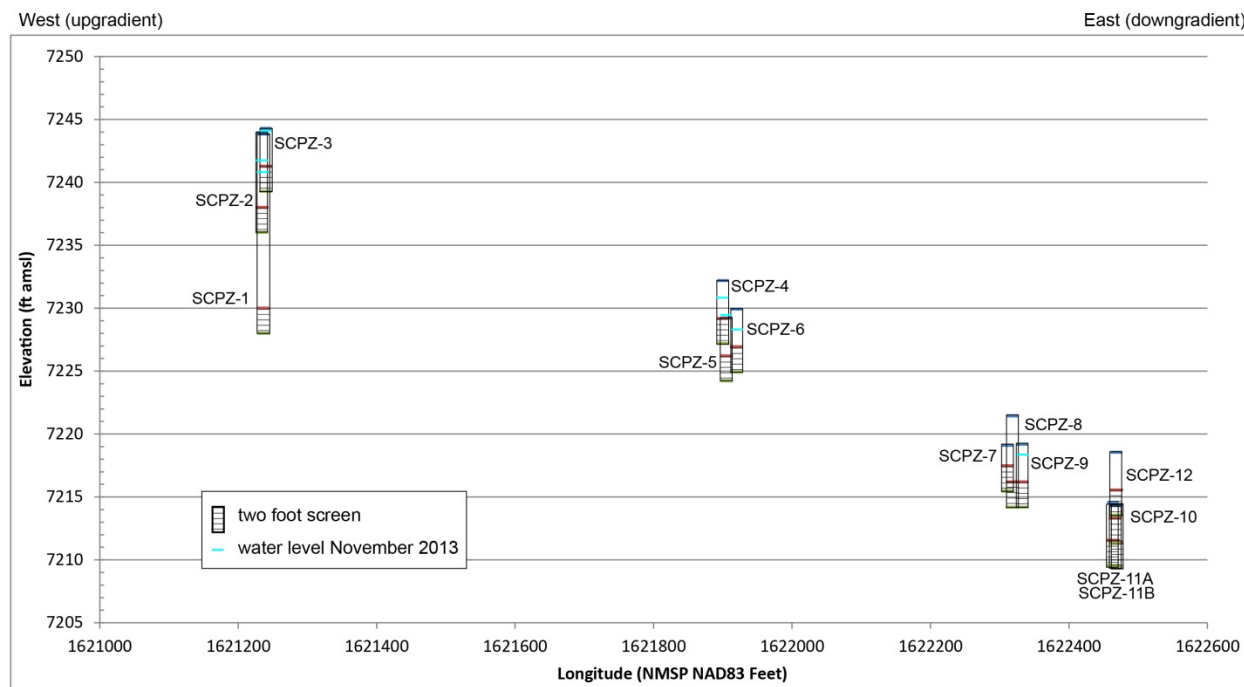


Figure 1.5-3 Schematic of piezometer transects and depths

Table 1.5-1
Completion Data for Alluvial Piezometers

| Parameter | Piezometer | | | | | | | | | | | | |
|------------------------|------------|--------|--------|--------|--------|--------|--------|--------|--------|---------|------------|------------|---------|
| | SCPZ-1 | SCPZ-2 | SCPZ-3 | SCPZ-4 | SCPZ-5 | SCPZ-6 | SCPZ-7 | SCPZ-8 | SCPZ-9 | SCPZ-10 | SCPZ-11(A) | SCPZ-11(B) | SCPZ-12 |
| Total length (ft) | 20.5 | 11.4 | 8.3 | 8.3 | 8.3 | 8.3 | 8.3 | 11.4 | 8.3 | 8.3 | 8.3 | 8.3 | 8.3 |
| Stick up (ft) | 4.3 | 3.1 | 3.0 | 3.0 | 3.0 | 3.0 | 4.3 | 3.8 | 3.0 | 3.0 | 3.0 | 5.0 | 3.0 |
| Top of screen (ft bgs) | 13.8 | 6.0 | 3 | 3 | 3 | 3 | 1.6 | 5.3 | 3 | 3 | 3 | 1 | 3 |
| Total depth (ft bgs) | 16.2 | 8.3 | 5.4 | 5.4 | 5.4 | 5.4 | 4.0 | 7.6 | 5.4 | 5.4 | 5.4 | 5.4 | 5.4 |

Table 1.5-2
Alluvial Groundwater Sampling and Analysis Plan for Sandia Wetland Stabilization Monitoring

| Suite | Frequency | Comment |
|--|-----------|---|
| EES Metals ^a (filtered) | Quarterly | Includes redox sensitive metals Fe, Mn, Cr, As |
| EES Anions ^b (filtered) | Quarterly | Includes redox sensitive anions sulfate and nitrate; nitrate is a wetland vegetation nutrient |
| Sulfide (filtered) | Quarterly | Redox indicator (reduction of sulfate) |
| Alkalinity/pH (unfiltered) | Quarterly | Organic matter degradation |
| Ammonia (filtered) | Quarterly | Indicator of organic matter degradation; wetland vegetation nutrient |
| TOC ^c (unfiltered) | Annually | Organic matter degradation |
| DOC ^d (filtered) | Annually | Organic matter degradation |
| Cr(VI) (filtered) | Annually | Indicator of Cr(III) oxidizing to Cr(VI) |
| $\delta^{15}\text{N}$ ammonia (filtered) | Quarterly | Indicator of nitrogen sources and redox-related transformations |
| $\delta^{15}\text{N}/\delta^{18}\text{O}$ nitrate (filtered) | Quarterly | Indicator of denitrification (redox process) and nitrogen sources |
| $\delta^{18}\text{O}/\delta\text{D}$ water (filtered) | Quarterly | Indicator of outfall discharge versus snowmelt and storm water runoff |

^a EES metals refers to metals analyses conducted at the Laboratory's Earth and Environmental Sciences (EES) analytical laboratory, and consists of the following suite: Ag, Al, As, B, Ba, Be, Cd, Co, Cr, Cs, Cu, Fe, K, Li, Mg, Mn, Na, Ni, Pb, Rb, Se, Si, Sr, Ti, Tl, U, V, Zn, Hg, Mo, Sb, Sn, Th.

^b EES anions refers to anion analyses conducted at the Laboratory's EES analytical laboratory, and consists of the following suite: Br, F, Cl, NO₂, NO₃, PO₄, SO₄, C₂O₄H₂ (oxalic acid).

^c TOC = Total organic carbon.

^d DOC = Dissolved organic carbon.

**Table 1.5-3
2012 and 2013 Storm Water Sampling
Planned at Gage Stations E121, E122, and E123**

| Bottle No. | Sample Collection Time (min) | Sandia Watershed, E121, E122, E123 | |
|------------|------------------------------|------------------------------------|---|
| | | Bottle Type | Analytical Suite |
| 1 | 10 | 1-L Poly | SSC, particle size |
| 2 | 11 | 1-L Poly | TAL ^a metals F ^b /UF ^c |
| 3 | 12 | 1-L Poly | Iso Pu |
| 4 | 13 | 1-L Glass | PCB |
| 5 | 14 | 1-L Glass | PCB |
| 6 | 15 | 1-L Poly | SSC |
| 7 | 16 | 1-L Poly | Extra |
| 8 | 17 | 1-L Glass | Extra |
| 9 | 18 | 1-L Glass | Extra |
| 10 | 19 | 1-L Poly | Extra |
| 11 | 20 | 1-L Poly | Extra |
| 12 | 21 | 1-L Glass | Extra |

^a TAL = Target analyte list.

^b F = Filtered.

^c UF = Unfiltered.

**Table 2.0-1
Precipitation at RG121.9 and Storm Water
Sampling at Gage Stations E121, E122, and E123**

| Discharge Date | RG121.9 Total Precipitation (in.) | E121 | E122 | E123 |
|----------------|-----------------------------------|---------------------|--------|--------|
| 07-Jul-12 | 0.16 | 2.2 NS ^a | 19 NS | 3 NS |
| 11-Jul-12 | 0.44 | 28 S ^b | 9.1 NS | 19 NS |
| 25-Jul-12 | 0.12 | 10 S | 3.5 NS | 4.8 NS |
| 10-Sep-12 | 0.27 | 14 S | 3.9 NS | 11 NS |
| 12-Oct-12 | 1.07 | 13 NS | 4.6 NS | 34 S |
| 14-Jun-13 | 0.44 | 10 NS | 3.2 NS | 16 NS |
| 30-Jun-13 | 0.4 | 21 S | 3.8 NS | 18 NS |
| 02-Jul-13 | 0.27 | 6 NS | 2.1 NS | 15 NS |
| 05-Jul-13 | 0.14 | 2.4 NS | 1.1 NS | 13 NS |
| 11-Jul-13 | 0.16 | 4.7 NS | 1.7 NS | 10 NS |
| 12-Jul-13 | 0.79 | 45 S | 3.6 NS | 36 NS |
| 13-Jul-13 | 0.24 | 4.2 NS | 1.3 NS | 11 NS |
| 14-Jul-13 | 0.22 | 13 NS | 2.6 NS | 13 NS |
| 25-Jul-13 | 0.29 | 4.8 NS | 1.6 NS | 12 NS |
| 26-Jul-13 | 0.19 | 4.9 NS | 1.5 NS | 15 NS |
| 05-Aug-13 | 0.35 | 6.6 NS | 2.1 NS | 16 NS |
| 18-Aug-13 | 0.2 | 5.5 NS | 2 NS | 16 NS |
| 20-Aug-13 | 0.14 | 13 NS | 2.1 NS | 15 NS |
| 30-Aug-13 | 0.12 | 3.9 NS | 1.6 NS | 14 NS |
| 10-Sep-13 | 1.35 | 9.4 NS | 2.3 NS | 15 NS |
| 12-Sep-13 | 2.31 | 20 S | 4.6 S | 48 NS |
| 13-Sep-13 | 2.35 | 68 NS | 18 NS | 110 NS |
| 18-Sep-13 | 0.74 | 4.5 NS | 3.2 NS | 19 NS |
| 23-May-14 | 0.36 | 13 NS | 5.8 NS | 18 NS |

^a NS = Sample not collected.

^b S = Sample collected.

**Table 2.0-2
Types, Locations, and Period of Record for Data Used in This Report**

| Data Type | Date | Piezometers | | | | | | | | | | | | Outfalls | | | Gaging Stations – Storm Water | | | Gaging Stations – Base Flow | | | Alluvial Wells | | | | | | | | | |
|----------------------|---|-------------|-----------|-----------|-----------|-----------|-----------|----------------|-----------|-----------|-----------|------------|------------|------------|---|--------------------------------------|-------------------------------|----------------------------|-----------------------------|-----------------------------|--|-------------------------------------|------------------------------------|---------------------|----------------|-------------|-----|-----|-----|-----|------------------|---|
| | | SCPZ-1 | SCPZ-2 | SCPZ-3 | SCPZ-4 | SCPZ-5 | SCPZ-6 | SCPZ-7 | SCPZ-8 | SCPZ-9 | SCPZ-10 | SCPZ-11(A) | SCPZ-11(B) | SCPZ-12 | 001 | 03A027 | 03A199 | E121 | E122 | E123 | E121 | E122 | E123 | SCA-1 | SCA-1-DP | | | | | | | |
| Water levels | Nov12 | MM, Trans | MM, Trans | MM, Trans | MM, Trans | MM, Trans | MM, Trans | — ^a | MM, Trans | MM, Trans | — | — | — | — | n/a ^b | n/a | n/a | n/a | n/a | n/a | n/a | n/a | n/a | n/a | X ^c | — | | | | | | |
| | Mar13 | MM, Trans | MM, Trans | MM, Trans | MM, Trans | MM, Trans | MM, Trans | — | MM, Trans | MM, Trans | silted in | silted in | silted in | silted in | n/a | n/a | n/a | n/a | n/a | n/a | n/a | n/a | n/a | n/a | x | — | | | | | | |
| | Jul13 | MM, Trans | MM, Trans | MM, Trans | MM, Trans | MM, Trans | MM, Trans | — | MM, Trans | MM, Trans | buried | DRY-gcsp | DRY-gcsp | DRY-gcsp | n/a | n/a | n/a | n/a | n/a | n/a | n/a | n/a | n/a | n/a | — | — | | | | | | |
| | Nov13 | MM, Trans | MM, Trans | MM, Trans | MM, Trans | MM, Trans | MM, Trans | — | MM, Trans | MM, Trans | buried | DRY-gcsp | DRY-gcsp | DRY-gcsp | n/a | n/a | n/a | n/a | n/a | n/a | n/a | n/a | n/a | n/a | — | — | | | | | | |
| | Mar14 | R | R | R | R | R | R | R | R | R | R | R | R | R | n/a | n/a | n/a | n/a | n/a | n/a | n/a | n/a | n/a | n/a | — | — | | | | | | |
| Notes | MM = manual measurement; Trans = transducer (hourly); R = requested; water level data starts in Jul12; SCPZ-7, -10, -11(A), -11(B), -12 no transducers installed (silt) | | | | | | | | | | | | | | n/a | n/a | n/a | n/a | n/a | n/a | n/a | n/a | n/a | n/a | n/a | n/a | n/a | n/a | n/a | n/a | from Oct06-May13 | manual for 2009 (4), 2010 (7), 2011 (2) |
| Field parameter data | Nov12 | NR | NR | NR | NR | NR | NR | NR | NR | NR | NR | NR | NR | DRY-P | pH, Temp | pH | pH | — | — | — | — | — | — | — | — | — | | | | | | |
| | Mar13 | S | S | S | S | S‡ | S | silted in | S | S‡ | silted in | silted in | silted in | silted in | pH, Temp | pH | pH | — | — | — | — | — | — | — | — | | | | | | | |
| | Jul13 | S | S | S | MM, S | MM, S‡ | MM, S | MM | MM, S | MM, S‡ | buried | DRY-gcsp | DRY-gcsp | DRY-gcsp | pH, Temp | pH | pH | — | — | — | x | x | x | — | — | | | | | | | |
| | Nov13 | MM, S | MM, S | MM, S | MM, S | MM | DRY | MM | MM, S | MM | buried | DRY-gcsp | DRY-gcsp | DRY-gcsp | pH, Temp | pH | pH | — | — | — | x | x | x | — | — | | | | | | | |
| | Mar14 | MM | MM | MM | MM | MM | DRY | DRY-P | NR | NR | DRY-P | DRY-P | MM | DRY-P | pH, Temp | pH | pH | — | — | — | — | — | — | — | — | | | | | | | |
| Notes | NR = not recorded; MM = manual measurement; S = Sonde data (hrly) incl. Temp. and Cond. ‡ = SCPZ-5, -9 sonde data lost in Sept flood, data recovery being attempted by sonde manufacturer; DRY-gcsp=Dry, downstream from GCS pond; SCPZ-10 was accidentally buried during construction of the GCS | | | | | | | | | | | | | | wkly from Oct11 | wkly from Jan12 | | | — | — | — | from Nov08, no 2012 | pH only Apr06-Jan08 | from Feb08, no 2012 | Oct06-Aug09 | Feb09-May11 | | | | | | |
| Analytical data | Nov12 | x | x | x | x | x | x | DRY-P | x | DRY-P | — | — | — | DRY-P | x | x | x | — | — | — | — | — | — | — | — | | | | | | | |
| | Mar13 | x | x | x | x | x | x | silted in | DRY-P | DRY-P | silted in | silted in | silted in | silted in | x | x | x | — | — | — | Apr13, May13 | — | Apr13, May13 | — | — | | | | | | | |
| | Jul13 | x | x | x | x | x | x | silted in | x | DRY | buried | DRY - gcsp | DRY - gcsp | DRY - gcsp | x | x | x | Jun13, Jul13, Sept13 | Sept13 | — | Jul13, Aug13 | — | Jul13, Aug13 | — | — | | | | | | | |
| | Nov13 | x | x | x | x | x | DRY | x | x | DRY-P | buried | DRY - gcsp | DRY - gcsp | DRY - gcsp | x | x | x | — | — | — | Dec13 | — | Dec13 | — | — | | | | | | | |
| | Mar14 | x | x | x | x | x | DRY | DRY-P | x | x | DRY-P | DRY-P | x | DRY-P | x | x | x | — | — | — | x | x | x | — | — | | | | | | | |
| Notes | DRY-P = dry, prioritized suite collected; DRY-gcsp = Dry, downstream from GCS pond; SCPZ-10 accidentally buried during GCS construction | | | | | | | | | | | | | | Al, TSS, NH3, Cl, NO2+NO3, TDS, TKN | PO4, TSS, NH3, Cl, NO3+NO2, TDS, TKN | PO4, TSS | Jul04-Jul07, Jul12-present | Jul00-Oct09, Sept13-present | Aug01-Oct12 | 2003–11; no 2012, 2013(5), Mar2014 | 2006–11, no 2012, 2013(3), Mar 2014 | 2002–11, no 2012, 2013(5), Mar2014 | Oct06-Aug09 | Aug09-May11 | | | | | | | |
| Flow data | Nov12 | n/a | n/a | n/a | n/a | n/a | n/a | n/a | n/a | n/a | n/a | n/a | n/a | n/a | x | x | x | — | — | — | x | x | x | n/a | n/a | | | | | | | |
| | Mar13 | n/a | n/a | n/a | n/a | n/a | n/a | n/a | n/a | n/a | n/a | n/a | n/a | n/a | x | x | x | — | — | — | x | x | x | n/a | n/a | | | | | | | |
| | Jul13 | n/a | n/a | n/a | n/a | n/a | n/a | n/a | n/a | n/a | n/a | n/a | n/a | n/a | x | x | x | Jun-Jul13, Sept13 | Sept13 | — | x | x | x | n/a | n/a | | | | | | | |
| | Nov13 | n/a | n/a | n/a | n/a | n/a | n/a | n/a | n/a | n/a | n/a | n/a | n/a | n/a | x | x | x | — | — | — | x | x | x | n/a | n/a | | | | | | | |
| | Mar14 | n/a | n/a | n/a | n/a | n/a | n/a | n/a | n/a | n/a | n/a | n/a | n/a | n/a | x | x | x | — | — | — | x | x | x | n/a | n/a | | | | | | | |
| Notes | — | | | | | | | | | | | | | | Daily total million gal./day from Dec11 | | | — | — | — | cfs evry 5 min.; Daily tot. in acre-ft. E121 and E122 from Oct06; E123 from Aug99; no data 2010; | | | — | — | | | | | | | |

^a — = No data available.

^b n/a = Not applicable.

^c x = Data available.

**Table 3.1-1
NMWQCC Surface Water Standards**

| Analytical Suite ^a | Analyte Code | Analyte Name | Field Prep | Acute Aquatic ^b | Human Health Persistent | Livestock Watering | Wildlife Habitat |
|-------------------------------|------------------|---------------------------|-----------------|----------------------------|-------------------------|--------------------|------------------|
| DIOX/FUR | n/a ^c | Dioxin (TEQ) | UF ^d | n/a | 0.000000051 | n/a | n/a |
| METALS | Al | Aluminum | F ^e | 658 | n/a | n/a | n/a |
| METALS | Sb | Antimony | F | n/a | 640 | n/a | n/a |
| METALS | As | Arsenic | F | 340 | 9 | 200 | n/a |
| METALS | B | Boron | F | n/a | n/a | 5000 | n/a |
| METALS | Cd | Cadmium | F | 0.59 | n/a | 50 | n/a |
| METALS | Cr | Chromium | F | n/a | n/a | 1000 | n/a |
| METALS | Cr(III) | Chromium(III) | F | 213 | n/a | n/a | n/a |
| METALS | Co | Cobalt | F | n/a | n/a | 1000 | n/a |
| METALS | Cu | Copper | F | 4.3 | n/a | 500 | n/a |
| METALS | Pb | Lead | F | 17 | n/a | 100 | n/a |
| METALS | Mn | Manganese | F | 2000 | n/a | n/a | n/a |
| METALS | Hg | Mercury | F | 1.4 | n/a | n/a | n/a |
| METALS | Hg | Mercury | UF | n/a | n/a | 10 | 0.77 |
| METALS | Ni | Nickel | F | 170 | 4600 | n/a | n/a |
| METALS | Se | Selenium | F | n/a | 4200 | 50 | n/a |
| METALS | Se | Selenium | UF | 20 | n/a | n/a | 5 |
| METALS | Ag | Silver | F | 0.41 | n/a | n/a | n/a |
| METALS | Tl | Thallium | F | n/a | 0.47 | n/a | n/a |
| METALS | V | Vanadium | F | n/a | n/a | 100 | n/a |
| METALS | Zn | Zinc | F | 54 | 26,000 | 25,000 | n/a |
| WET_CHEM | CN(TOTAL) | Cyanide (Total) | UF | 22 | 140 | n/a | 5.2 |
| PCB_CONG | 1336-36-3 | Total PCB | UF | n/a | 0.00064 | n/a | 0.014 |
| RAD | GROSSA | Gross alpha | UF | n/a | n/a | 15 | n/a |
| RAD | Ra-226+228 | Radium-226 and Radium-228 | UF | n/a | n/a | 30 | n/a |

^a All units are µg/L except for RAD, which are pCi/L.

^b Hardness-dependent values are calculated using a water hardness value of 30 mg CaCO₃/L.

^c n/a = Not applicable.

^d UF= Unfiltered.

^e F = Filtered.

**Table 3.1-2
Maximum Detected Results by Station and Event above Comparison Values in Sandia Storm Water Samples Since 1999**

| Station | Collection Date | Total PCBs | Aluminum | Arsenic | Cadmium | Cyanide (Total) | Cobalt | Chromium | Copper | Gross Alpha | Mercury | Nickel | Lead | Radium-226 | Radium-228 | Antimony | Selenium | Thallium | Vanadium | Zinc |
|-------------------------------------|-----------------|-----------------------|----------------------|----------|------------|-----------------|-------------|------------|------------|-------------|----------------|------------|-----------|------------|------------|------------|-----------|------------|------------|-----------|
| Comparison Value^a | | 0.00064 | 658 | 9 | 0.6 | 5.2 | 1000 | 210 | 4.3 | 15 | 0.77 | 170 | 17 | 30 | 30 | 640 | 5 | 6.3 | 100 | 54 |
| Field Preparation | | UF^b | F^c | F | F | UF | F | F | F | UF | UF | F | F | UF | UF | F | UF | F | F | F |
| E121 | 5/28/1999 | NA ^d | NA | NA | NA | NA | NA | NA | NA | NA | — ^e | NA | NA | NA | NA | NA | 60 | NA | NA | NA |
| E121 | 6/21/1999 | NA | NA | NA | NA | NA | NA | NA | NA | NA | NA | NA | NA | NA | NA | NA | 50 | NA | NA | NA |
| E121 | 6/21/2002 | NA | NA | NA | NA | 37.2 | NA | NA | NA | NA | NA | NA | NA | NA | NA | NA | — | NA | NA | NA |
| E121 | 7/4/2002 | NA | NA | NA | NA | 6.83 | NA | NA | NA | NA | NA | NA | NA | NA | NA | NA | — | NA | NA | NA |
| E121 | 7/23/2002 | NA | — | NA | NA | NA | NA | — | — | NA | — | NA | — | NA | NA | NA | NA | NA | — | — |
| E121 | 5/24/2003 | NA | NA | NA | NA | NA | NA | NA | NA | NA | 0.883 | NA | NA | NA | NA | NA | — | NA | NA | NA |
| E121 | 7/27/2004 | NA | — | NA | NA | — | NA | — | — | — | — | NA | — | NA | NA | NA | NA | NA | — | — |
| E121 | 8/11/2004 | NA | — | NA | — | NA | NA | — | 9.3 | NA | NA | NA | — | NA | NA | NA | NA | — | — | — |
| E121 | 8/18/2004 | NA | — | — | NA | NA | — | — | 4.9 | 24.7 | — | NA | — | NA | NA | NA | — | NA | NA | — |
| E121 | 9/27/2004 | NA | 5590 | NA | NA | — | — | — | 10.2 | 32 | — | NA | NA | NA | NA | NA | NA | — | NA | — |
| E121 | 4/16/2005 | NA | — | NA | NA | NA | NA | — | 7.1 | 19.3 | — | — | — | NA | NA | — | NA | NA | — | — |
| E121 | 7/15/2005 | NA | — | NA | NA | NA | NA | — | 5.6 | 26.6 | — | — | — | NA | NA | — | NA | NA | — | — |
| E121 | 7/20/2005 | NA | — | NA | NA | NA | NA | — | 9 | — | — | — | NA | NA | NA | NA | NA | NA | — | — |
| E121 | 8/4/2005 | NA | — | NA | NA | NA | NA | — | 6 | NA | — | — | NA | NA | NA | — | NA | NA | — | — |
| E121 | 8/12/2005 | NA | — | NA | NA | NA | NA | — | NA | 17.3 | NA | NA | NA | NA | NA | NA | NA | NA | — | — |
| E121 | 6/22/2006 | NA | — | NA | NA | NA | NA | — | 10.8 | 26.5 | NA | NA | — | NA | NA | NA | NA | NA | — | — |
| E121 | 7/3/2006 | NA | — | NA | NA | NA | NA | — | — | 30.1 | — | NA | NA | — | NA | NA | NA | NA | — | — |
| E121 | 7/6/2006 | NA | — | NA | NA | NA | NA | — | — | NA | NA | NA | NA | NA | NA | NA | NA | NA | — | — |
| E121 | 5/13/2007 | NA | — | NA | NA | NA | — | — | 5.8 | NA | — | NA | — | NA | NA | — | NA | NA | — | — |
| E121 | 6/16/2007 | NA | — | NA | NA | 8.4 | NA | NA | 6.4 | 45.1 | — | — | — | NA | NA | NA | NA | NA | — | — |
| E121 | 7/14/2007 | NA | — | NA | NA | NA | NA | — | 5.1 | 16.9 | — | — | — | NA | NA | NA | NA | NA | NA | NA |
| E121 | 7/30/2007 | NA | — | NA | NA | NA | NA | — | 5.6 | — | — | — | NA | NA | NA | NA | NA | NA | NA | — |
| E121 | 8/29/2007 | NA | NA | NA | NA | NA | NA | NA | NA | — | NA | NA | NA | — | NA | NA | NA | NA | NA | NA |
| E121 | 7/11/2012 | 0.259 | — | NA | NA | NA | — | — | 20.4 | NA | — | — | — | NA | NA | — | NA | NA | — | 259 |
| E121 | 7/25/2012 | 0.148 | — | NA | NA | NA | — | — | 6.63 | NA | — | — | NA | NA | NA | NA | NA | NA | — | — |
| E121 | 9/10/2012 | 0.129 | — | NA | NA | NA | — | NA | 6.86 | NA | — | — | NA | NA | NA | NA | NA | NA | — | — |
| E121 | 9/28/2012 | 0.112 | — | NA | NA | NA | NA | — | 5.57 | NA | — | — | NA | NA | NA | NA | NA | NA | — | — |
| E121 | 6/30/2013 | 0.142 | — | NA | NA | NA | — | NA | 6.48 | NA | — | — | — | NA | NA | NA | NA | NA | — | — |
| E121 | 7/12/2013 | 0.217 | — | NA | NA | NA | — | — | — | NA | 1.17 | — | — | NA | NA | NA | NA | NA | — | — |
| E121 | 9/12/2013 | 0.093 | — | NA | NA | NA | NA | — | — | NA | — | — | — | NA | NA | NA | NA | NA | — | — |
| E121 | 4/3/2014 | NA | — | — | NA | NA | NA | — | — | NA | NA | NA | NA | NA | NA | NA | — | NA | — | — |
| E122 | 5/28/1999 | NA | NA | NA | NA | NA | NA | NA | NA | NA | 1.3 | NA | NA | NA | NA | NA | NA | NA | NA | NA |
| E122 | 7/17/2000 | NA | NA | NA | NA | NA | NA | NA | NA | — | — | NA | NA | NA | NA | NA | NA | NA | NA | NA |
| E122 | 10/11/2000 | NA | — | NA | NA | NA | NA | NA | 7.92 | — | NA | NA | — | — | — | — | NA | — | — | 60.2 |
| E122 | 8/20/2002 | NA | NA | NA | NA | — | NA | NA | NA | NA | — | NA | NA | NA | NA | NA | NA | NA | NA | NA |

Table 3.1-2 (continued)

| Station | Collection Date | Total PCBs | Aluminum | Arsenic | Cadmium | Cyanide (Total) | Cobalt | Chromium | Copper | Gross Alpha | Mercury | Nickel | Lead | Radium-226 | Radium-228 | Antimony | Selenium | Thallium | Vanadium | Zinc |
|-------------------------------------|-----------------|-----------------------|----------------------|----------|------------|-----------------|-------------|------------|------------|-------------|-------------|------------|-----------|------------|------------|------------|-----------|------------|------------|-----------|
| Comparison Value^a | | 0.00064 | 658 | 9 | 0.6 | 5.2 | 1000 | 210 | 4.3 | 15 | 0.77 | 170 | 17 | 30 | 30 | 640 | 5 | 6.3 | 100 | 54 |
| Field Preparation | | UF^b | F^c | F | F | UF | F | F | F | UF | UF | F | F | UF | UF | F | UF | F | F | F |
| E122 | 8/28/2002 | NA | NA | NA | — | — | NA | — | 14.1 | — | NA | NA | — | NA | NA | — | NA | NA | — | 107 |
| E122 | 9/4/2002 | NA | NA | NA | — | — | NA | — | 13.2 | — | NA | NA | — | NA | — | NA | NA | — | — | 92.9 |
| E122 | 9/7/2002 | NA | NA | NA | — | NA | NA | NA | 12.3 | NA | NA | NA | — | NA | NA | — | NA | NA | — | 86.3 |
| E122 | 9/10/2002 | NA | NA | NA | NA | NA | NA | NA | NA | — | — | NA | NA | NA | — | NA | NA | NA | NA | NA |
| E122 | 10/1/2002 | NA | NA | NA | NA | — | NA | NA | NA | NA | NA | NA | NA | NA | NA | NA | NA | NA | NA | NA |
| E122 | 10/22/2002 | NA | NA | NA | — | NA | — | NA | 7.53 | NA | — | NA | — | NA | NA | — | NA | NA | — | 52.4 |
| E122 | 2/25/2004 | NA | NA | NA | NA | 15.3 | NA | NA | NA | NA | NA | NA | NA | NA | NA | NA | NA | NA | NA | NA |
| E122 | 4/6/2004 | NA | NA | NA | NA | NA | NA | NA | NA | NA | — | NA | NA | NA | NA | NA | NA | NA | NA | NA |
| E122 | 4/11/2004 | NA | — | NA | NA | NA | NA | NA | — | NA | NA | NA | — | NA | NA | NA | NA | — | NA | — |
| E122 | 7/27/2004 | NA | — | NA | NA | NA | NA | NA | — | NA | — | NA | — | NA | NA | NA | NA | NA | — | NA |
| E122 | 8/11/2004 | NA | — | NA | — | NA | NA | NA | 12.6 | NA | NA | NA | — | NA | NA | NA | NA | NA | — | 43.4 |
| E122 | 8/18/2004 | NA | 4080 | — | 1.9 | — | — | — | 86.7 | NA | — | — | 145 | NA | NA | — | NA | — | — | 1100 |
| E122 | 4/5/2006 | NA | — | — | NA | 11.1 | NA | — | 10.5 | NA | — | NA | — | NA | NA | NA | NA | NA | — | — |
| E122 | 6/22/2006 | NA | — | NA | NA | — | NA | — | 15.7 | 32.2 | NA | NA | — | — | NA | NA | NA | NA | — | 62.9 |
| E122 | 6/28/2006 | NA | — | NA | NA | — | NA | — | 9.9 | NA | NA | NA | NA | NA | NA | NA | NA | — | — | 52.4 |
| E122 | 7/2/2006 | NA | — | NA | NA | — | NA | — | 10.5 | NA | NA | NA | NA | NA | NA | NA | NA | NA | — | 50.7 |
| E122 | 3/21/2007 | NA | — | NA | NA | 30.2 | — | — | 13.9 | 18.6 | NA | — | — | NA | NA | NA | NA | NA | — | 285 |
| E122 | 4/9/2007 | NA | — | NA | NA | — | NA | — | NA | — | NA | — | — | NA | NA | NA | NA | NA | — | — |
| E122 | 5/1/2007 | NA | NA | NA | NA | NA | NA | NA | 10.5 | NA | — | — | NA | NA | NA | — | NA | NA | NA | — |
| E122 | 5/8/2007 | NA | — | NA | NA | NA | — | — | 8.6 | — | NA | — | NA | NA | NA | NA | NA | NA | — | — |
| E122 | 11/30/2007 | NA | NA | NA | NA | NA | NA | NA | NA | — | NA | NA | NA | NA | NA | NA | NA | NA | NA | NA |
| E122 | 6/3/2009 | NA | NA | NA | NA | NA | NA | NA | NA | 18.9 | NA | NA | NA | NA | NA | NA | NA | NA | NA | NA |
| E122 | 9/12/2013 | 0.406 | 795 | NA | NA | NA | NA | NA | — | NA | — | — | — | NA | NA | NA | — | NA | — | — |
| E123 | 8/10/1999 | NA | NA | NA | NA | NA | NA | NA | NA | NA | 1.1 | NA | NA | NA | NA | NA | NA | NA | NA | NA |
| E123 | 8/5/2001 | NA | 832 | NA | NA | NA | NA | — | 5.64 | — | NA | — | — | — | — | — | NA | NA | — | 42.2 |
| E123 | 7/4/2002 | NA | NA | NA | — | NA | NA | NA | NA | NA | NA | NA | — | NA | NA | NA | — | — | NA | NA |
| E123 | 7/14/2002 | NA | NA | NA | NA | 5.88 | NA | NA | NA | NA | NA | NA | NA | NA | NA | NA | NA | NA | NA | NA |
| E123 | 7/22/2002 | NA | — | — | NA | — | NA | — | 7.97 | NA | NA | NA | — | NA | NA | — | — | — | — | — |
| E123 | 8/7/2002 | NA | — | NA | NA | — | NA | — | NA | NA | — | NA | — | NA | NA | NA | NA | NA | NA | — |
| E123 | 7/26/2003 | NA | NA | NA | NA | 5.42 | — | — | 10.3 | NA | 1.18 | NA | — | NA | NA | — | NA | NA | — | 86.4 |
| E123 | 8/7/2003 | NA | NA | NA | NA | 6.89 | NA | — | 5.66 | NA | 0.932 | NA | — | NA | NA | NA | NA | — | — | — |
| E123 | 8/23/2003 | NA | — | — | NA | — | NA | — | 6.9 | 28.5 | 0.954 | NA | — | — | — | — | NA | NA | — | 52.9 |
| E123 | 8/29/2003 | NA | — | — | NA | — | NA | — | 5.37 | NA | 0.972 | NA | — | NA | NA | NA | NA | NA | — | — |
| E123 | 9/3/2003 | NA | NA | NA | NA | NA | NA | NA | NA | 43.3 | NA | NA | NA | — | — | — | NA | NA | NA | NA |
| E123 | 7/21/2004 | NA | — | NA | NA | NA | — | — | 4.72 | NA | — | NA | — | NA | NA | NA | NA | — | — | 48.4 |
| E123 | 7/23/2004 | NA | — | NA | NA | NA | NA | NA | 9.64 | NA | 0.921 | NA | — | NA | NA | NA | NA | NA | — | 49.6 |
| E123 | 7/27/2004 | NA | — | NA | NA | NA | — | — | 4.7 | NA | — | NA | — | NA | NA | NA | NA | NA | — | — |

Table 3.1-2 (continued)

| Station | Collection Date | Total PCBs | Aluminum | Arsenic | Cadmium | Cyanide (Total) | Cobalt | Chromium | Copper | Gross Alpha | Mercury | Nickel | Lead | Radium-226 | Radium-228 | Antimony | Selenium | Thallium | Vanadium | Zinc |
|-------------------------------------|-----------------|-----------------------|----------------------|----------|------------|-----------------|-------------|------------|------------|-------------|-------------|------------|-----------|------------|------------|------------|-----------|------------|------------|-----------|
| Comparison Value^a | | 0.00064 | 658 | 9 | 0.6 | 5.2 | 1000 | 210 | 4.3 | 15 | 0.77 | 170 | 17 | 30 | 30 | 640 | 5 | 6.3 | 100 | 54 |
| Field Preparation | | UF^b | F^c | F | F | UF | F | F | F | UF | UF | F | F | UF | UF | F | UF | F | F | F |
| E123 | 8/11/2004 | NA | — | NA | NA | NA | NA | — | 8.4 | NA | 0.87 | NA | — | NA | NA | NA | NA | NA | — | — |
| E123 | 4/24/2005 | NA | — | NA | NA | NA | NA | — | 5.9 | NA | NA | — | — | NA | NA | — | NA | NA | — | 108 |
| E123 | 5/1/2005 | NA | — | NA | NA | NA | — | — | NA | NA | NA | — | — | NA | NA | NA | NA | NA | — | 42.5 |
| E123 | 5/3/2005 | NA | — | NA | NA | NA | NA | — | NA | NA | NA | — | — | NA | NA | NA | — | NA | — | — |
| E123 | 7/15/2005 | NA | 871 | NA | NA | NA | — | — | 5.4 | NA | 0.93 | — | — | NA | NA | NA | NA | NA | — | — |
| E123 | 7/20/2005 | NA | NA | NA | NA | NA | NA | NA | NA | NA | — | NA | NA | NA | NA | NA | NA | NA | NA | NA |
| E123 | 6/22/2006 | NA | NA | NA | NA | NA | NA | NA | NA | NA | — | NA | NA | NA | NA | NA | NA | NA | NA | NA |
| E123 | 6/25/2006 | NA | NA | NA | NA | NA | NA | — | 10 | NA | NA | NA | — | NA | NA | NA | NA | NA | — | 47 |
| E123 | 6/28/2006 | NA | — | NA | NA | — | NA | — | 11.5 | 29.8 | NA | NA | — | — | NA | NA | NA | NA | — | — |
| E123 | 7/3/2006 | NA | — | NA | NA | 12.4 | NA | — | 8 | NA | NA | NA | NA | NA | NA | NA | NA | NA | — | NA |
| E123 | 7/6/2006 | NA | NA | NA | NA | NA | NA | NA | NA | NA | — | NA | NA | NA | NA | NA | NA | NA | NA | NA |
| E123 | 7/8/2006 | NA | — | — | NA | NA | NA | — | 6.3 | NA | — | NA | — | NA | NA | NA | NA | NA | — | — |
| E123 | 10/9/2006 | NA | NA | NA | NA | NA | NA | NA | NA | NA | — | NA | NA | NA | NA | NA | NA | NA | NA | NA |
| E123 | 3/23/2007 | NA | — | NA | NA | 50.7 | — | — | 7.7 | 66.9 | 1.3 | — | — | NA | NA | NA | NA | NA | — | — |
| E123 | 4/13/2007 | NA | — | NA | NA | — | — | — | — | 36 | — | — | NA | NA | NA | NA | NA | NA | — | — |
| E123 | 5/2/2007 | NA | — | NA | NA | NA | — | — | — | 30.1 | 2.7 | — | — | NA | NA | NA | NA | NA | — | — |
| E123 | 5/8/2007 | NA | NA | NA | NA | 11.4 | NA | — | 6.2 | 35.5 | — | — | NA | NA | NA | — | NA | NA | — | — |
| E123 | 7/16/2008 | NA | — | NA | NA | — | — | — | 5.3 | 20.6 | NA | — | NA | NA | NA | NA | NA | NA | — | — |
| E123 | 7/27/2008 | NA | — | — | NA | 34.1 | NA | — | 5.6 | 21.3 | NA | — | NA | NA | NA | NA | — | NA | — | — |
| E123 | 8/4/2008 | NA | NA | — | NA | NA | NA | — | 4.8 | — | NA | — | — | NA | NA | NA | — | — | — | — |
| E123 | 8/7/2008 | NA | NA | NA | NA | NA | NA | NA | NA | 32.8 | NA | NA | NA | NA | NA | NA | NA | NA | NA | NA |
| E123 | 8/12/2009 | NA | — | — | NA | NA | — | — | 5.7 | 17.7 | NA | — | NA | — | NA | — | NA | — | — | — |
| E123 | 8/23/2009 | NA | NA | — | NA | — | NA | — | 7.5 | — | NA | — | NA | — | — | NA | NA | NA | — | — |
| E123 | 8/30/2009 | NA | — | — | NA | NA | — | — | 4.7 | NA | NA | — | NA | NA | NA | NA | NA | NA | — | — |
| E123 | 9/6/2009 | NA | NA | NA | NA | NA | NA | NA | NA | — | NA | NA | NA | — | — | NA | NA | NA | NA | NA |
| E123 | 9/10/2009 | NA | — | NA | NA | — | — | — | 6.9 | — | NA | — | NA | — | — | NA | NA | NA | — | — |
| E123 | 10/7/2009 | NA | — | NA | NA | NA | — | — | 6.5 | NA | — | — | NA | — | — | NA | NA | NA | — | — |
| E123 | 10/2/2010 | 0.797 | — | NA | NA | NA | — | NA | 6.2 | 15.5 | NA | — | — | NA | NA | NA | NA | NA | — | — |
| E123 | 7/28/2011 | 0.464 | — | — | NA | NA | — | — | 13.9 | — | NA | — | — | NA | NA | NA | — | NA | — | — |
| E123 | 8/4/2011 | 0.903 | — | — | NA | NA | — | — | 17.5 | — | — | — | — | NA | NA | NA | NA | NA | — | — |
| E123 | 10/12/2012 | 0.431 | — | NA | NA | NA | NA | — | 4.89 | — | — | — | — | NA | NA | NA | NA | NA | — | — |
| E123 | 4/3/2014 | NA | — | — | NA | NA | NA | — | — | NA | NA | NA | NA | NA | NA | NA | — | NA | — | — |

Note: All units are µg/L, except gross alpha, radium-226, and radium-228, are in pCi/L.

^a Hardness-dependent comparison values based on 30 mg CaCO₃/L hardness.

^b UF = Unfiltered.

^c F = Filtered.

^d NA = Not analyzed.

^e — = Analyte was not detected above comparison value.

**Table 4.5-1
Efficacy of Locations for Monitoring Recent Hydrologic
and Geochemical Forcing Function and Associated Impacts**

| Hydrologic and Geochemical Forcing Function | Impact | Gage E123 | Gage E121 | Piezometers |
|---|---|--|-----------|--|
| Decreased outfall discharge | Dewatering and associated chemical transformations (e.g., oxidation) | Yes | Yes | Yes |
| Change in outfall chemistry | Scavenging waters Desorption/dissolution | Yes, but modified by wetland biogeochemical reactions and potential mixing with alluvial water | Yes | Yes, but modified by wetland subsurface biogeochemical reactions |
| Natural disturbance (e.g., flooding) | Alteration of Flow Changes in alluvial saturation Physical transport of contaminants | Yes | Yes | Yes |
| GCS Stabilization | Maintaining physical stability of lower portion of wetland Maintaining reducing conditions in lower portion of wetland | Yes | No | Yes, for eastern transects |

**Table 4.6-1
Modified Sample Analytes and Preservation Requirements for Sandia Wetland**

| Suite | Frequency | Filtered? | Preservation | Field Storage | Holding Time | Minimum Volume | Comment |
|---------------------------|-----------|-----------|-------------------------|---------------|------------------------------|------------------|--|
| EES Metals | Qtrly | Y | Nitric acid | <4°C | 6 mo | 125 mL | 3 subsamples filtered at 0.45, 0.2, and 0.02 µm |
| EES Anions | Qtrly | Y | None | <4°C | 1 mo; NO ₃ 2 d | 125 mL | —* |
| Alkalinity/pH | Qtrly | N | None | <4°C | ASAP | 125 mL | — |
| Ammonia | Qtrly | N | Sulfuric acid | <4°C | 1 mo | 125 mL | — |
| Sulfide | Qtrly | N | sulfide buffer pH 12 | <4°C | 24 h | 15 mL | — |
| DOC | Annually | Y | Sulfuric acid | <4°C | 1 mo | 40 mL | Collect during June sample event |
| δ ¹⁵ N Ammonia | Qtrly | Y | Sulfuric acid | <4°C | 6 mo if frozen | 100 mL for 1 ppm | Use polytetrafluoroethylene bottles if freezing. |
| ¹⁸ O/δD | Qtrly | N | None | <4°C | 1 yr | 10 mL | — |

*— = None.

Table 4.6-2
ISCO Bottle Configurations and Analytical Suites,
Calendar Year 2013 Storm Water Sampling Plan, and ISCO Analytical Suites and Bottle Sequence

| Configuration | Storm Sampling | | | Storm Sampling | |
|---------------|--|-------------------------|--|--|--|
| Program | Storm/Delay 0-1×4@1min/Delay 40-2×4@1min | | | Storm/Delay 0-6×1@5min/Delay 30-18×1@20min | |
| Bottle No. | Sample Collection Time (min) | Sandia E121, E122, E123 | | Sandia E121, E122, E123 | |
| | | Bottle Type | Analytical Suite | Sample Collection Time (min) | Analytical Suite 24 Bottle ISCO 1-L Poly Wedge |
| 1 | Max + 10 | 1-L Glass | PCB Congener (UF ^a) | Trigger + 0 | SSC |
| 2 | Max + 10 | 1-L Glass | PAH (UF) | Trigger + 5 | SSC |
| 3 | Max + 10 | 1-L Glass | SVOC (UF) | Trigger + 10 | SSC, Particle Size |
| 4 | Max + 10 | 1-L Poly | TAL ^b metals (F ^c /UF) | Trigger + 15 | SSC |
| 5 | Max + 50 | 1-L Glass | PCB Congener (UF) | Trigger + 20 | SSC |
| 6 | Max + 50 | 1-L Glass | PAH (UF) | Trigger + 25 | DOC+Cl+SO4+Alk+pH |
| 7 | Max + 50 | 1-L Glass | SVOC ^d (UF) | Trigger + 30 | SSC |
| 8 | Max + 50 | 1-L Poly | TAL metals (F/UF) | Trigger + 50 | SSC, Particle Size |
| 9 | Max + 90 | 1-L Glass | PCB Congener (UF) | Trigger + 70 | SSC |
| 10 | Max + 90 | 1-L Glass | PAH (UF) | Trigger + 90 | SSC, Particle Size |
| 11 | Max + 90 | 1-L Glass | SVOC (UF) | Trigger + 110 | SSC |
| 12 | Max + 90 | 1-L Poly | TAL metals (F/UF) | Trigger + 130 | SSC |
| 13 | — ^e | — | — | Trigger + 150 | SSC |
| 14 | — | — | — | Trigger + 170 | SSC |
| 15 | — | — | — | Trigger + 190 | SSC |
| 16 | — | — | — | Trigger + 210 | SSC |
| 17 | — | — | — | Trigger + 230 | SSC |
| 18 | — | — | — | Trigger + 250 | SSC |
| 19 | — | — | — | Trigger + 270 | SSC |
| 20 | — | — | — | Trigger + 290 | SSC |
| 21 | — | — | — | Trigger + 310 | SSC |
| 22 | — | — | — | Trigger + 330 | SSC |
| 23 | — | — | — | Trigger + 350 | SSC |
| 24 | — | — | — | Trigger + 370 | SSC |

Note: E121 = Sandia right fork at Pwr Plant, E122 = Sandia left fork at Asph Plant, E123 = Sandia below Wetlands.

^a UF = Unfiltered

^b TAL = Target analyte list.

^c F = Filtered.

^d SVOC = Semivolatile organic compound.

^e — = None.

Appendix A

*Acronyms and Abbreviations,
Metric Conversion Table, and Data Qualifier Definitions*

A-1.0 ACRONYMS AND ABBREVIATIONS

| | |
|--------|---|
| bgs | below ground surface |
| csf | cubic foot per second |
| DC | direct current |
| DOC | dissolved organic carbon |
| EES | Earth and Environmental Sciences |
| ENV | Environmental Protection (Laboratory division) |
| F | filtered |
| GCS | grade-control structure |
| gpd | gallons per day |
| gps | global positioning system |
| HFO | hydrous ferrous oxide |
| ID | identification |
| IR | investigation report |
| LANL | Los Alamos National Laboratory |
| LDCC | Laboratory Data Communications Center |
| NMED | New Mexico Environment Department |
| NMWQCC | New Mexico Water Quality Control Commission |
| NPDES | National Pollutant Discharge Elimination System |
| PAH | polycyclic aromatic hydrocarbon |
| PCB | polychlorinated biphenyl |
| RO | reverse osmosis |
| RPF | Records Processing Facility |
| SCC | Strategic Computing Complex |
| SERF | Sanitary Effluent Reclamation Facility |
| SOM | solid organic matter |
| SSC | suspended sediment concentration |
| SWWS | Sanitary Waste Water System |
| TA | technical area |
| TAL | target analyte list |
| TDS | total dissolved solids |
| TKN | total Kjeldahl nitrogen |
| TOC | total organic compound |

TSS total suspended sediments
 UF unfiltered
 VE vertical exaggeration

A-2.0 METRIC CONVERSION TABLE

| Multiply SI (Metric) Unit | by | To Obtain U.S. Customary Unit |
|---|-----------|---|
| kilometers (km) | 0.622 | miles (mi) |
| kilometers (km) | 3281 | feet (ft) |
| meters (m) | 3.281 | feet (ft) |
| meters (m) | 39.37 | inches (in.) |
| centimeters (cm) | 0.03281 | feet (ft) |
| centimeters (cm) | 0.394 | inches (in.) |
| millimeters (mm) | 0.0394 | inches (in.) |
| micrometers or microns (µm) | 0.0000394 | inches (in.) |
| square kilometers (km ²) | 0.3861 | square miles (mi ²) |
| hectares (ha) | 2.5 | acres |
| square meters (m ²) | 10.764 | square feet (ft ²) |
| cubic meters (m ³) | 35.31 | cubic feet (ft ³) |
| kilograms (kg) | 2.2046 | pounds (lb) |
| grams (g) | 0.0353 | ounces (oz) |
| grams per cubic centimeter (g/cm ³) | 62.422 | pounds per cubic foot (lb/ft ³) |
| milligrams per kilogram (mg/kg) | 1 | parts per million (ppm) |
| micrograms per gram (µg/g) | 1 | parts per million (ppm) |
| liters (L) | 0.26 | gallons (gal.) |
| milligrams per liter (mg/L) | 1 | parts per million (ppm) |
| degrees Celsius (°C) | 9/5 + 32 | degrees Fahrenheit (°F) |

A-3.0 DATA QUALIFIER DEFINITIONS

| Data Qualifier | Definition |
|----------------|--|
| U | The analyte was analyzed for but not detected. |
| J | The analyte was positively identified, and the associated numerical value is estimated to be more uncertain than would normally be expected for that analysis. |
| J+ | The analyte was positively identified, and the result is likely to be biased high. |
| J- | The analyte was positively identified, and the result is likely to be biased low. |
| UJ | The analyte was not positively identified in the sample, and the associated value is an estimate of the sample-specific detection or quantitation limit. |
| R | The data are rejected as a result of major problems with quality assurance/quality control (QA/QC) parameters. |

Appendix B

*Baseline Geomorphic Conditions
and Vegetation Monitoring in Sandia Canyon Reach S2*

CONTENTS

B-1.0 INTRODUCTION B-1

B-2.0 HYDROLOGIC EVENTS DURING 2013 MONSOON SEASON B-1

B-3.0 SURVEYS AT REACH S-2 IN SANDIA CANYON B-1

 B-3.1 Plunge Pool Area B-2

 B-3.2 Wetland Transitional Area B-2

 B-3.3 Alluvial Fan Depositional Area B-2

 B-3.4 Grade-Control Structure Area B-3

 B-3.5 Vegetation Monitoring Survey B-3

B-4.0 SUMMARY B-3

B-5.0 REFERENCES AND MAP DATA SOURCES B-4

 B-5.1 References B-4

 B-5.2 Map Data Sources B-4

Figures

Figure B-1.0-1 Orthophoto showing the locations of surveyed cross-sections and thalweg profiles at Reach S-2 in Sandia Canyon B-7

Figure B-1.0-2 Geomorphic map of Reach S-2 showing the locations of surveyed cross-sections and thalweg surveys at Sandia Canyon B-8

Figure B-3.0-1 Geomorphic map overlain on an orthophoto showing the locations of baseline photographs, surveyed cross-sections and thalweg surveys at the plunge pool area in Sandia Canyon Reach S-2 B-9

Figure B-3.0-2 Geomorphic map overlain on an orthophoto showing the locations of piezometers, baseline photographs, surveyed cross-sections and thalweg surveys at the wetland transition area in Sandia Canyon Reach S-2 B-10

Figure B-3.0-3 Geomorphic map overlain on an orthophoto showing the locations of piezometers, baseline photographs, surveyed cross-sections and thalweg surveys at the alluvial fan deposition area in Sandia Canyon Reach S-2 B-11

Figure B-3.0-4 Geomorphic map overlain on an orthophoto showing the locations of piezometers, baseline photographs, surveyed cross-sections and thalweg surveys at the GCS area in Sandia Canyon Reach S-2 B-12

Figure B-3.1-1 Cross-sections at the plunge pool area in Sandia Canyon B-13

Figure B-3.1-2 Plan view of the plunge pool area in Sandia Canyon B-14

Figure B-3.1-3 Thalweg profile in Sandia Canyon B-15

Figure B-3.2-1 Cross-sections at the wetland transitional area in Sandia Canyon B-16

Figure B-3.3-1 Cross-sections at the alluvial fan depositional area in Sandia Canyon B-17

Figure B-3.4-1 Cross-sections at the GCS area in Sandia Canyon B-18

Tables

Table B-2.0-1 Daily Total Precipitation and Peak Discharge for September 2013 Flood B-19

Table B-3.0-1 Baseline Photograph Survey Location Coordinates B-20

Attachments

- Attachment B-1 Baseline Photographs of Geomorphic Conditions in Sandia Canyon Reach S-2
- Attachment B-2 Baseline Photographs of the Vegetation Monitoring Survey
- Attachment B-3 Baseline Cross-Section Survey Data (on CD included with this document)

B-1.0 INTRODUCTION

This report presents geodetic survey data obtained in 2014 from above the grade-control structure (GCS) in Sandia Canyon Reach S-2 within the Los Alamos National Laboratory (LANL or the Laboratory). The survey data document the baseline geomorphic conditions in Reach S-2 prior to the 2014 monsoon season, as specified in the “Work Plan and Final Design for Stabilization of the Sandia Canyon Wetland” (LANL 2011, 207053) and in the modified version of this work plan was approved by NMED on April 3, 2013 (Cobrain 2013, 256726). These surveys will be repeated after the 2014 monsoon season and the results will be presented the 2015 Sandia wetland performance report. The 2015 report will include estimates of net sediment deposition in each area since the previous surveys and will evaluate if any unintended geomorphic changes have occurred, such as net sediment erosion. The “Work Plan and Final Design for Stabilization of the Sandia Canyon Wetland” (LANL 2011, 207053) also specified semiannual vegetation photo monitoring to occur every 2 yr beginning in 2012. To meet this requirement, a baseline vegetation photo survey was conducted on May 21, 2014, and these photos are included herein. Figures B-1.0-1 and B-1.0-2 shows the locations of sites discussed in this report. Attachment B-1 presents photographs of the baseline geomorphic conditions in Sandia Canyon Reach S-2. Attachment B-2 presents photographs of baseline vegetation monitoring surveys.

B-2.0 HYDROLOGIC EVENTS DURING 2013 MONSOON SEASON

Historically, stream gage E121 (upstream of the wetland) and stream gage E123 (downstream of the wetland and GCS) have experienced peak flows of approximately 140 cubic feet per second (cfs) and 88 cfs, respectively, during the period of record 1999 to 2010 (LANL 2011, 207053). During the week of September 9, 2013, a significant amount of rain fell in and around Los Alamos, with a peak discharge of 68 cfs at E121 and 110 cfs at E123 on September 13 (Table B-2.0-1). Heavy rainfall occurred on the 3 d before the peak discharge event (Table B-2.0-1).

B-3.0 SURVEYS AT REACH S-2 IN SANDIA CANYON

A total of 16 cross-sections were established and surveyed in February and March 2014 at varying intervals across the approximate 2100-ft length of Sandia Canyon Reach S-2, from the outlet of the plunge pool to just upstream of the Sandia Canyon GCS (Figures B-1.0-1 and B-1.0-2). The cross-sections are labeled as SGCS-16 through SGCS-1 from upstream to downstream. In the following discussion, the sections are grouped into the following areas: the plunge pool area, wetland transitional area, the alluvial fan depositional area, and the GCS area (Figures B-1.0-1 and B-1.0-2). Figures B-3.0-1 to B-3.0-4 show the piezometer and photograph locations discussed within this report at these cross-section areas (Table 3.0-1). A longitudinal channel thalweg profile was surveyed in two segments, one from the plunge pool to the western edge of the wetland and one in the eastern part of the wetland immediately upstream of the GCS where the thalweg is once again a defined feature (Figures B-1.0-1 and B-1.0-2). There was no defined thalweg through the central and western portions of the wetland area.

All cross-sections were monumented with rebar at each end and baseline surveys were conducted using a combination of a differentially corrected global positioning system (GPS) and a total station tied to GPS control points, depending on tree cover. The general locations of all survey areas are shown on an orthophotograph in Figure B-1.0-1 and are also shown on a geomorphic map in Figure B-1.0-2 (LANL 2009, 107453). The locations of piezometers and photographs are shown on an orthophotograph overlain with a geomorphic map in Figures 3.0-1 to 3.0-4. GPS coordinates of the photograph locations are presented in Table 3.0-1. Surveyed cross-sections are shown in figures with a vertical exaggeration (VE)

of 2.5 times, and channel thalweg profile is shown with a VE of 7.5 times. Raw survey data are included electronically as Attachment B-3 (on CD). The calculated distances along each cross-section and along each thalweg profile that are used for the figures in this report are also included in Attachment B-3. These calculations involved basic trigonometry (Pythagorean theorem).

B-3.1 Plunge Pool Area

Three cross-sections were surveyed directly downstream of the plunge pool in the western end of reach S-2. SGCS-16 was surveyed across the outlet at the eastern edge of the plunge pool and SGCS-15 and SGCS-14 are downstream at 20-ft intervals. A channel thalweg profile was surveyed over this interval, continuing downstream to cross section SGCS-12 in the wetland transitional area as described below. The perimeter of the plunge pool was also surveyed. Rebar monuments were established at various locations around the plunge pool to allow repeat measurements and evaluate changes in the plunge pool perimeter over time. Cross-section and thalweg-profile locations are shown in Figures B-1.0-1 and B-1.0-2. Cross-sections for the plunge pool area and a plan view of the plunge pool are shown in Figures B-3.1-1 and B-3.1-2. The thalweg profile is shown in Figure B-3.1-3. Baseline photographs of the plunge pool area are shown in Photos B1-1 and B1-2 in Attachment B-1. Photograph locations are presented in Figure B-3.0-1 and Table 3.0-1.

B-3.2 Wetland Transitional Area

Five cross-sections were surveyed in the wetland transitional area, located in the western third of S-2. This area is about 400 ft downstream of the plunge pool area, where the main stream channel begins to widen into the main wetland area. A channel thalweg profile was surveyed from the eastern edge of the plunge pool area to cross-section line SGCS-12. Below line SGCS-12 the thalweg is poorly defined (diffuse) or absent as a mappable feature as a result of spreading of flow within the active wetland. SGCS-13 is approximately 400 ft downstream of the plunge pool area cross-sections and is characterized as having a main active stream channel. Cross-section lines SGCS-12 through SGCS-9 are spaced sequentially at 100-ft intervals below SGCS-13. The five cross-sections document the uneven transition from channelized flow (upstream) to diffuse, nonchannelized flow in the wetland area. Cross-section and thalweg-profile locations are shown in Figures B-1.0-1 and B-1.0-2. Cross-sections for the wetland transitional area and the thalweg profile are shown in Figures B-3.2-1 and B-3.1-3, respectively. Baseline photographs of the wetland transition area are shown in Photos B1-3 to B1-5 in Attachment B-1. Photograph and piezometer locations are presented in Figure B-3.0-2 and Table 3.0-1.

B-3.3 Alluvial Fan Depositional Area

Two cross-sections were surveyed in the alluvial fan depositional area, approximately 300 ft downstream of the wetland transitional area in the central part of S-2. SGCS-8 and SGCS-7 share a northern endpoint. The intention of these cross-sections is to monitor active deposition on a prograding fan that enters the wetland from a south tributary drainage that flows into the primary wetland. The southern end of these two cross-sections are on the tributary fan deposits, with the northern end of each section extending across the main wetland, providing representative sections in the central portion of the primary wetland. Cross-section locations are shown in Figures B-1.0-2 and B-1.0-3. Cross-sections for the alluvial fan depositional area are shown in Figure B-3.3-1. Baseline photographs of the alluvial fan depositional area are shown in Photos B1-6 and B1-7 in Attachment B-1. Photograph and piezometer locations are presented in Figure B-3.0-3 and Table 3.0-1.

B-3.4 Grade-Control Structure Area

Six cross-sections were surveyed directly upstream of the grade-control structure. SGCS-1, SGCS-2, SGCS-3, SGCS-4, SGCS-5 and SGCS-6 are 20 ft, 45 ft, 70 ft, 105 ft, 165 ft, and 265 ft upstream of the grade-control structure, respectively. SGCS-6 is approximately 400 ft downstream of the alluvial fan depositional area. SGCS-4, SGCS-5 and SGCS-6 have established cattails in the wetland area and established willows on the northern edge of the wetland. SGCS-2 and SGCS-3 have established cattails in the wetland area, established willows on the northern edge, and planted willows on the southern edge. SGCS-1 has planted cattails and planted willows, with some established willows on the northern edge of the wetland. The purpose of the closely spaced cross sections above the GCS is to provide detailed monitoring of the area immediately upstream of the GCS, including the area where the head cut was located prior to construction of the GCS. Cross-section and thalweg-profile locations are shown in Figures B-1.0-2 and B-1.0-3. Cross-sections for the area upstream of the grade-control structure and the thalweg profile are shown in Figures B-3.4-1 and B-3.1-3, respectively. The piezometers in Figure B-3.4-1 are projected onto the section and hung on ground surface (Figure B-3.0-4). Baseline photographs of the grade control structure area are shown in Photos B1-8 through B1-10 in Attachment B-1. Photograph and piezometer locations are presented in Figure B-3.0-4 and Table B-3.0-1.

B-3.5 Vegetation Monitoring Survey

The density and composition of plant communities both within the wetland and along its margins provide another indicator of wetland extent and condition. Water-loving species such as cattails and willows that thrive when their roots are saturated delineate the heart of the wetland. Ponderosa pine, piñon pine and juniper require drier conditions and die if their roots remain saturated for extended periods. Ten photo locations (Table B-3.0-1; Figures B-3.0-1 to B-3.0-4 and Attachment B-2) were chosen to document specific areas of the wetland:

- At the newly planted GCS (plantings include rushes, sedges, cattails, and willows (LANL 2013, 251743),
- Along the margins of the wetland where dewatering or expansion is most likely to occur,
- At the head of the wetland where floods have the greatest impact, and
- Along the inset channel to the west of the active wetland where rapid expansion of cattails has occurred in the past.

B-4.0 SUMMARY

Baseline geomorphic conditions for the Sandia wetland investigation area were established following the installation of the Sandia Canyon GCS. The surveys will be repeated following the 2014 monsoon season. Photographic surveys of baseline geomorphic and vegetation conditions were established and repeat surveys will be conducted annually and semiannually, respectively.

B-5.0 REFERENCES AND MAP DATA SOURCES

B-5.1 References

The following list includes all documents cited in this report. Parenthetical information following each reference provides the author(s), publication date, and ER ID. This information is also included in text citations. ER IDs are assigned by the Environmental Programs Directorate's Records Processing Facility (RPF) and are used to locate the document at the RPF and, where applicable, in the master reference set.

Copies of the master reference set are maintained at the NMED Hazardous Waste Bureau and the Directorate. The set was developed to ensure that the administrative authority has all material needed to review this document, and it is updated with every document submitted to the administrative authority. Documents previously submitted to the administrative authority are not included.

Cobrain, D., April 3, 2013. FW: Sandia Wetland cross sections. E-mail message to D. Katzman (LANL) from D. Cobrain (NMED), Santa Fe, New Mexico. (Cobrain 2013, 256726)

LANL (Los Alamos National Laboratory), October 2009. "Investigation Report for Sandia Canyon," Los Alamos National Laboratory document LA-UR-09-6450, Los Alamos, New Mexico. (LANL 2009, 107453)

LANL (Los Alamos National Laboratory), September 2011. "Work Plan and Final Design for Stabilization of the Sandia Canyon Wetland," Los Alamos National Laboratory document LA-UR-11-5337, Los Alamos, New Mexico. (LANL 2011, 207053)

LANL (Los Alamos National Laboratory), December 2013. "Completion Report for Sandia Canyon Grade-Control Structure," Los Alamos National Laboratory document LA-UR-13-29285, Los Alamos, New Mexico. (LANL 2013, 251743)

B-5.2 Map Data Sources

The following list provides data sources for maps included in the main body of this report.

2000 LIDAR Hypsography; Los Alamos National Laboratory, Earth and Environmental Sciences GISLab; 1:1,200; Work in progress.

Drainage; Los Alamos National Laboratory, Environment and Remediation Support Services; 1:24,000; May 15, 2006.

Gaging stations; Los Alamos National Laboratory, Waste and Environmental Services Division; 1:2,500; March 19, 2011.

Grade control structures; Los Alamos National Laboratory, Environment and Remediation Support Services; Unknown; May 17, 2011.

LANL boundary; Los Alamos National Laboratory, KSL Site Support Services, Planning, Locating and Mapping Section; Unknown; August 16, 2010.

LANL area orthophoto; Los Alamos National Laboratory, Earth and Environmental Sciences GISLab; 1"=200'; April 22-30, 2011.

Location IDs; Los Alamos National Laboratory, ESH&Q Waste and Environmental Services Division; 1:2,500; May 19, 2011.

Other property boundary; Los Alamos National Laboratory, Earth and Environmental Sciences GISLab; Unknown; August 16, 2010.

Roads, surfaced; Los Alamos National Laboratory, KSL Site Support Services, Planning, Locating and Mapping Section; Unknown; November 30, 2010.

Technical area boundary; Los Alamos National Laboratory, Site Planning and Project Initiation Group, Infrastructure Planning Office; Unknown; August 16, 2010.

Watershed; Los Alamos National Laboratory, Environment and Remediation Support Services; 1:2,500; November 2, 2006.

Wells; Los Alamos National Laboratory, ESH&Q Waste and Environmental Services Division; 1:2,500; May 19, 2011.



Figure B-1.0-1 Orthophoto showing the locations of surveyed cross-sections and thalweg profiles at Reach S-2 in Sandia Canyon

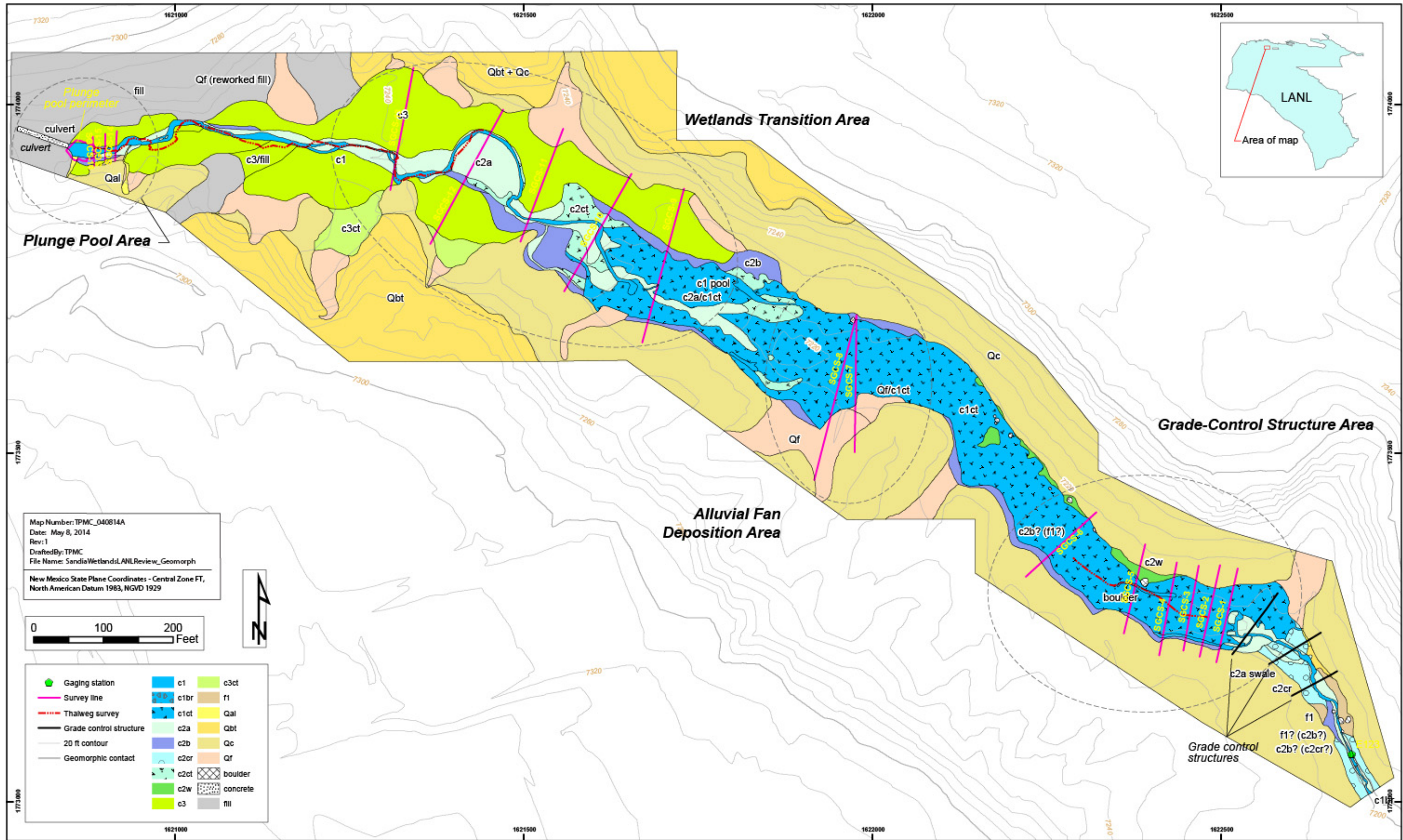


Figure B-1.0-2 Geomorphologic map of Reach S-2 showing the locations of surveyed cross-sections and thalweg surveys at Sandia Canyon

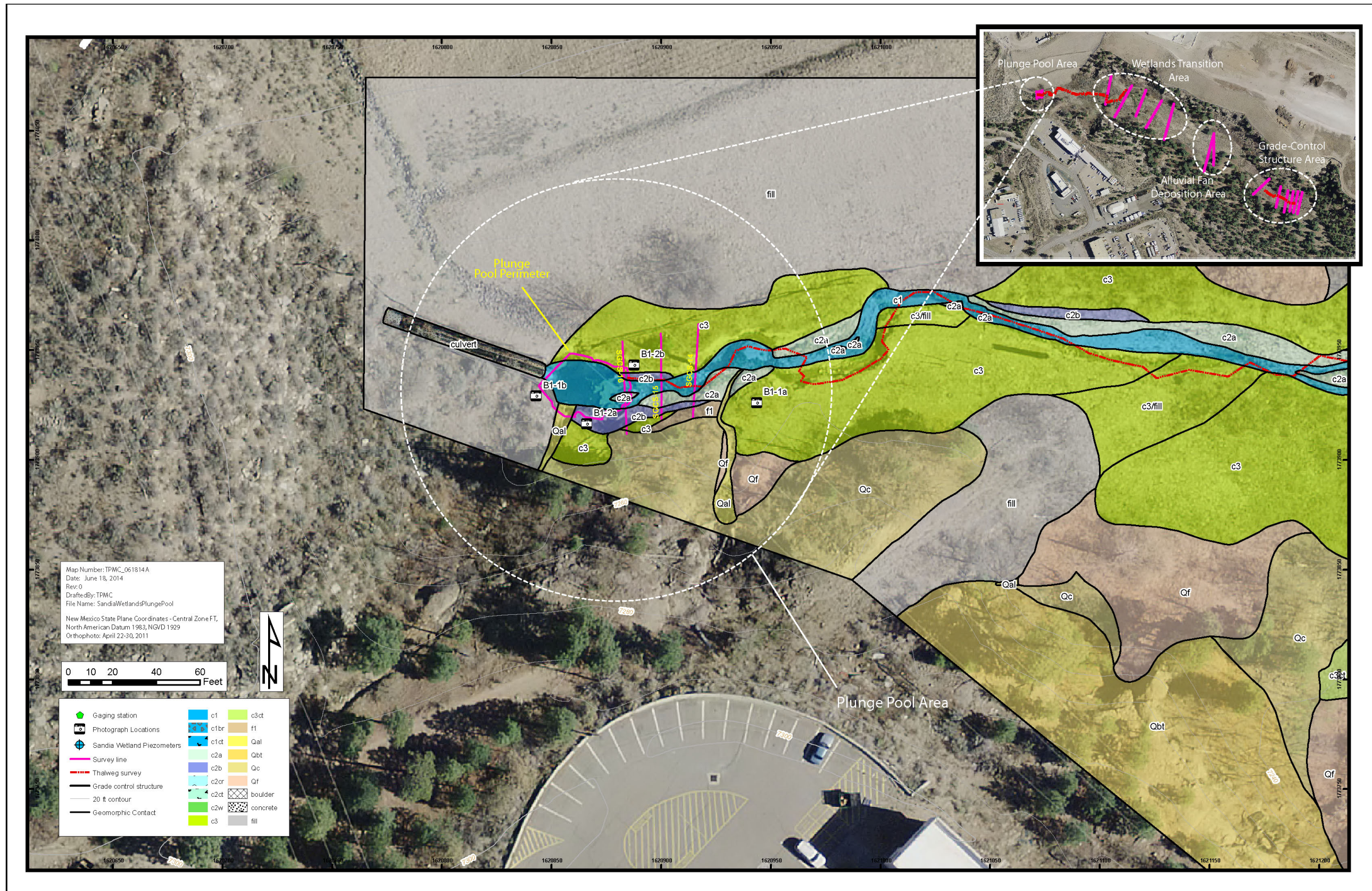


Figure B-3.0-1 Geomorphic map overlain on an orthophoto showing the locations of baseline photographs, surveyed cross-sections and thalweg surveys at the plunge pool area in Sandia Canyon Reach S-2

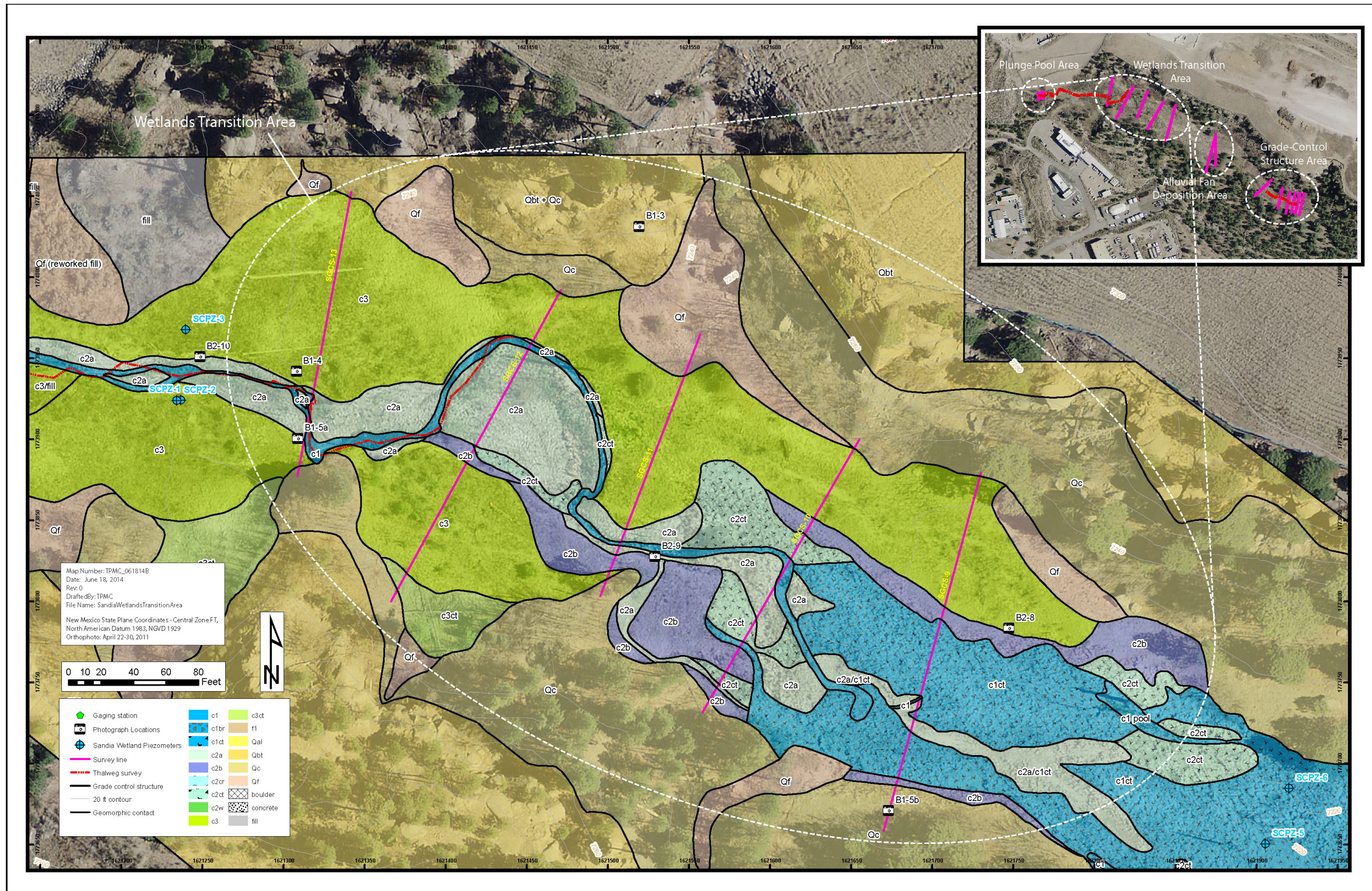


Figure B-3.0-2 Geomorphic map overlain on an orthophoto showing the locations of piezometers, baseline photographs, surveyed cross-sections and thalweg surveys at the wetland transition area in Sandia Canyon Reach S-2

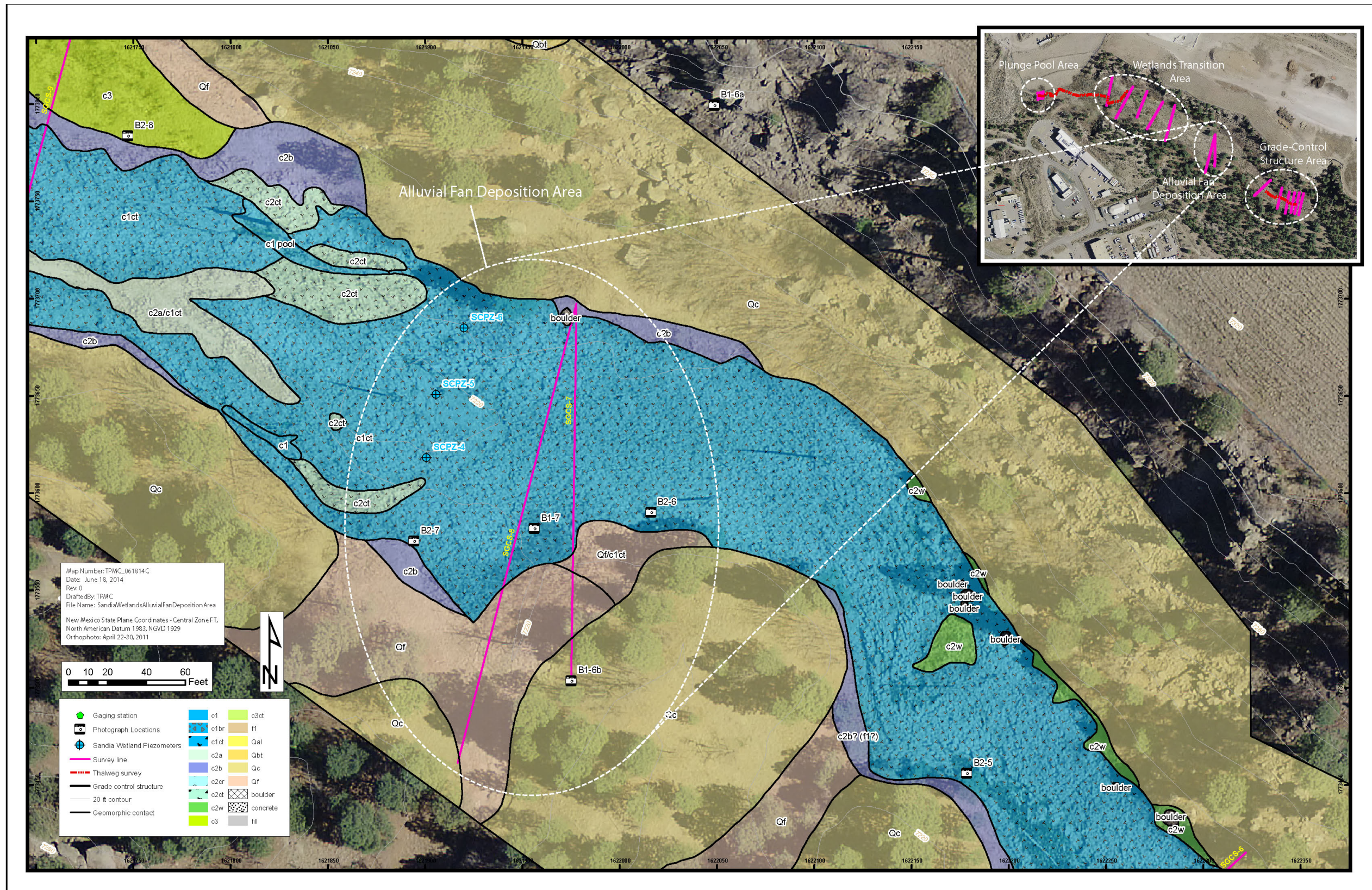


Figure B-3.0-3 Geomorphic map overlain on an orthophoto showing the locations of piezometers, baseline photographs, surveyed cross-sections and thalweg surveys at the alluvial fan deposition area in Sandia Canyon Reach S-2

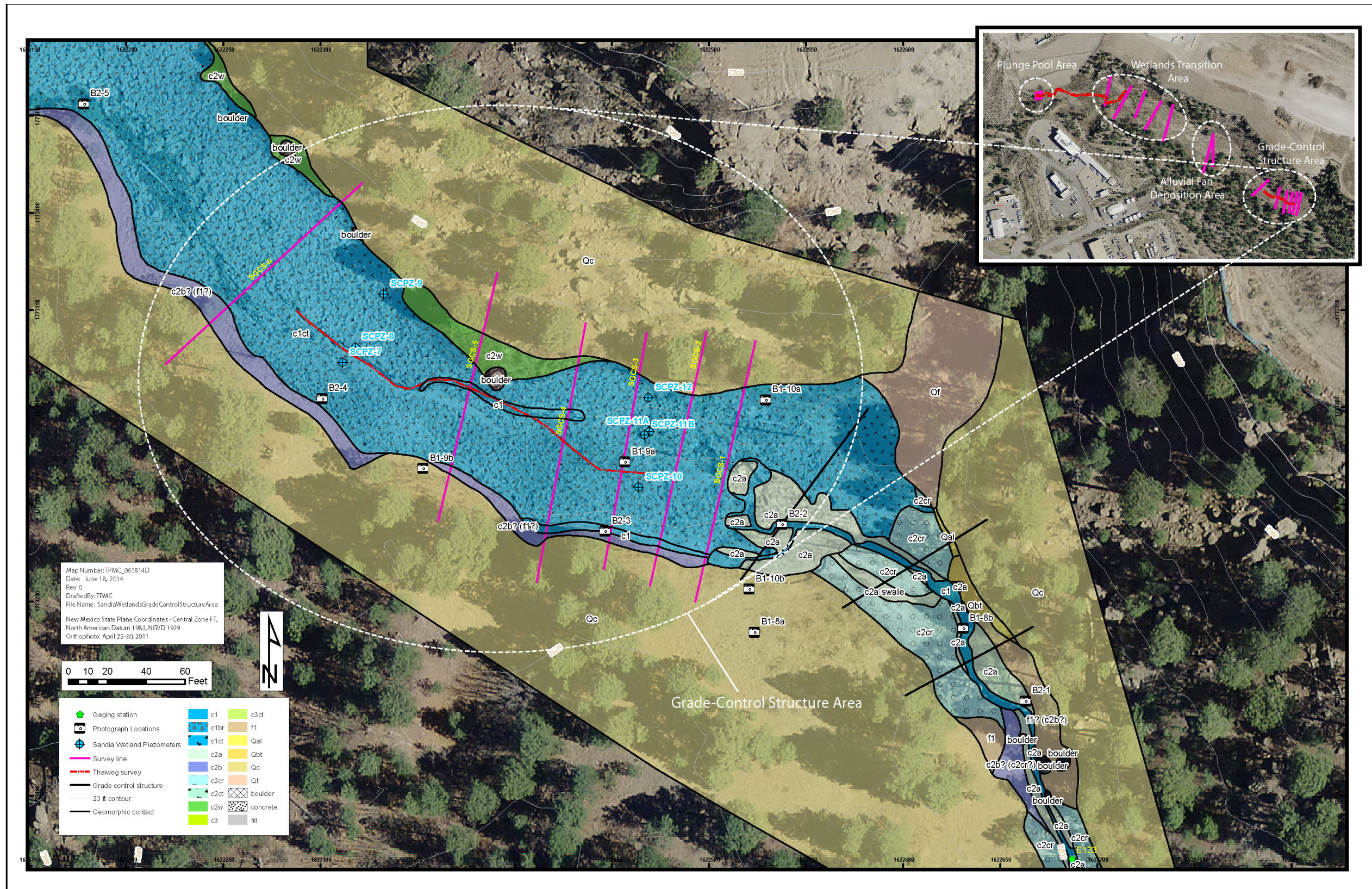


Figure B-3.0-4 Geomorphologic map overlain on an orthophoto showing the locations of piezometers, baseline photographs, surveyed cross-sections and thalweg surveys at the GCS area in Sandia Canyon Reach S-2

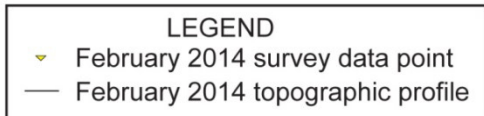
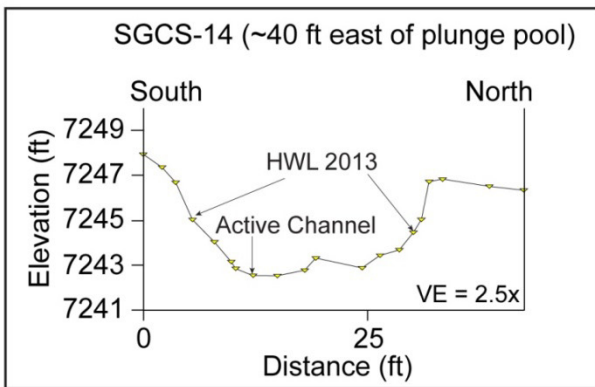
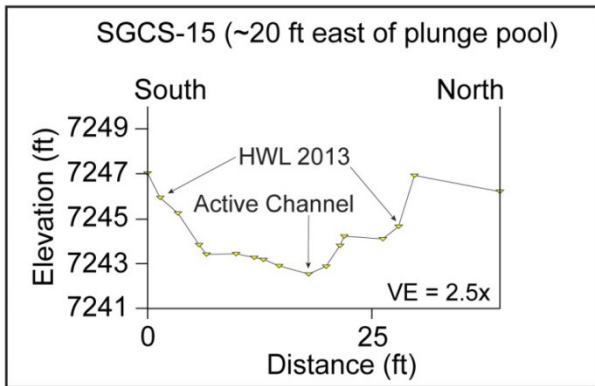
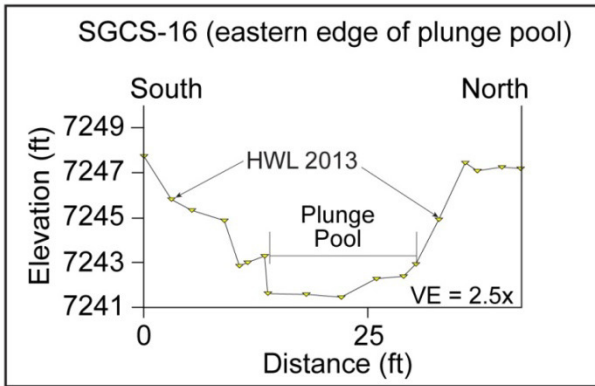


Figure B-3.1-1 Cross-sections at the plunge pool area in Sandia Canyon

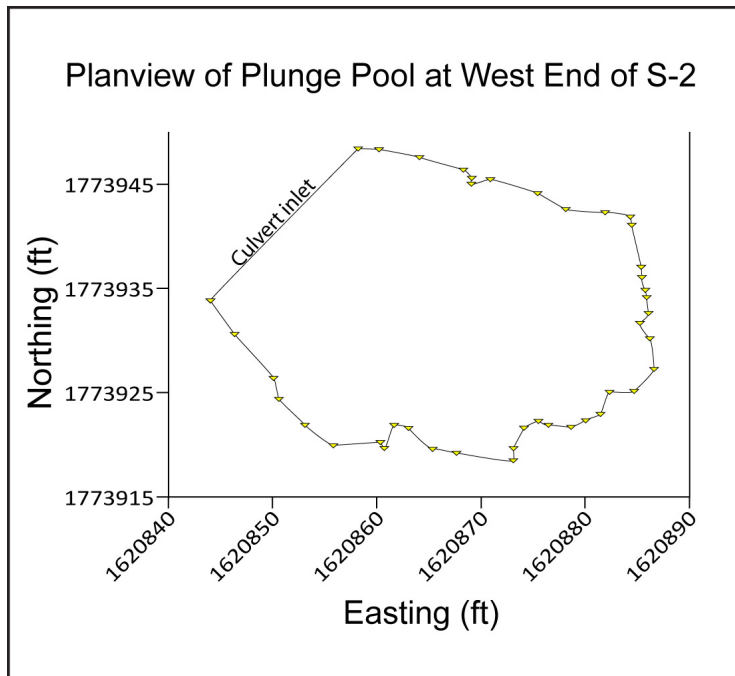


Figure B-3.1-2 Plan view of the plunge pool area in Sandia Canyon

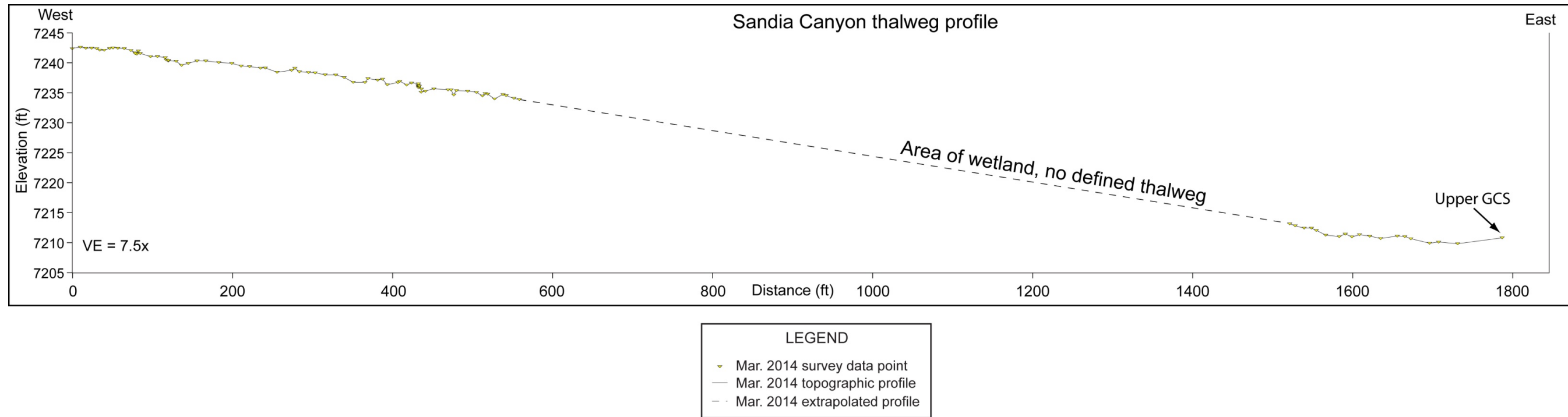


Figure B-3.1-3 Thalweg profile in Sandia Canyon

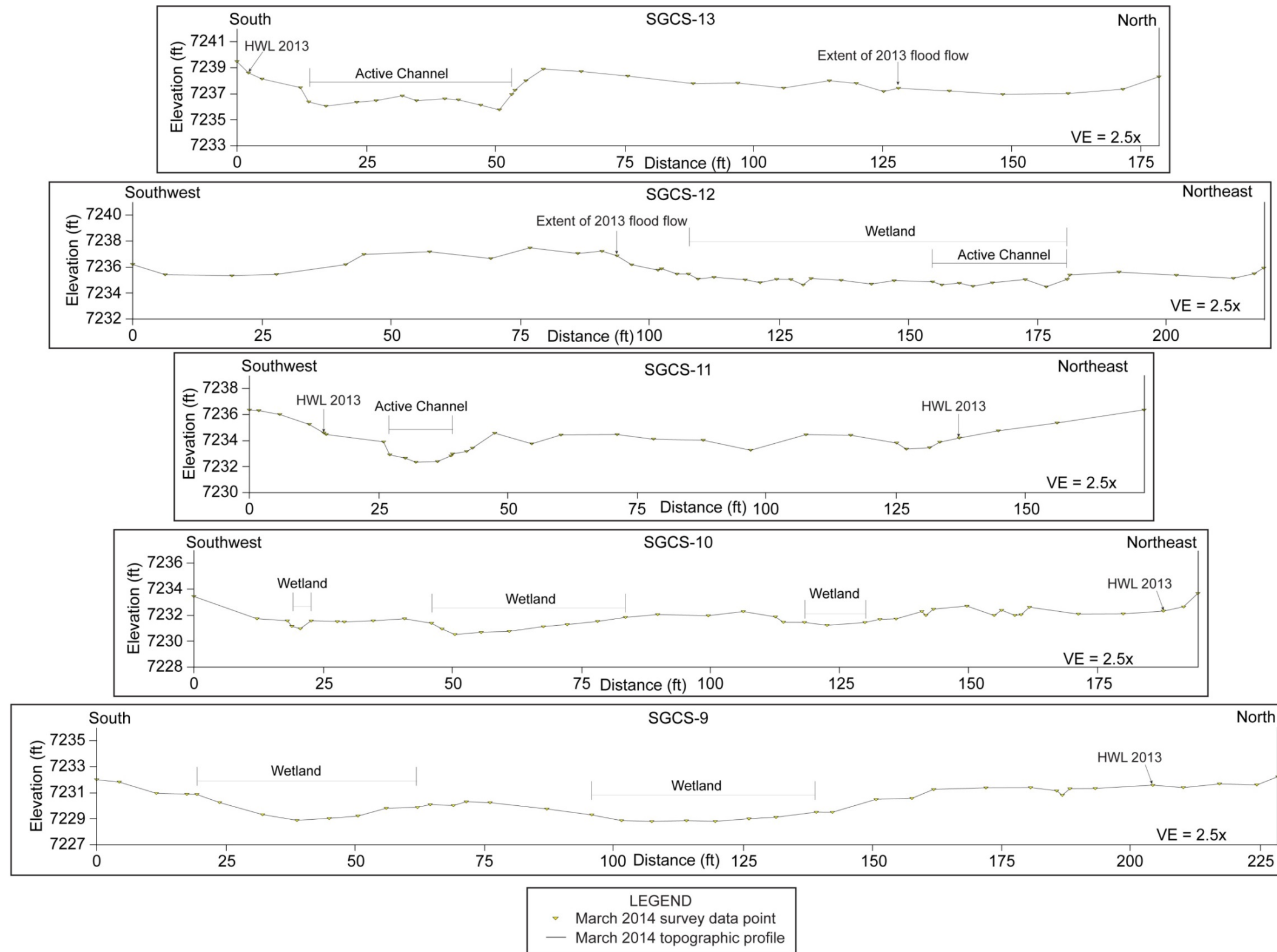
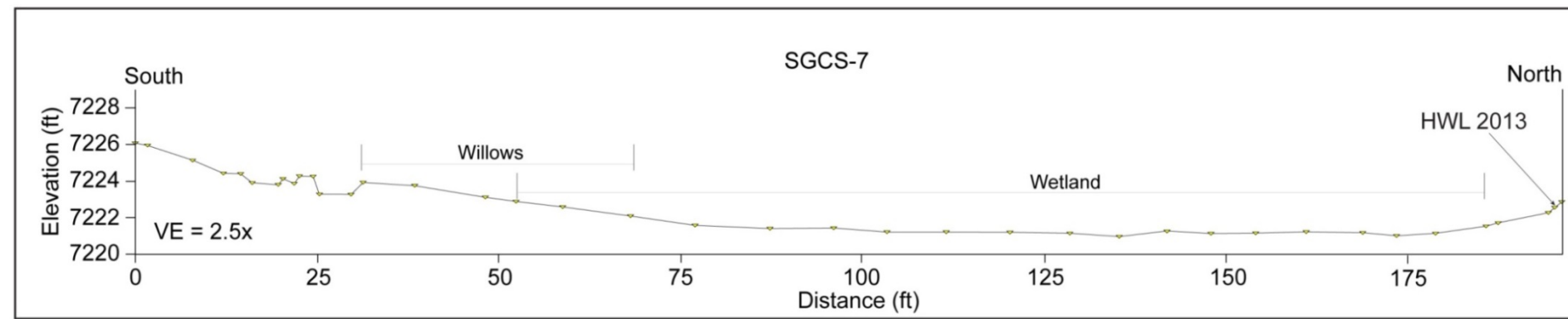
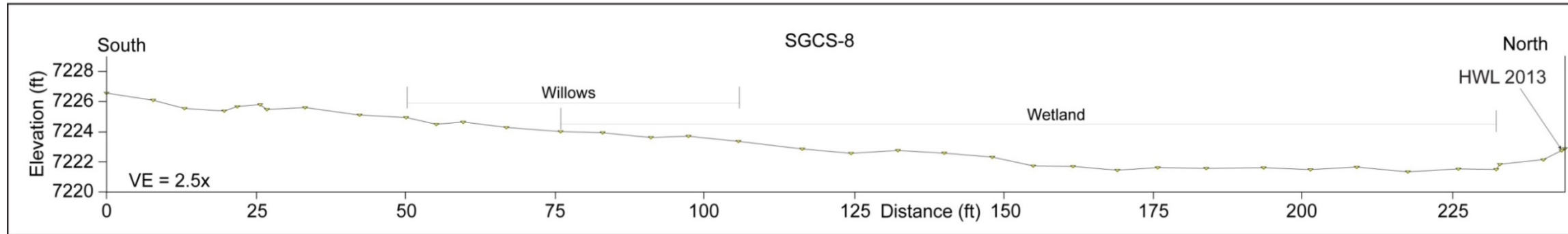


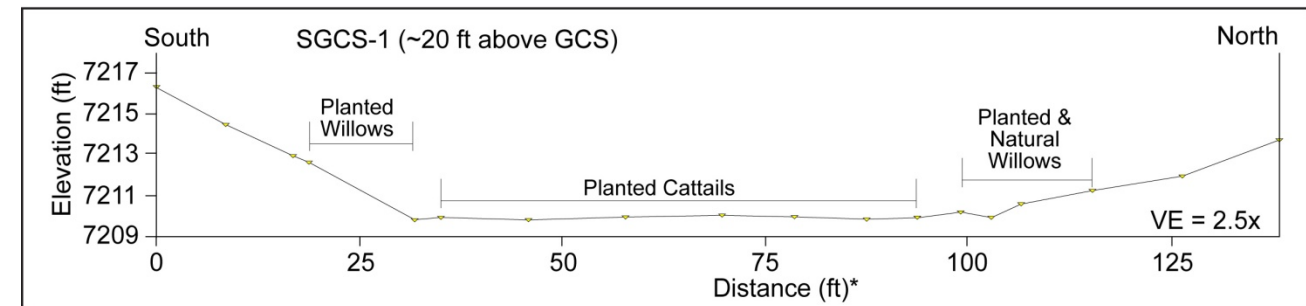
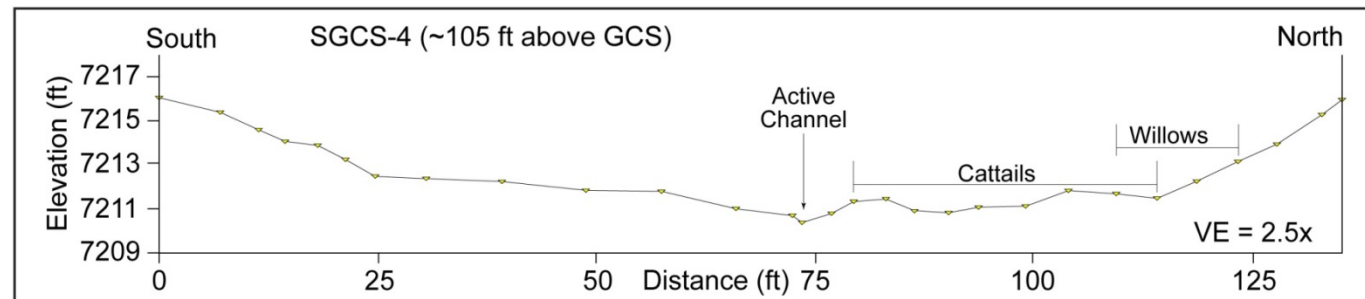
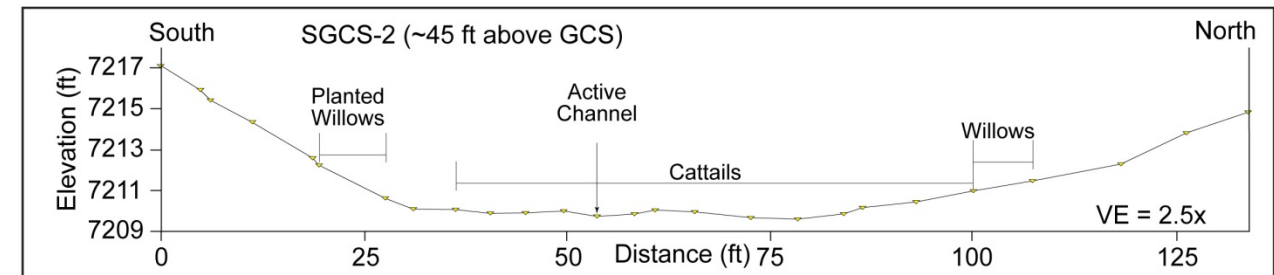
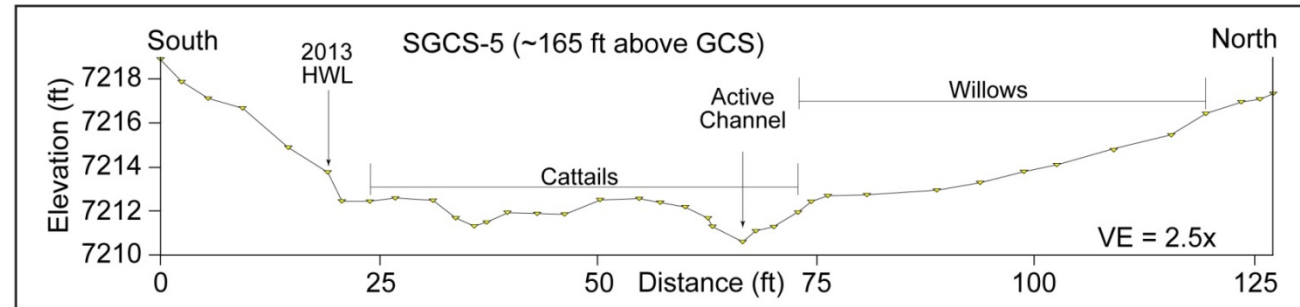
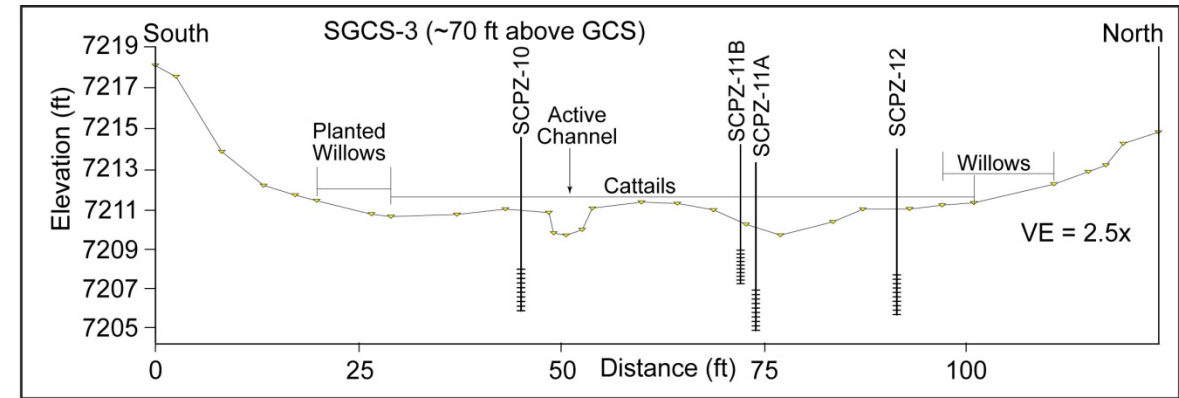
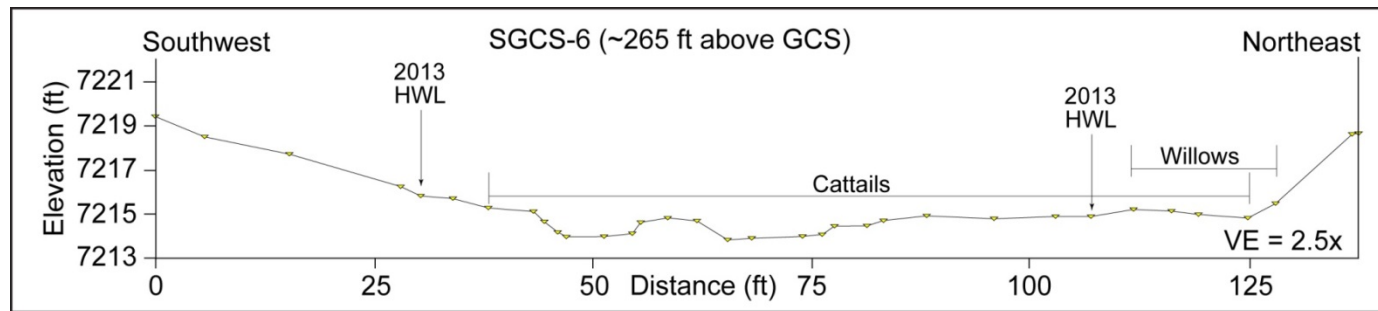
Figure B-3.2-1 Cross-sections at the wetland transitional area in Sandia Canyon



LEGEND

- ▼ March 2014 survey data point
- March 2014 topographic profile

Figure B-3.3-1 Cross-sections at the alluvial fan depositional area in Sandia Canyon



LEGEND

- ▼ March 2014 survey data point
- March 2014 topographic profile
- SCPZ-12 Piezometer showing screened interval*
- ← Screen

*Piezometer projected onto section, shown schematically

Figure B-3.4-1 Cross-sections at the GCS area in Sandia Canyon

Table B-2.0-1
Daily Total Precipitation and Peak Discharge for September 2013 Flood

| Date | Daily Total Precipitation (in.) Rain Gage 121.9 | Max Daily Discharge (cfs) Stream Gage E121 | Max Daily Discharge (cfs) Stream Gage E123 |
|-------------|--|---|---|
| 9/09/2013 | 0 | 0.64 | 2.2 |
| 9/10/2013 | 1.4 | 9.4 | 15 |
| 9/11/2013 | 0.02 | 1.3 | 2.8 |
| 9/12/2013 | 2.3 | 20 | 48 |
| 9/13/2013 | 2.4 | 68 | 110 |
| 9/14/2013 | 0.19 | 2.0 | 5.9 |
| 9/15/2013 | 0.07 | 0.77 | 3.9 |

**Table B-3.0-1
Baseline Photograph Survey Location Coordinates**

| Photograph ID | X Coordinate ^a | Y Coordinate ^a | Elevation (ft) |
|---|---------------------------|---------------------------|----------------|
| Baseline Photographs of Geomorphic Conditions in Sandia Canyon Reach S-2^b | | | |
| B1-1a | 1620944 | 1773926 | 7248 |
| B1-1b | 1620843 | 1773929 | 7252 |
| B1-2a | 1620866 | 1773917 | 7248 |
| B1-2b | 1620888 | 1773943 | 7248 |
| B1-3 | 1621519 | 1774032 | 7253 |
| B1-4 | 1621308 | 1773942 | 7242 |
| B1-5a | 1621309 | 1773901 | 7242 |
| B1-5b | 1621673 | 1773671 | 7229 |
| B1-6a | 1622048 | 1773799 | 7267 |
| B1-6b | 1621975 | 1773504 | 7218 |
| B1-7 | 1621956 | 1773582 | 7221 |
| B1-8a | 1622523 | 1773184 | 7215 |
| B1-8b | 1622631 | 1773186 | 7207 |
| B1-9a | 1622457 | 1773272 | 7211 |
| B1-9b | 1622353 | 1773269 | 7213 |
| B1-10a | 1622529 | 1773304 | 7213 |
| B1-10b | 1622521 | 1773207 | 7211 |
| Baseline Photographs of the Vegetation Monitoring Survey^c | | | |
| B2-1 | 1622662.91 | 1773148.90 | 7206.11 |
| B2-2 | 1622537.67 | 1773239.87 | 7212.86 |
| B2-3 | 1622446.62 | 1773236.35 | 7212.42 |
| B2-4 | 1622300.88 | 1773304.53 | 7212.48 |
| B2-5 | 1622178.18 | 1773456.19 | 7217.98 |
| B2-6 | 1622015.84 | 1773590.32 | 7222.10 |
| B2-7 | 1621894.05 | 1773575.48 | 7224.93 |
| B2-8 | 1621747.14 | 1773783.76 | 7229.09 |
| B2-9 | 1621528.98 | 1773827.97 | 7233.24 |
| B2-10 | 1621248.41 | 1773951.28 | 7239.07 |
| B2-1 | 1622662.91 | 1773148.90 | 7206.11 |

^a State Plane Coordinate System New Mexico Central Zone, feet, North American Datum 83.

^b Coordinates were estimated using field notes and topographic map.

^c Coordinates were determined using a Trimble GeoExplorer® 16000 series handheld unit.

Attachment B-1

*Baseline Photographs of the
Sandia Canyon Sediment Transport Mitigation Site*



(a)



(b)

Note: Laths visible around perimeter of plunge pool mark locations where rebar was set to allow repeat surveys.

Photo B1-1 (a) Looking west (upstream) at plunge pool and outfall and (b) looking east (downstream) at plunge pool



(a)



(b)

Note: South end of section SGCS-14 is just off photo b to the left (east)

Photo B1-2 (a) Looking northeast at north endpoints of sections SGCS-16, SGCS-15, and SGCS-14 with the east end of the plunge pool in the foreground and (b) looking south at south endpoints of sections SGCS-16 and SGCS-15



Notes: Section SGCS-13 is the uppermost section in the transitional area, and SGCS-9 is in the main wetland at the downstream (east) end of the transition area. Photo is taken looking south from the north canyon wall.

Photo B1-3 Photomosaic of the wetland transitional area



Note: Tallest willows in this stand measure 5.2 m high.

Photo B1-4 Willow stand just upstream of section SGCS-13 with the tallest willows in the wetland transition area



(a)



(b)

Photo B1-5 (a) View north along section SGCS-13 at the upper (west) end of the wetland transition area with active channel (mappable thalweg) in foreground and (b) view north along section SGCS-9 in the active wetland area at the downstream (east) end of the wetland transition area



(a)



(b)

Note: Photo b taken from south endpoint of section line.

Photo B1-6 (a) View south of area of prograding fan deposits with wetland area and approximate locations of sections SGCS-7 and SGCS-8 in foreground and (b) view north along section SGCS-7



Note: Tallest willows in this stand measure 4.0 m high.

Photo B1-7 Looking south at willow stand between sections SGCS-7 and SGCS-8 in the alluvial fan depositional area



(a)



(b)

Note: Photo b taken standing in the middle of the downstream-most grade-control structure.

Photo B1-8 (a) View north from parking area across upper grade-control structure and area encompassed by sections SGCS-1 and SGCS-2 and (b) view west across upper two grade-control structures



(a)



(b)

Notes: Photo a taken from center of section SGCS-3. Note defined thalweg in foreground and established willows on north bank of wetland. Photo b taken from south bank of wetland at section SGCS-6.

Photo B1-9 (a) View west of cattail wetland and (b) view east of cattail wetland



(a)



(b)

Photo B1-10 (a) View east of willow planting area on north bank of the grade-control structure and (b) view east of willow planting area on south bank of the grade-control structure

Attachment B-2

Vegetation Monitoring Photographs



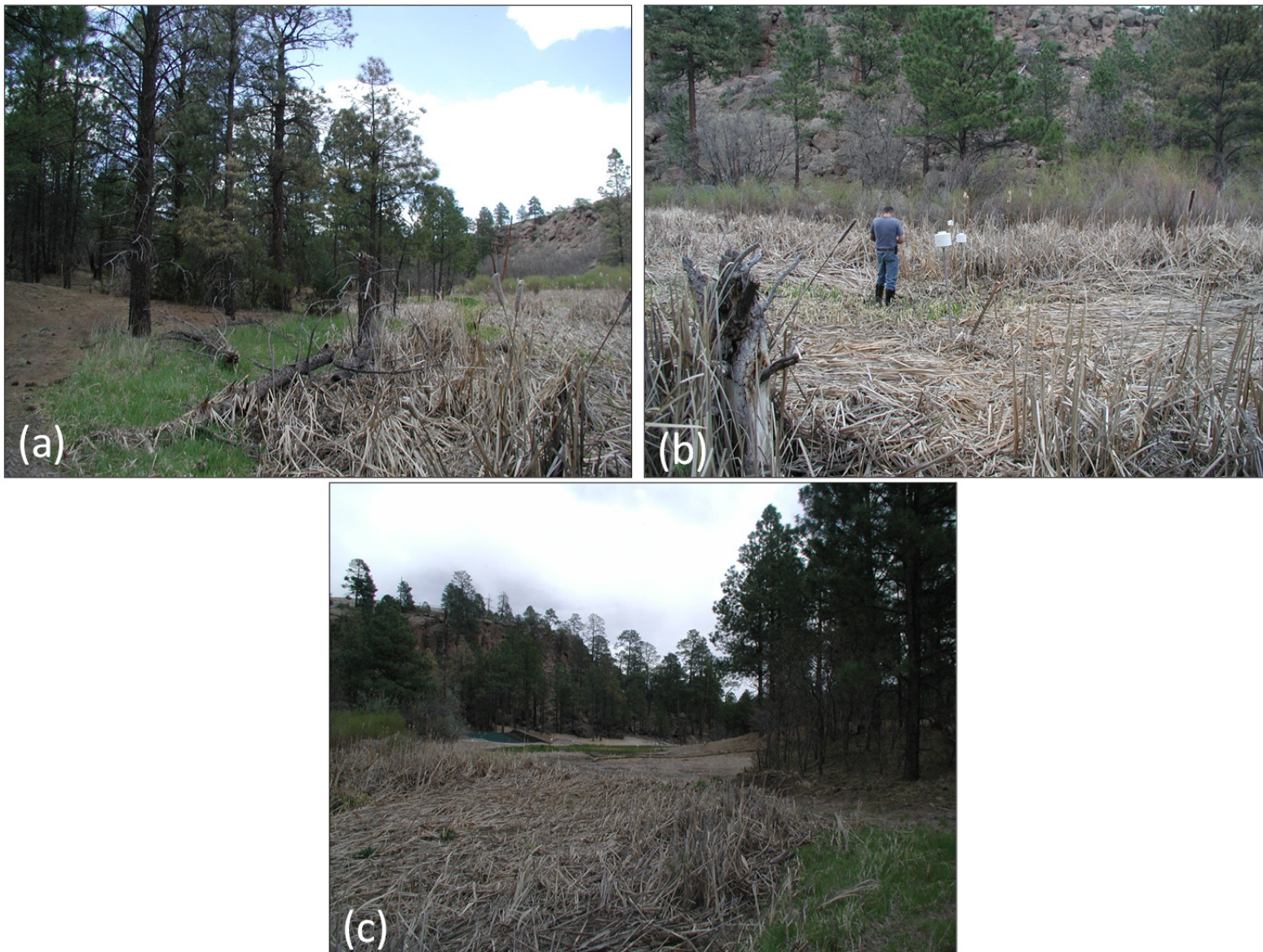
Photo B2-1 View east of GCS and west of catch pool looking west (upstream) at grade-control structure from boulders



Photo B2-2 Looking west (upstream) from westernmost step of grade-control structure

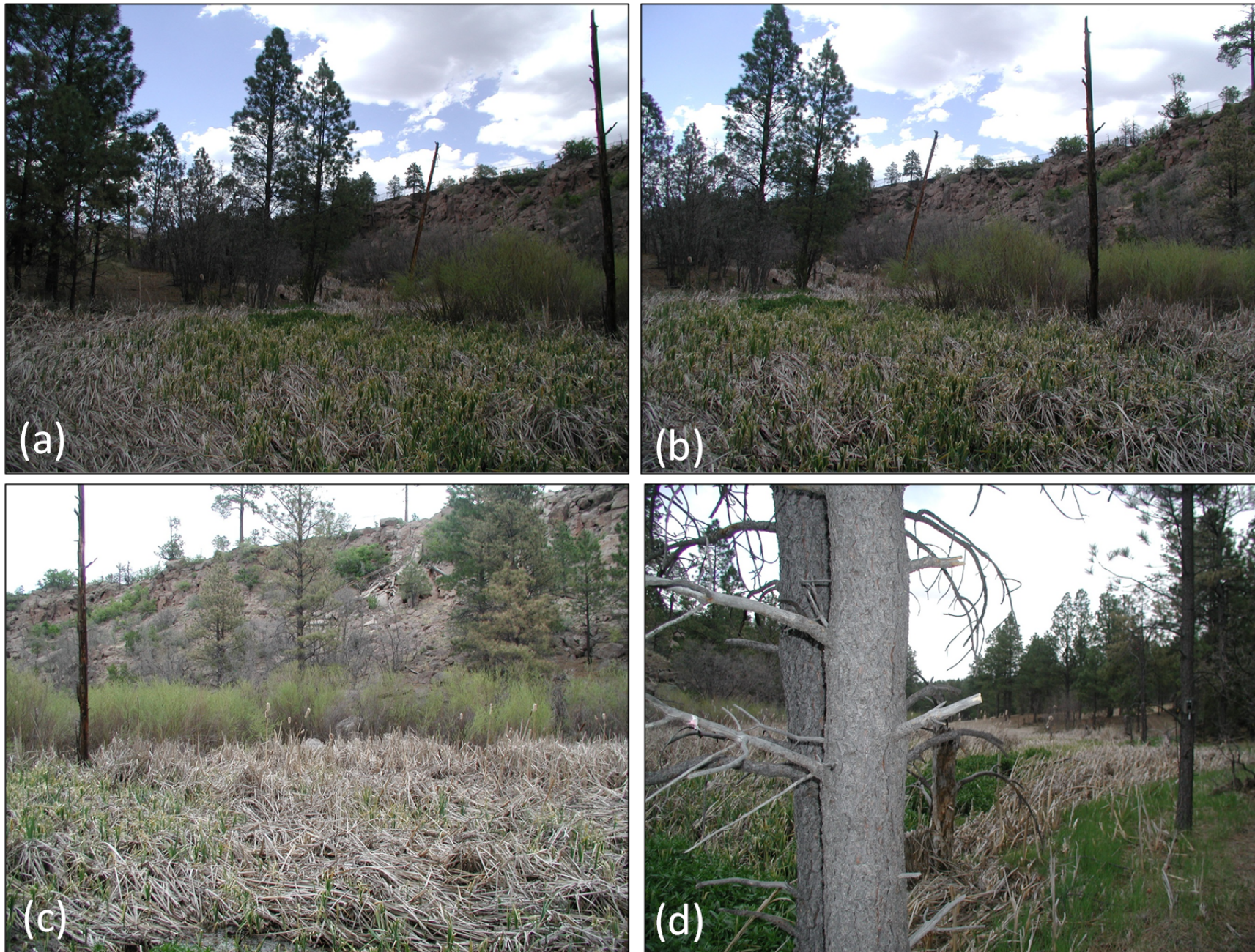


Photo B2-3 Views from south side of drive point transect SCPZ 10-12 looking (a) west, (b) north, and (c) east



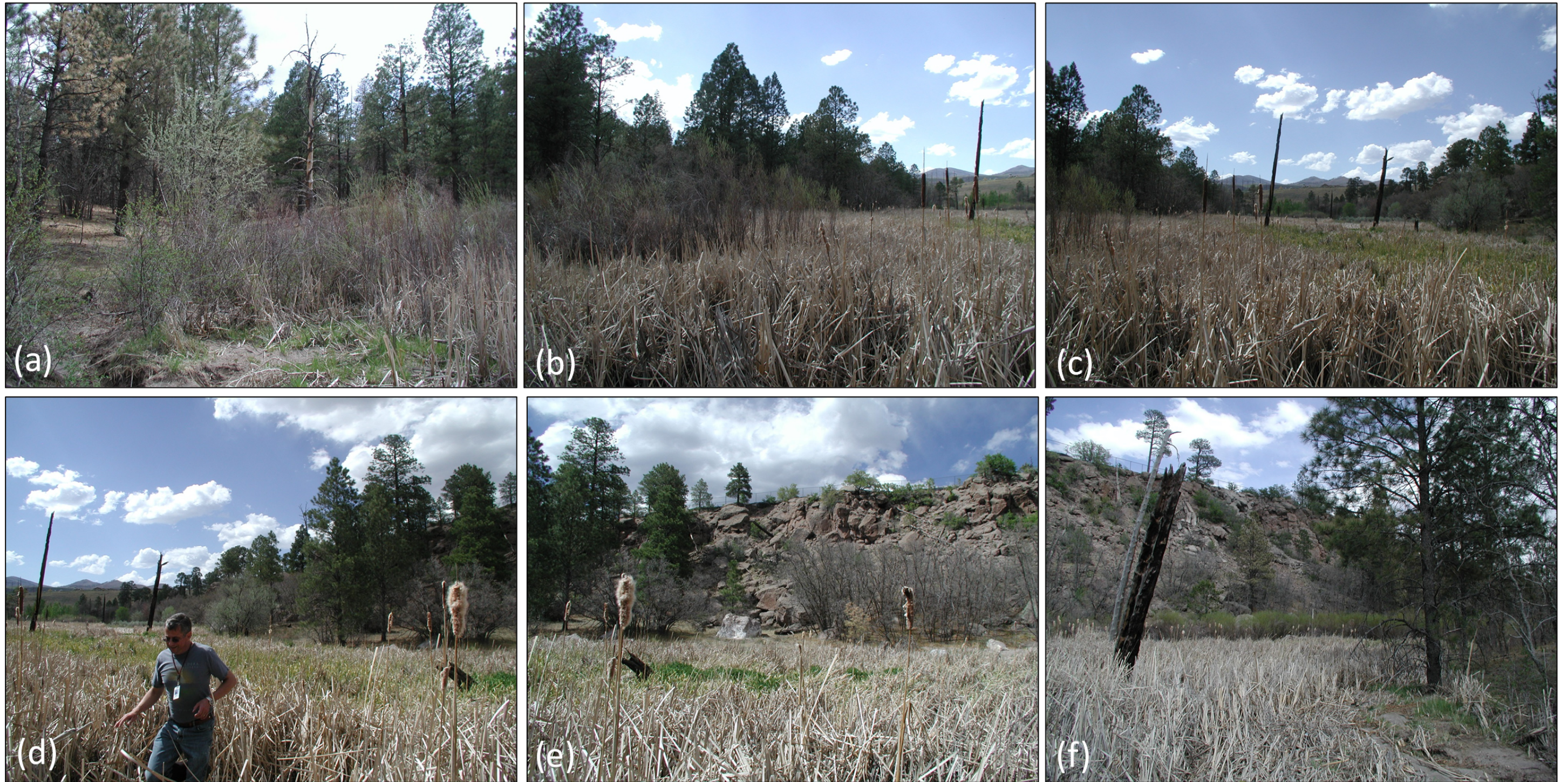
B2-4

Photo B2-4 Views from south side of drive point transect SCPZ 7-9 looking (a) west, (b) north, and (c) east



Notes: In photos b and c, note encroaching willows from north.

Photo B2-5 Views west of drive-point transect SCPZ 7-9 looking (a) west, (b) northwest, (c) north-northwest, and (d) east at ponderosas next to photo location



Notes: In photo e, note the small dying ponderosa (roots were not wet). In photo f, note the willows on the north side.

Photo B2-6 Views from south side of wetland where alluvial fan comes in from the south looking (a) southwest, (b) west, (c) west, (d) northwest, (e) north, and (f) northeast

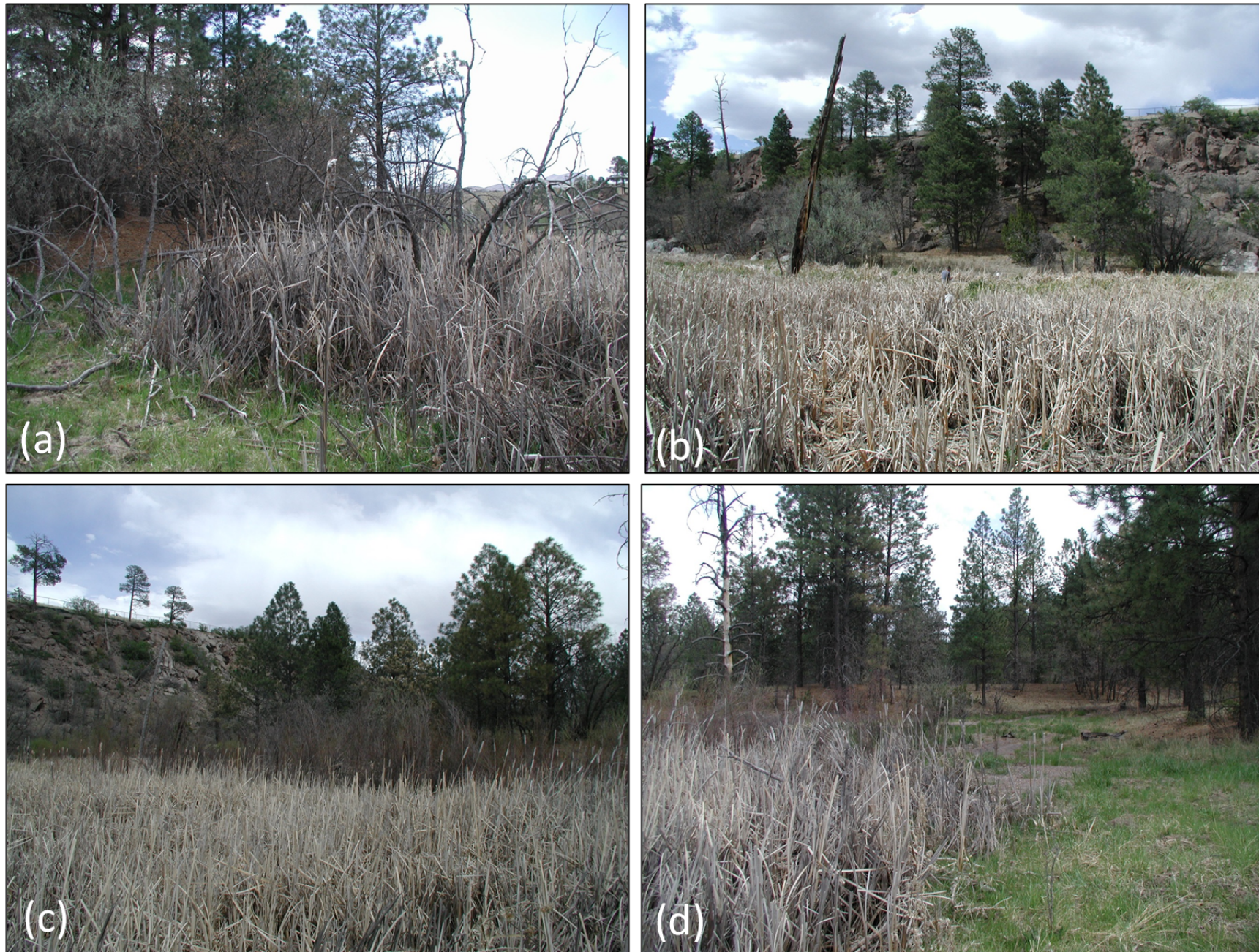
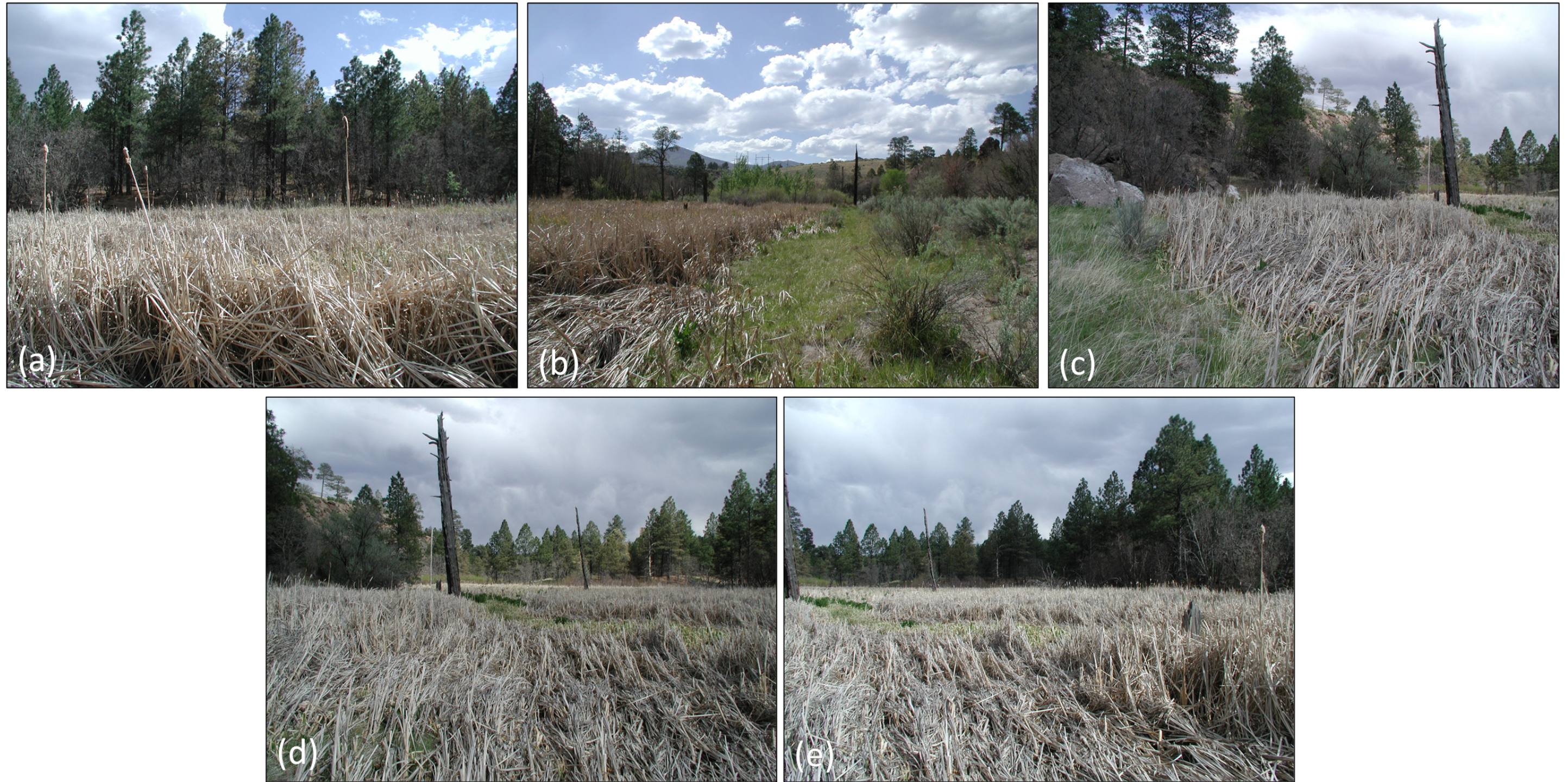


Photo B2-7 Views from south side of drive point transect SCPZ 4-6, just west of alluvial fan looking (a) west, (b) north, (c) northeast, and (d) east



Note: In photo d, note visible interior gravel bar.

Photo B2-8 Views from north side of wetland, west of photo location B2-7 looking (a) south (b) west, (c) northeast, (d) east, and (e) southeast



Notes: In photo a, note planted poplars to the north. In photo b, note planted poplars.

Photo B2-9 Views from south side of channel just inside south edge of wetland looking (a) west, (b) north, (c) northeast, and (d) east



B2-10

Photo B2-10 Views of channel in alluvial fill along SCPZ 1-3 transect between SCPZ-1/2 and SPCZ-3 looking (a) west, (b) northeast, and (c) east

Attachment B-3

*Baseline Cross-Section Survey Data
(on CD included with this document)*

Appendix C

Geochemical and Hydrologic Trends

This appendix presents geochemical and hydrologic trends based on recent monitoring in and around the Sandia Wetland. Interpretation of the data is discussed in the main body of this report.

C-1.0 BASEFLOW AND STORM WATER CHEMISTRY AT SURFACE WATER GAGING STATIONS E121, E122, AND E123

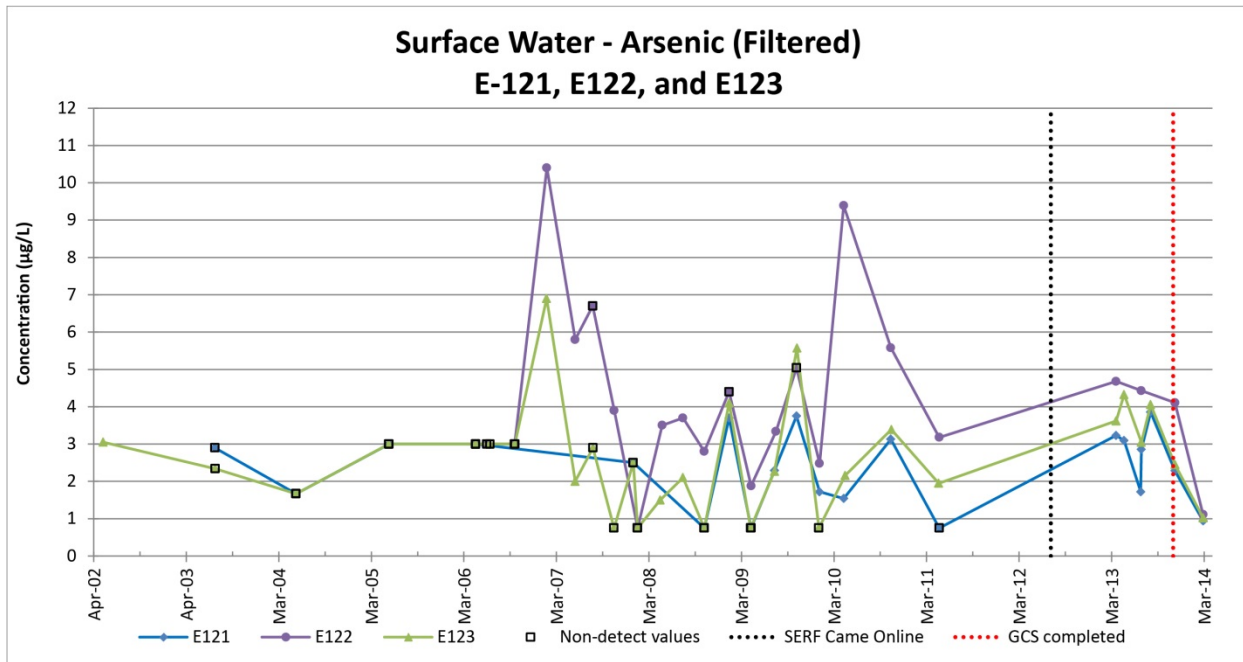
Figures C-1.0-1 through C-1.0-13 present time-series plots of analytical chemistry data of several different chemical constituents and nitrogen isotopes for base-flow samples collected at surface water gaging stations E121, E122, and E123. Figures C-1.0-14 through C-1.0-20 present time-series plots of analytical chemistry data of several different chemical constituents and nitrogen isotopes for storm water samples collected at the three gaging stations. Figure C-1.0-21 shows the monthly flow passing each of the three gaging stations.

C-2.0 ALLUVIAL WATER CHEMISTRY IN THE SANDIA WETLAND PIEZOMETER ARRAY

Analytical results for water chemistry from the piezometer array are presented in Figures C-2.0-1 to C-2.0-24.

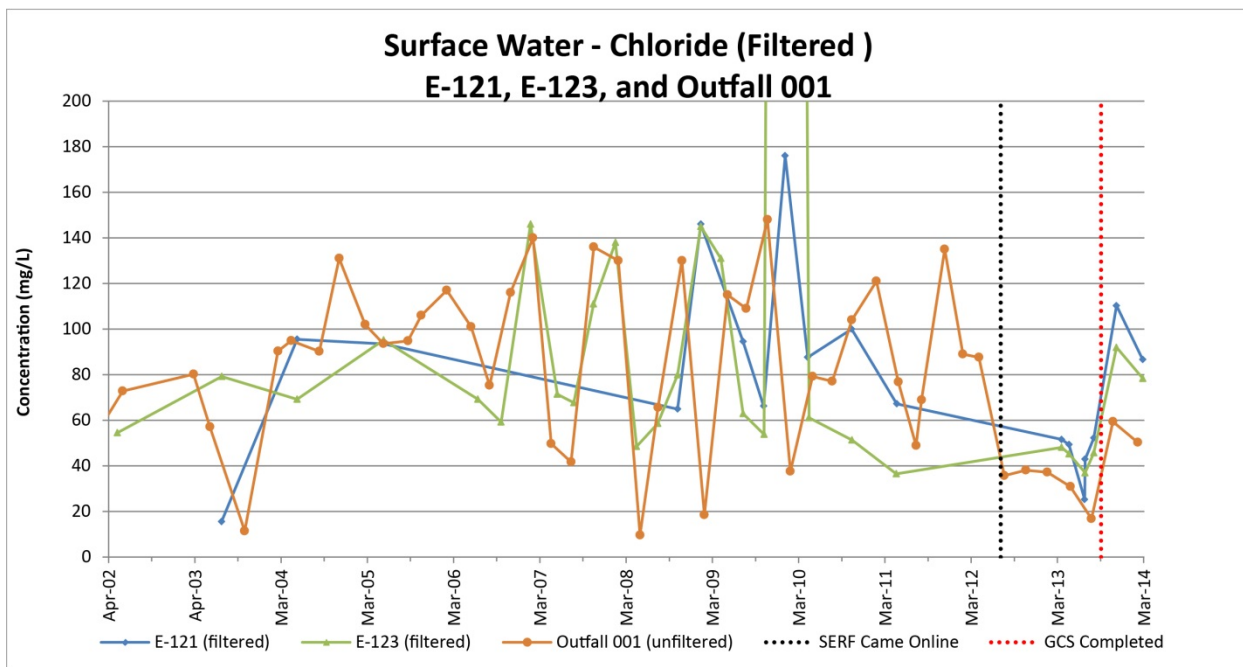
C-3.0 WATER LEVELS IN THE SANDIA WETLAND PIEZOMETER ARRAY

Water-level data for the piezometer array are presented in Figure C-3.0-1. The plots are arranged within the figure to represent the spatial distribution of the piezometers throughout the wetland. Daily flows at gage E121 are plotted along with the piezometer water-level data.



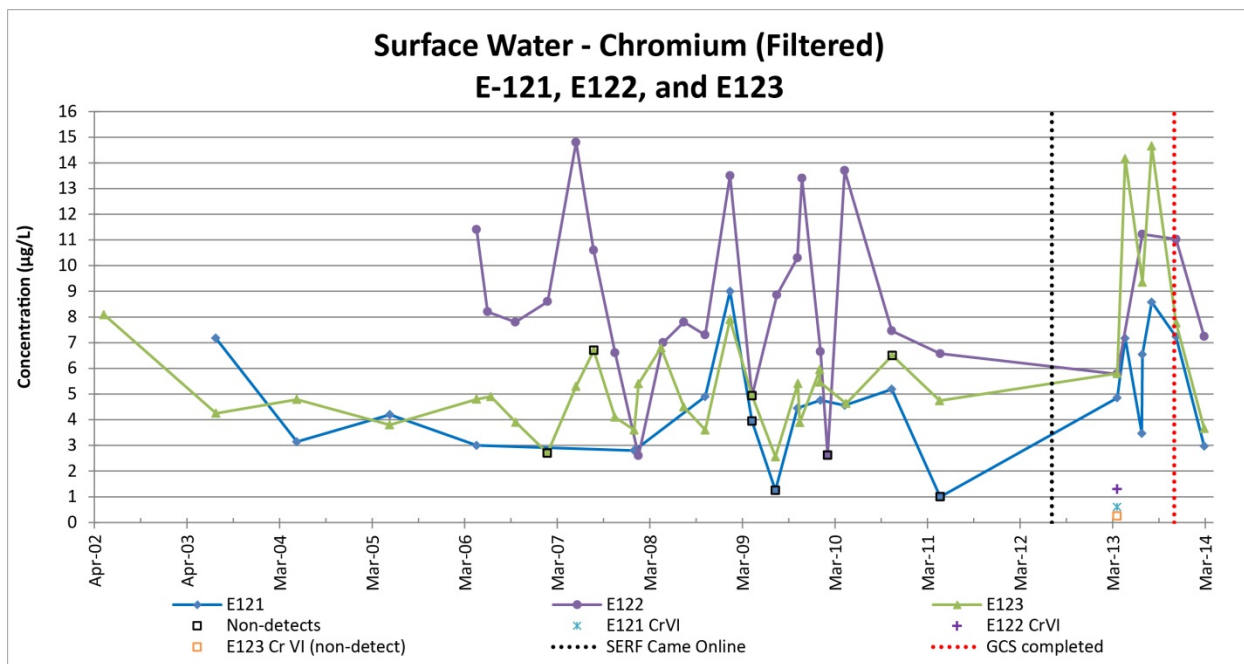
Non-detect values are estimates when above the MDL; otherwise values equal to half the MDL are used

Figure C-1.0-1 Time-series plot showing arsenic concentrations at gaging stations E121, E122, and E123



All values are detects

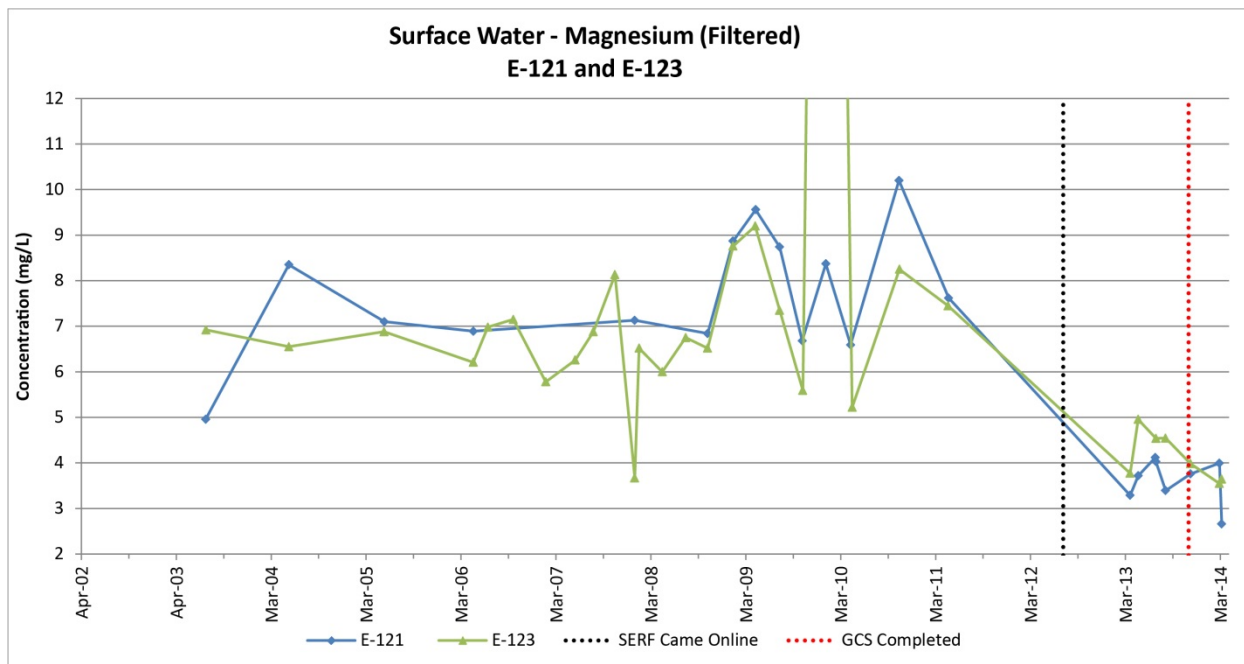
Figure C-1.0-2 Time-series plot showing chloride concentrations at gaging stations E121, E123, and National Pollutant Discharge Elimination System– (NPDES-) permitted Outfall 001



Non-detect values are estimates when above the MDL; otherwise values equal to half the MDL are used

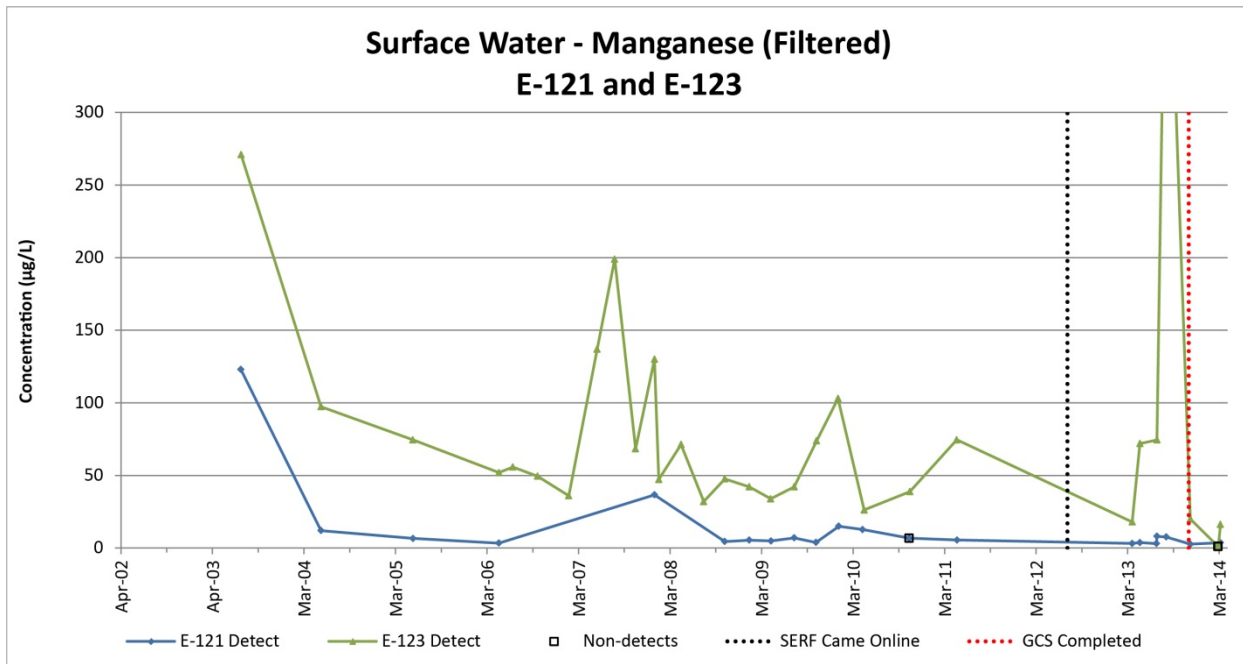
Note low concentrations of Cr(VI).

Figure C-1.0-3 Time-series plot showing chromium concentrations at gaging stations E121, E122, and E123



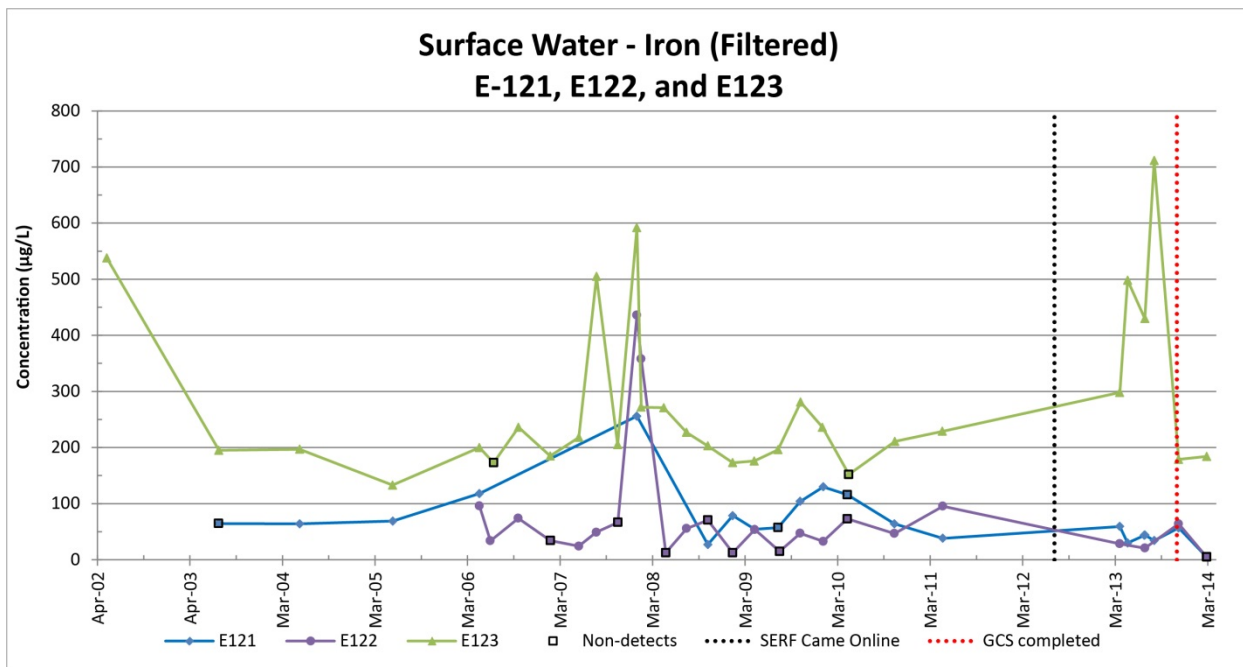
All values are detects

Figure C-1.0-4 Time-series plot showing magnesium concentrations at gaging stations E121 and E123



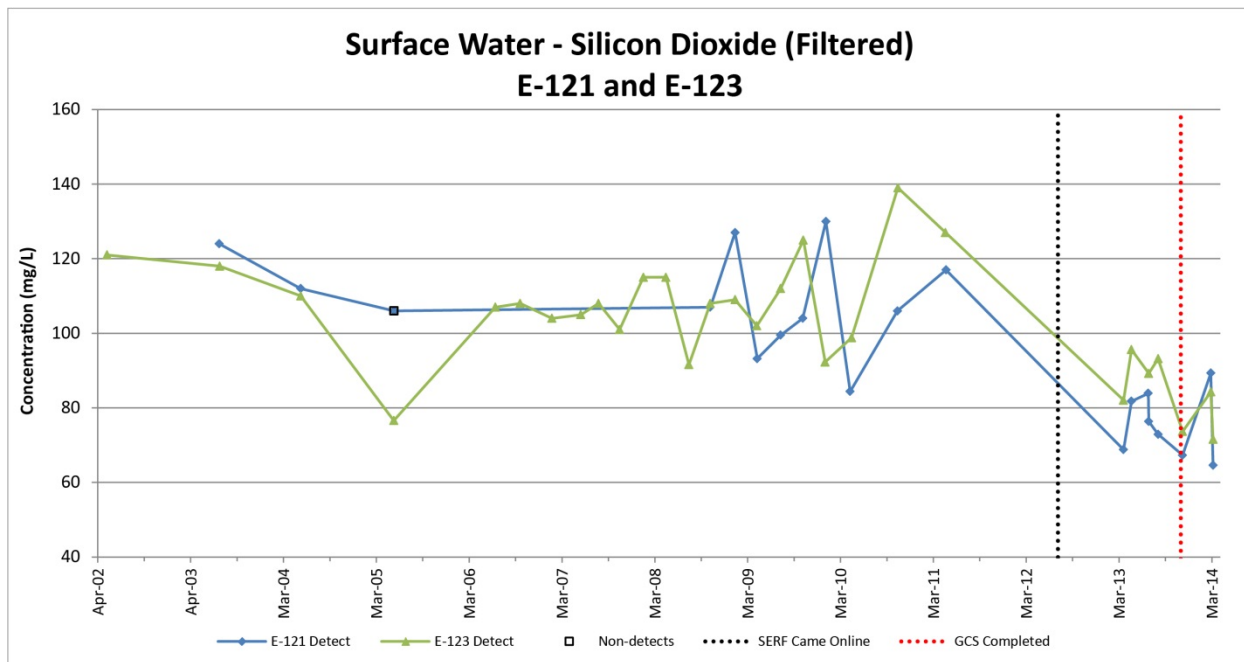
Non-detect values are estimates when above the MDL; otherwise values equal to half the MDL are used

Figure C-1.0-5 Time-series plot showing manganese concentrations at gaging stations E121 and E123



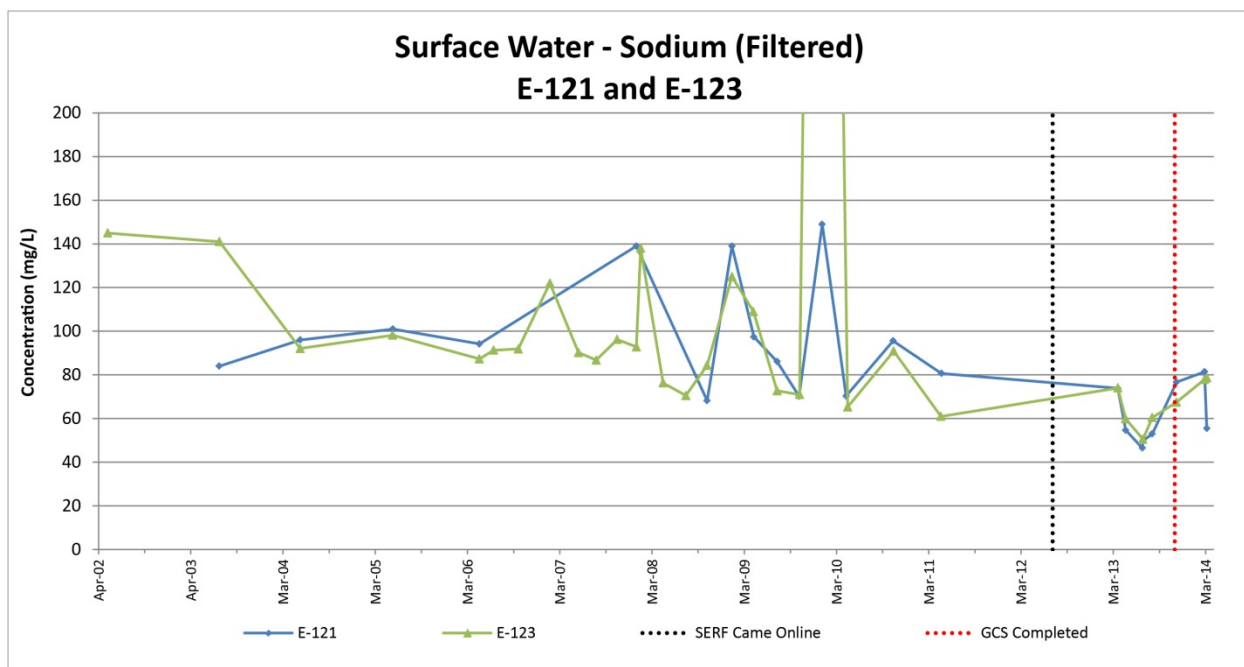
Non-detect values are estimates when above the MDL; otherwise values equal to half the MDL are used

Figure C-1.0-6 Time-series plot showing iron concentrations at gaging stations E121 and E123



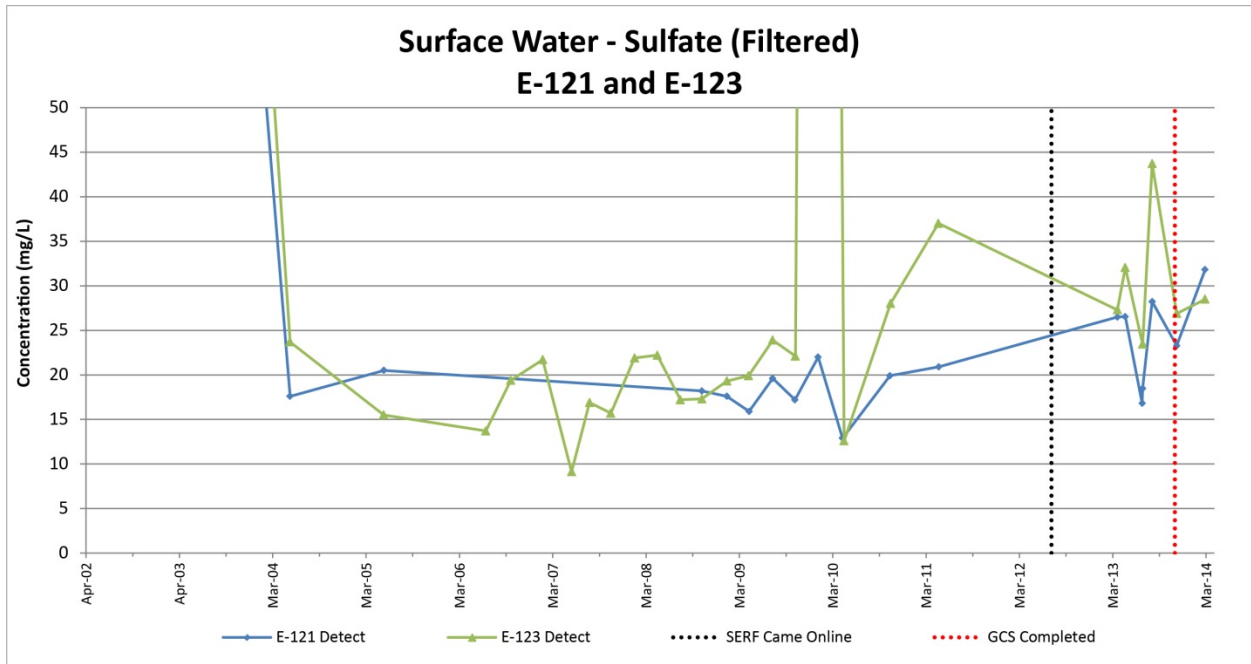
Non-detect values are estimates where above the MDL; otherwise values equal to half the MDL are used

Figure C-1.0-7 Time-series plot showing silicon dioxide concentrations at gaging stations E121 and E123



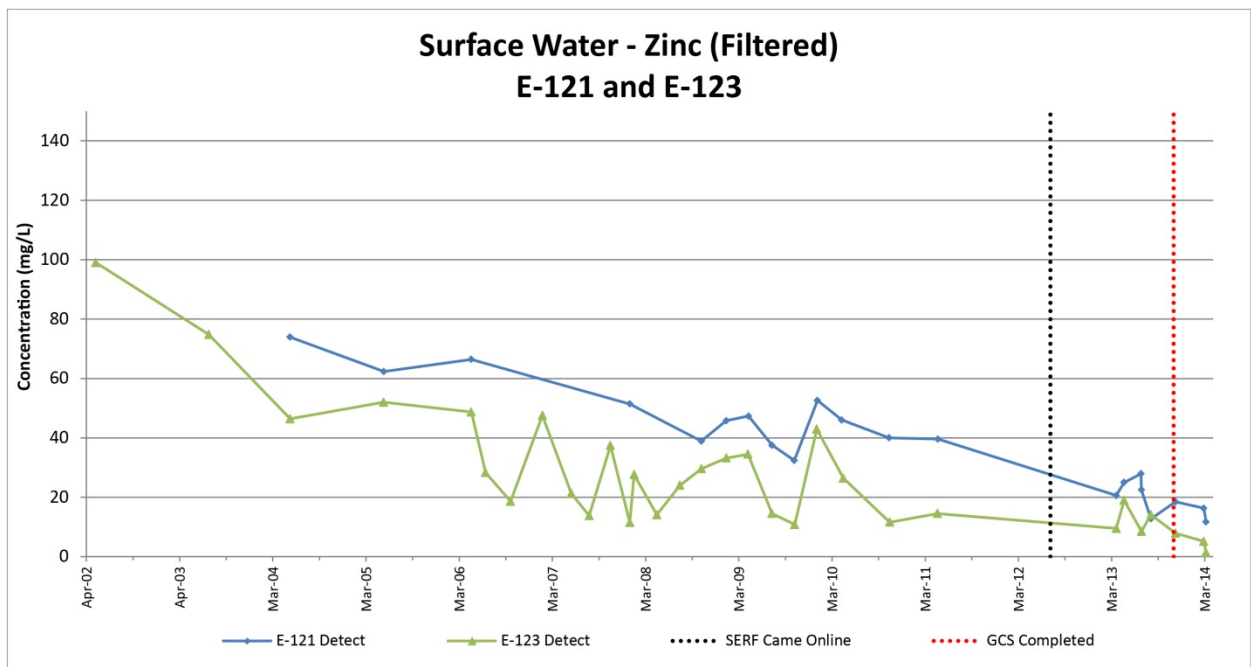
All values are detects

Figure C-1.0-8 Time-series plot showing sodium concentrations at gaging stations E121 and E123



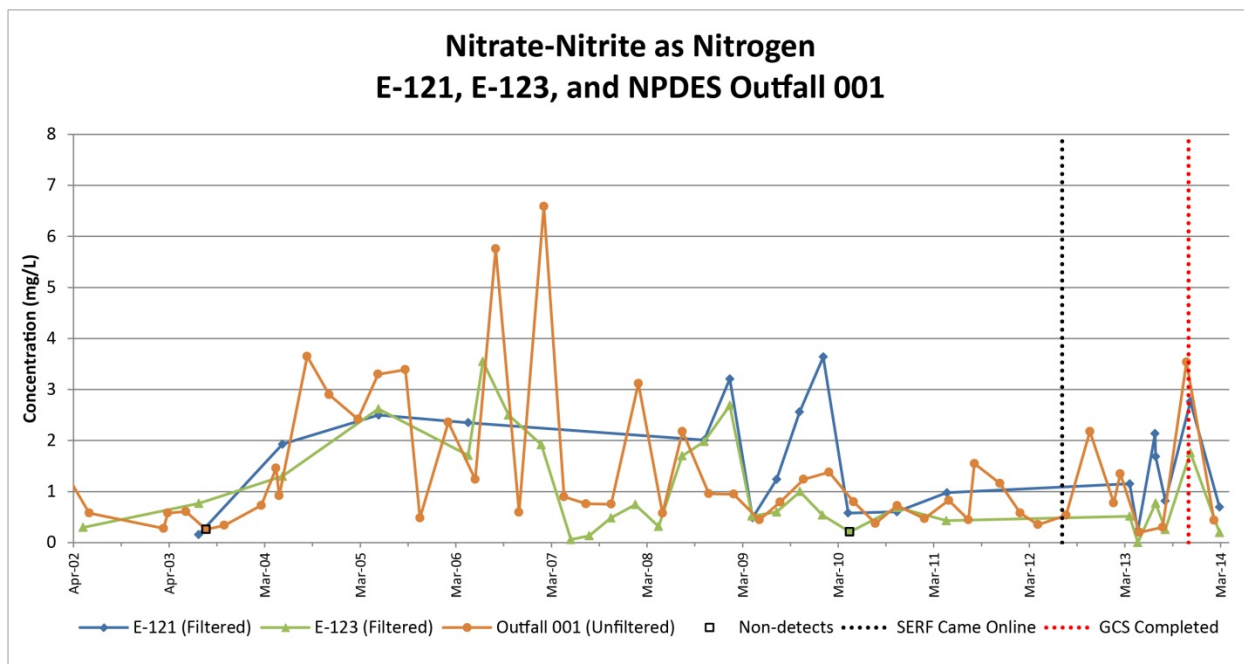
All values are detects

Figure C-1.0-9 Time-series plot showing sulfate concentrations at gaging stations E121 and E123



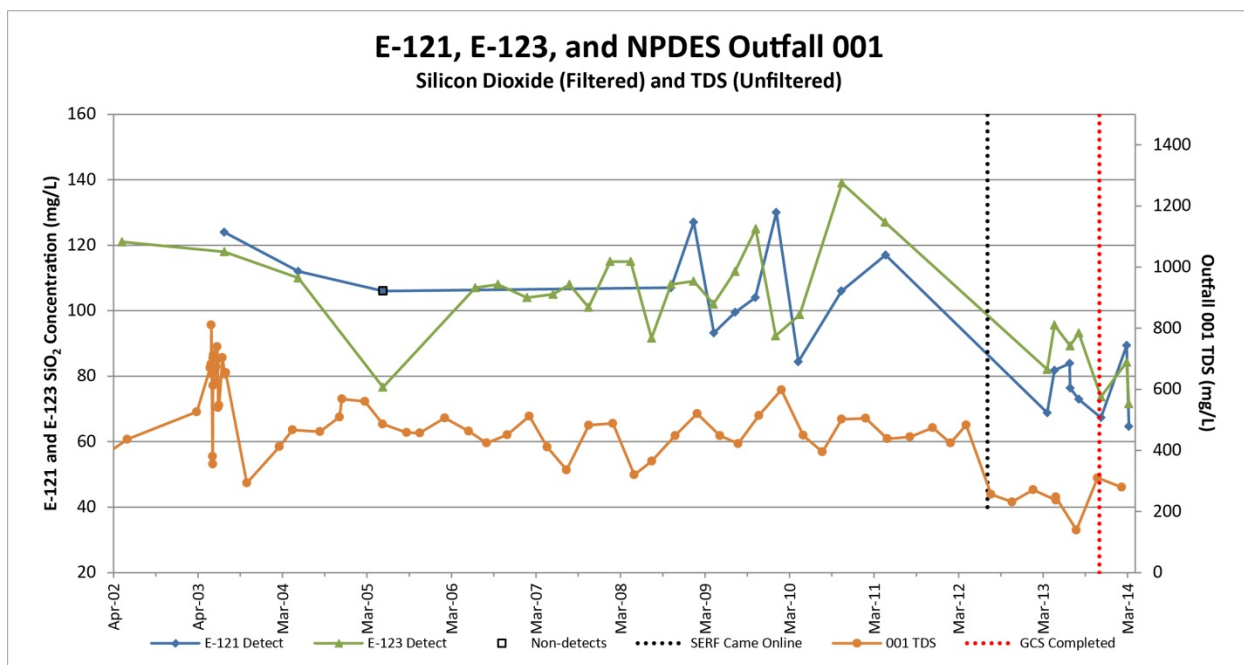
All values are detects

Figure C-1.0-10 Time-series plot showing zinc concentrations at gaging stations E121 and E123



Non-detect values are estimates where above the MDL; otherwise values equal to half the MDL are used

Figure C-1.0-11 Time-series plot showing nitrate plus nitrite as nitrogen concentrations at gaging stations E121, E123, and NPDES Outfall 001



Non-detect values are estimates when above the MDL; otherwise values equal to half the MDL are used

Figure C-1.0-12 Time-series plot showing silicon dioxide and total dissolved solids (TDS) at gaging stations E121, E123, and NPDES Outfall 001

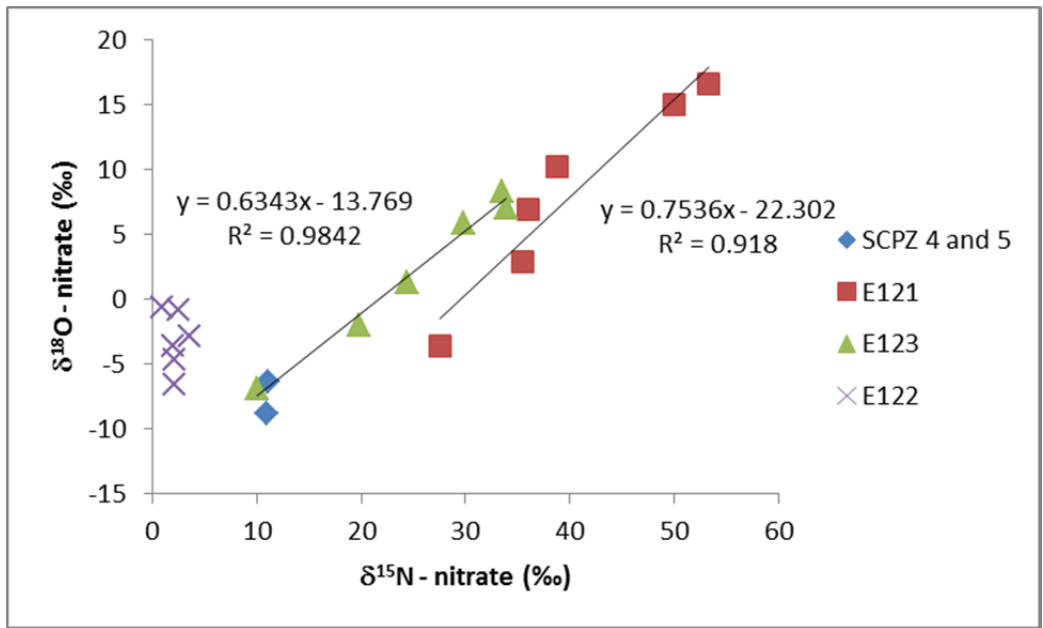
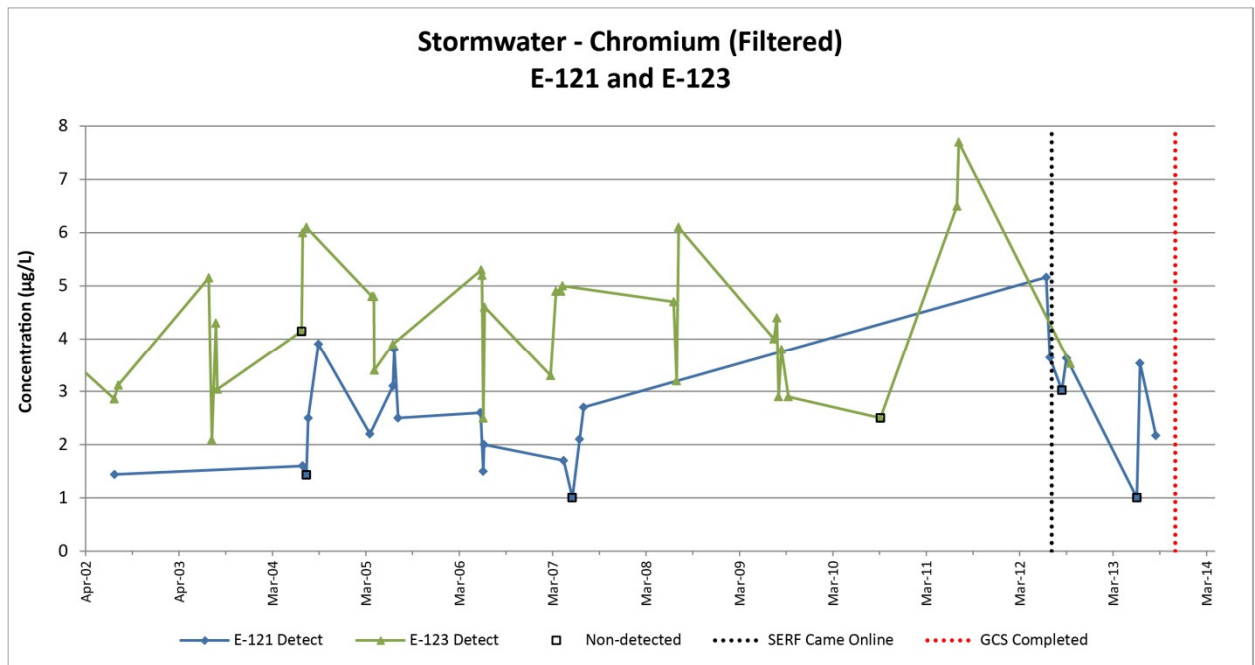
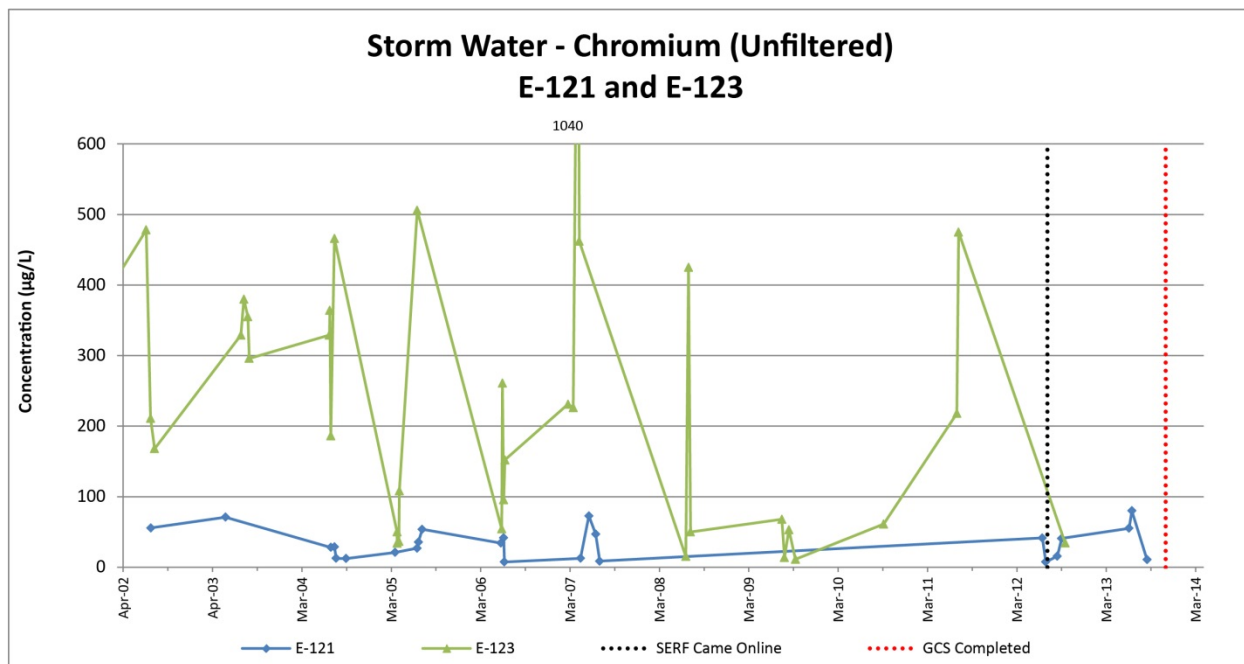


Figure C-1.0-13 Nitrogen isotope results from surface water



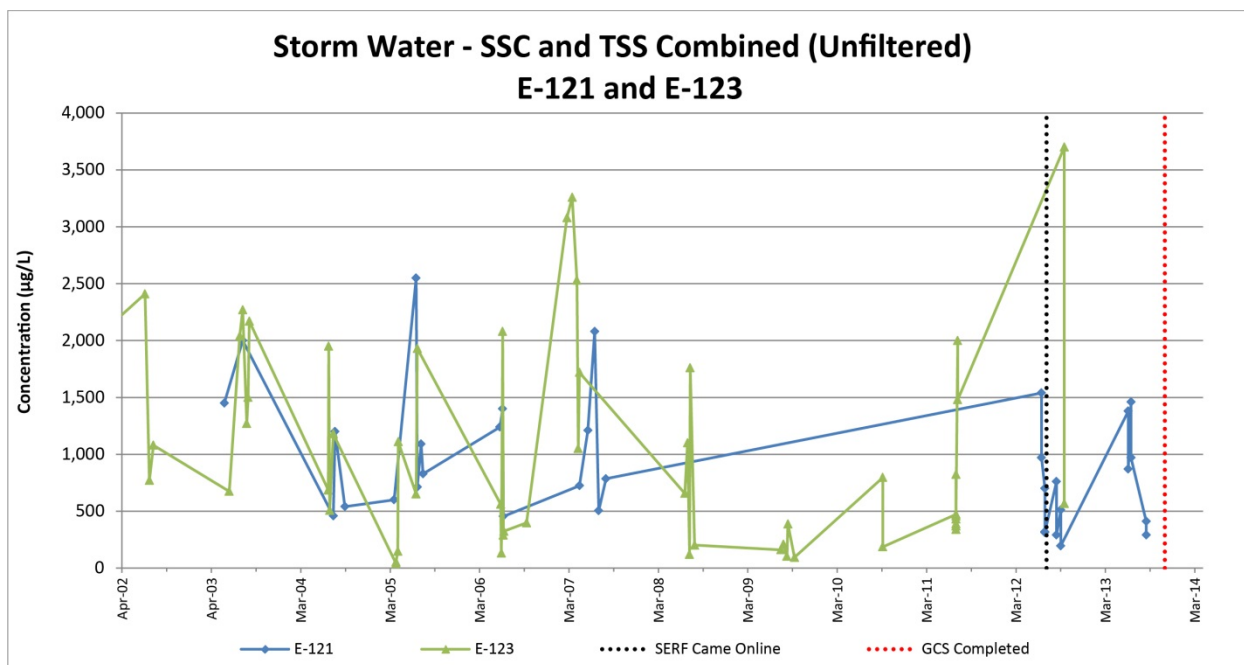
Non-detected values are estimates when above the MDL; otherwise values equal to half the MDL are used

Figure C-1.0-14 Time-series plot showing filtered chromium concentrations in storm water at gaging stations E121 and E123



All values are detects

Figure C-1.0-15 Time-series plot showing unfiltered chromium concentrations in storm water at gaging stations E121 and E123



All values are detects

Figure C-1.0-16 Time-series plot showing unfiltered suspended sediment concentrations (SSC) and total suspended sediment (TSS) in storm water at gaging stations E121 and E123

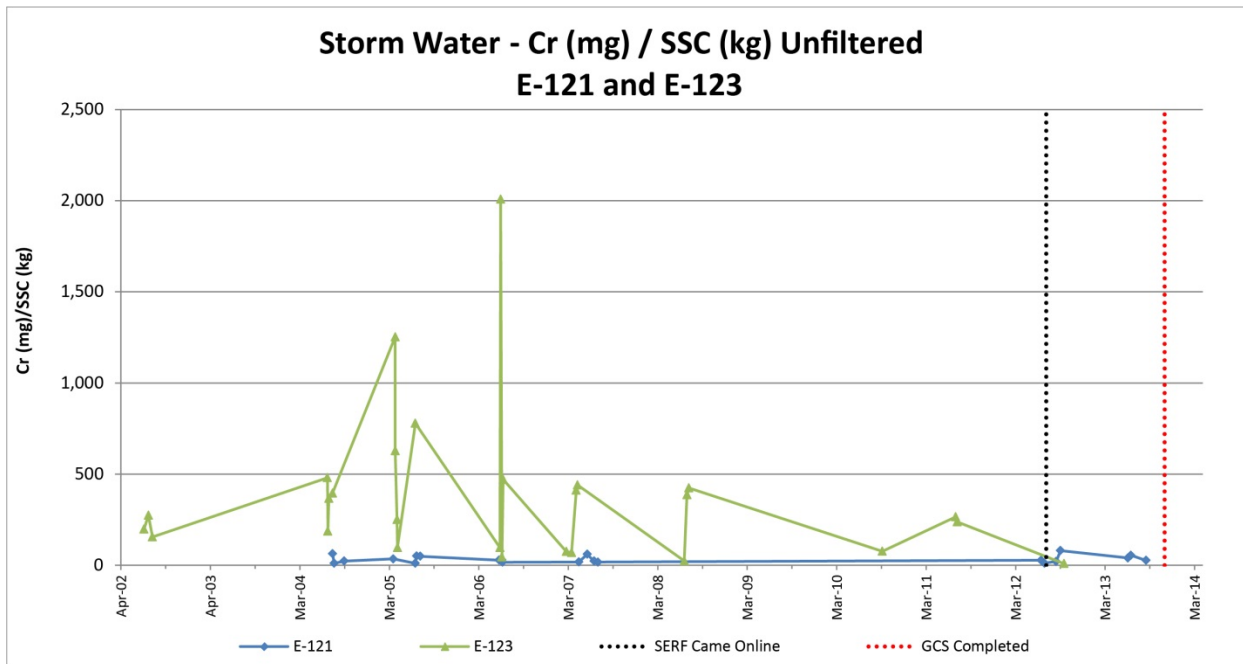
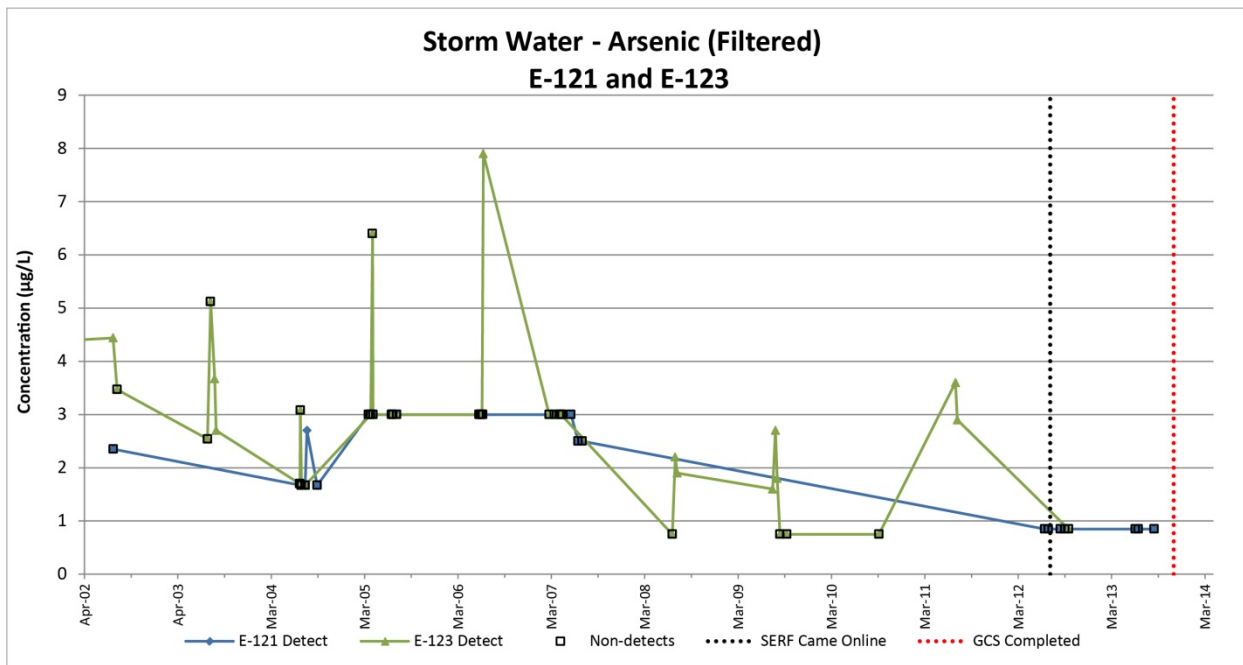
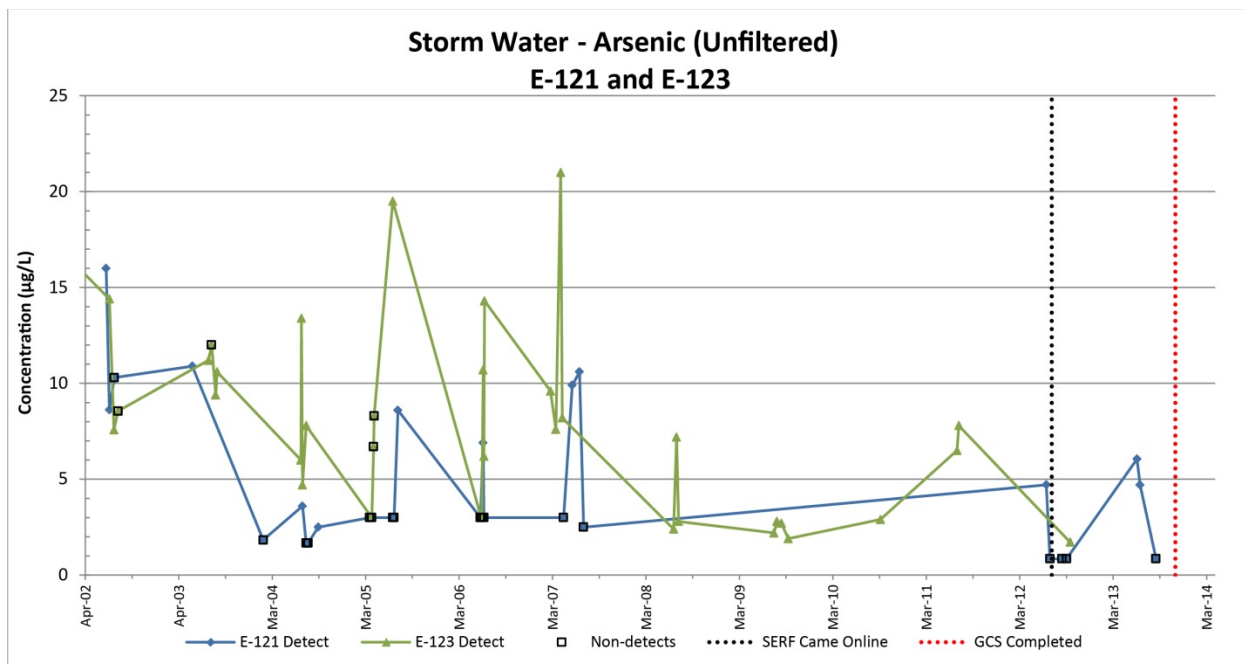


Figure C-1.0-17 Time-series plot showing unfiltered chromium normalized to SSC in storm water at gaging stations E121 and E123



Non-detect values are estimates when above the MDL; otherwise values equal to half the MDL are used

Figure C-1.0-18 Time-series plot showing filtered arsenic concentrations in storm water at gaging stations E121 and E123



Non-detect values are estimates when above the MDL; otherwise values equal to half the MDL are used

Figure C-1.0-19 Time-series plot showing unfiltered arsenic concentrations in storm water at gaging stations E121 and E123

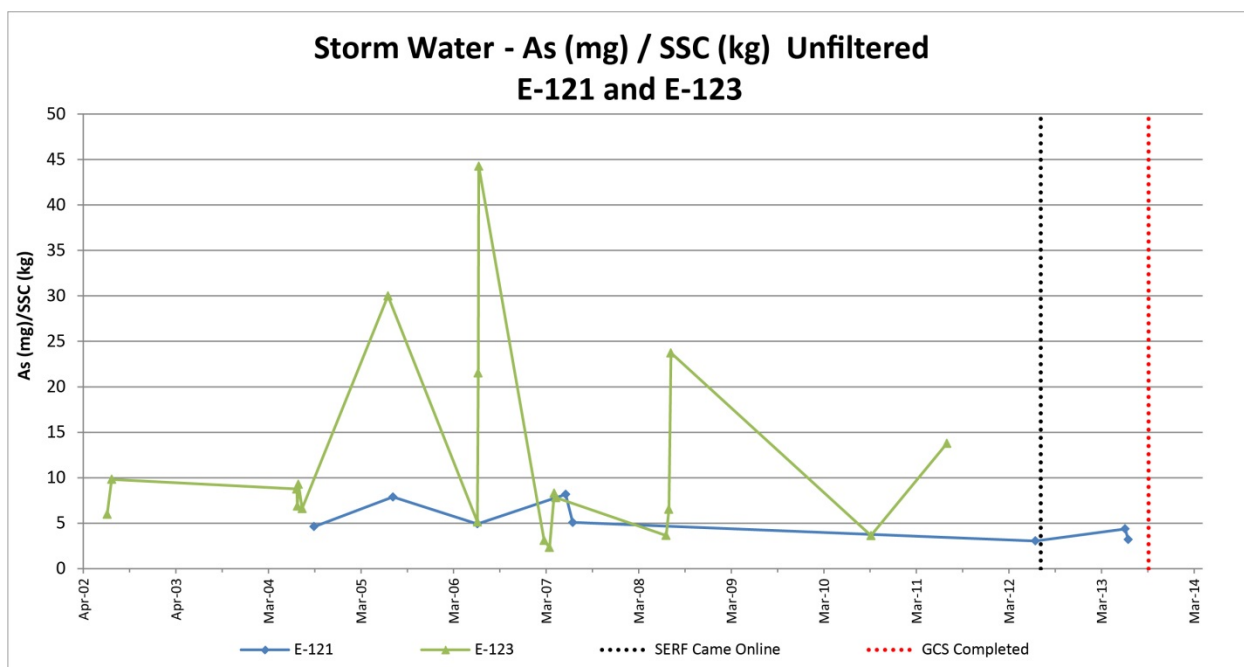


Figure C-1.0-20 Time-series plot showing unfiltered arsenic normalized to SSC in storm water at gaging stations E121 and E123

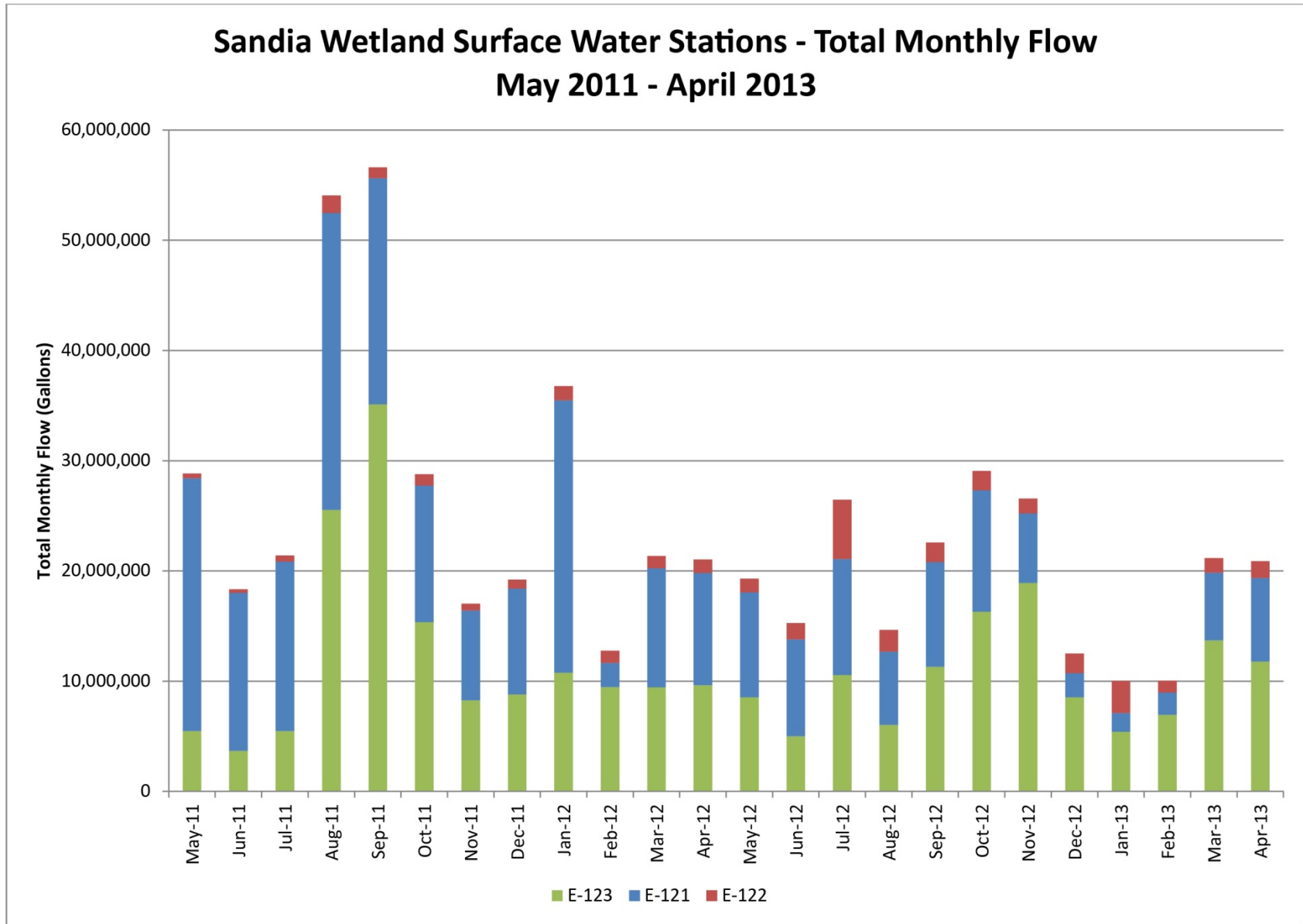


Figure C-1.0-21 Hydrograph for gaging stations E121, E122, and E123

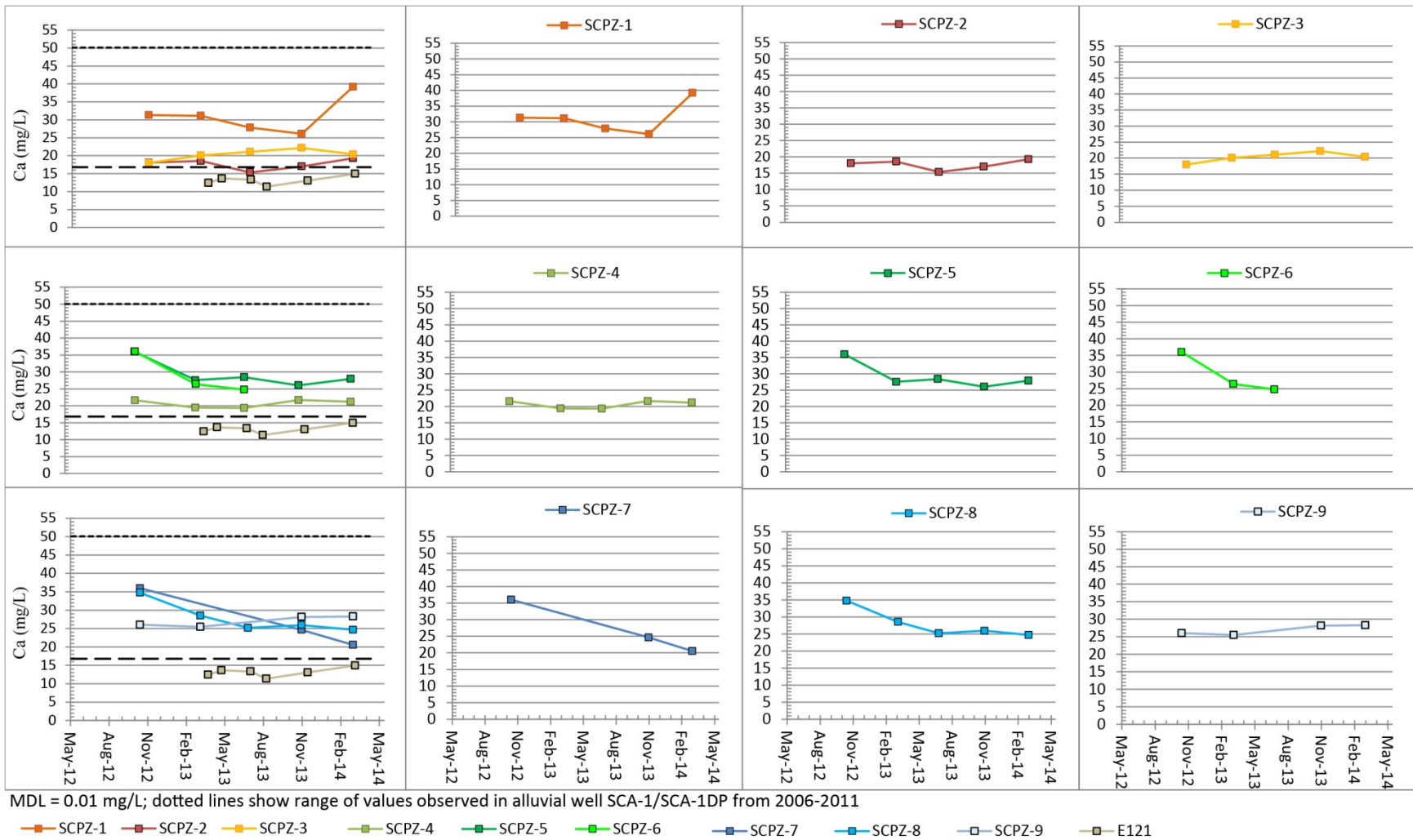


Figure C-2.0-1 Time-series plot showing calcium concentrations at Sandia Canyon piezometers and gaging station E121

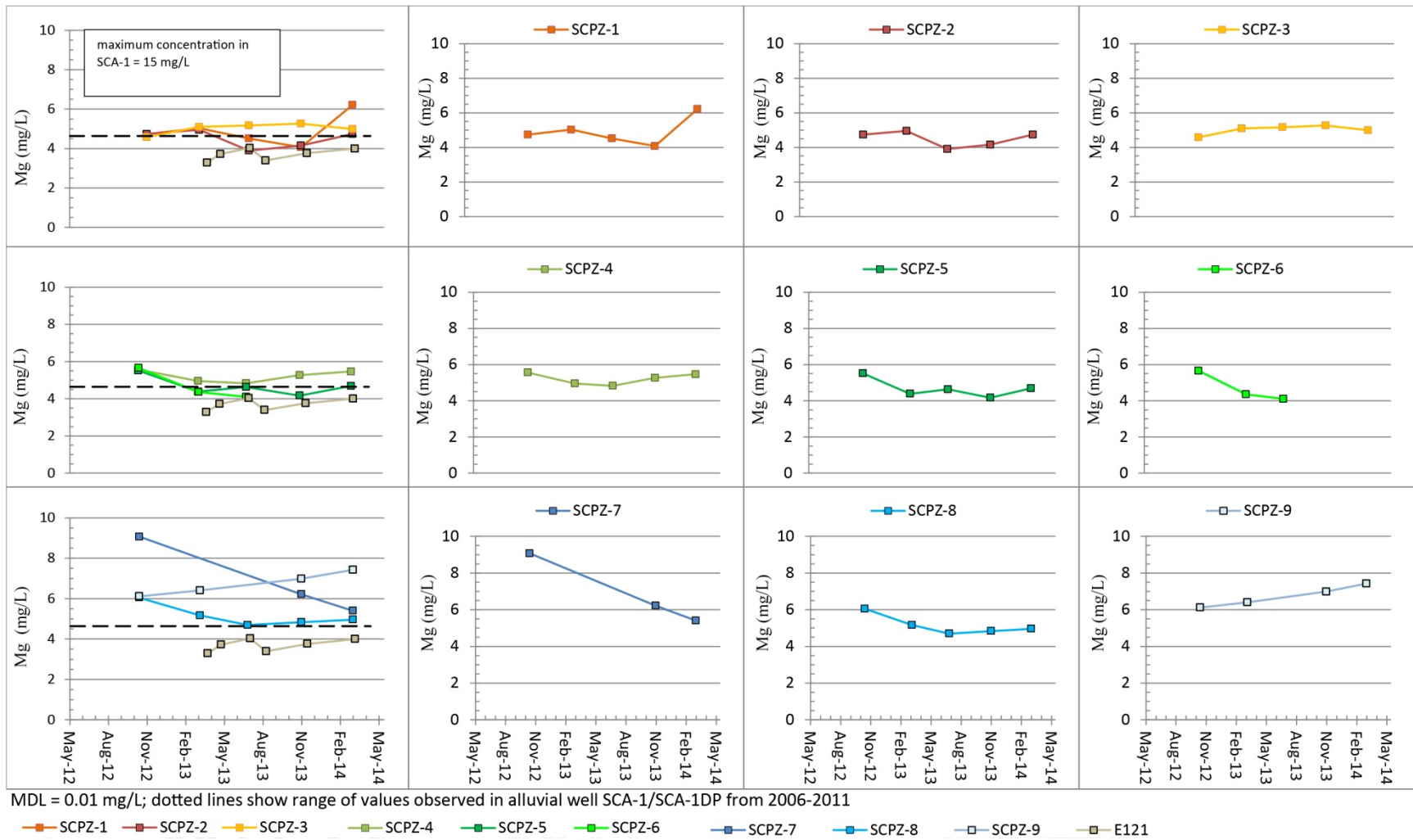


Figure C-2.0-2 Time-series plot showing magnesium concentrations at Sandia Canyon piezometers and gaging station E121

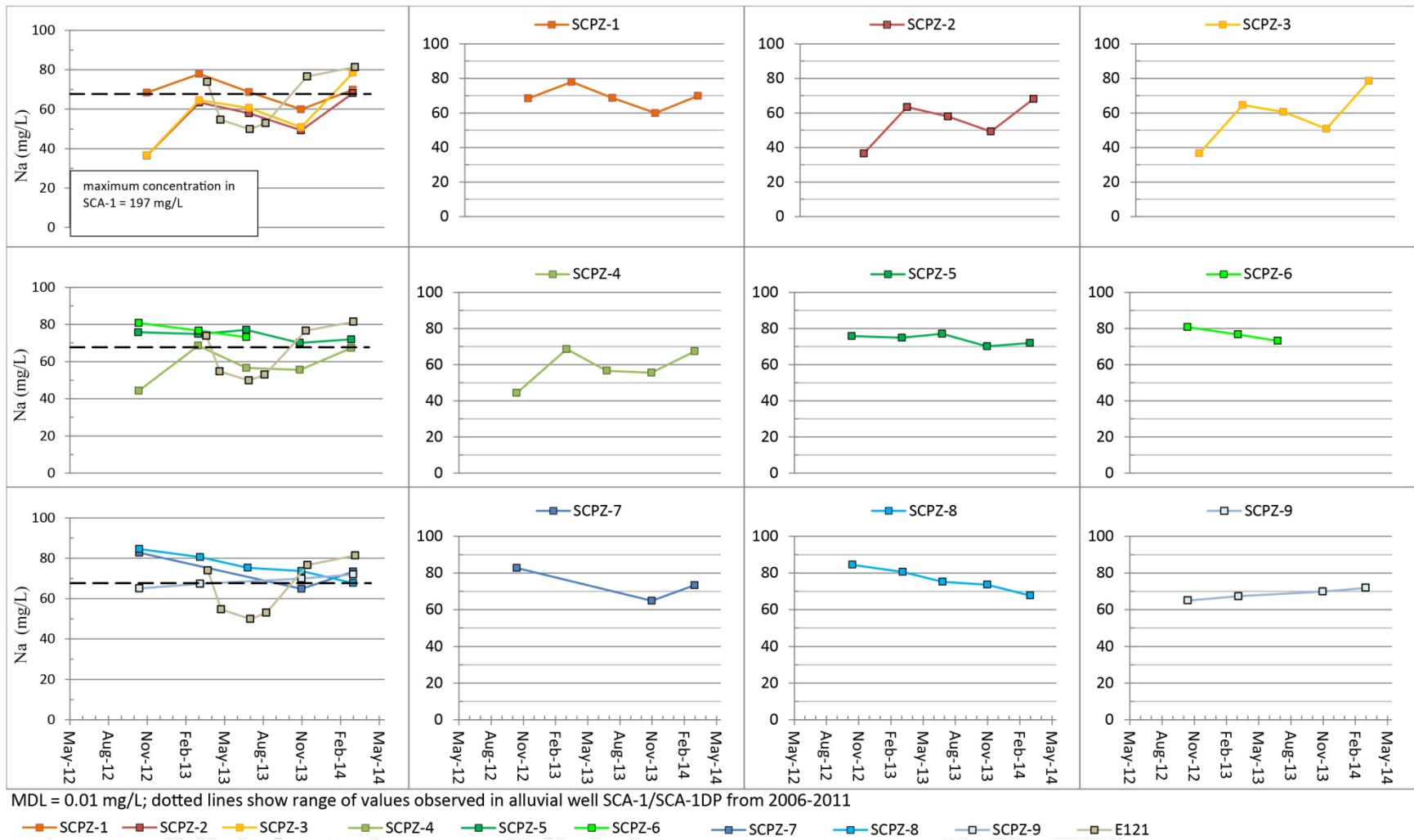


Figure C-2.0-3 Time-series plot showing sodium concentrations at Sandia Canyon piezometers and gaging station E121

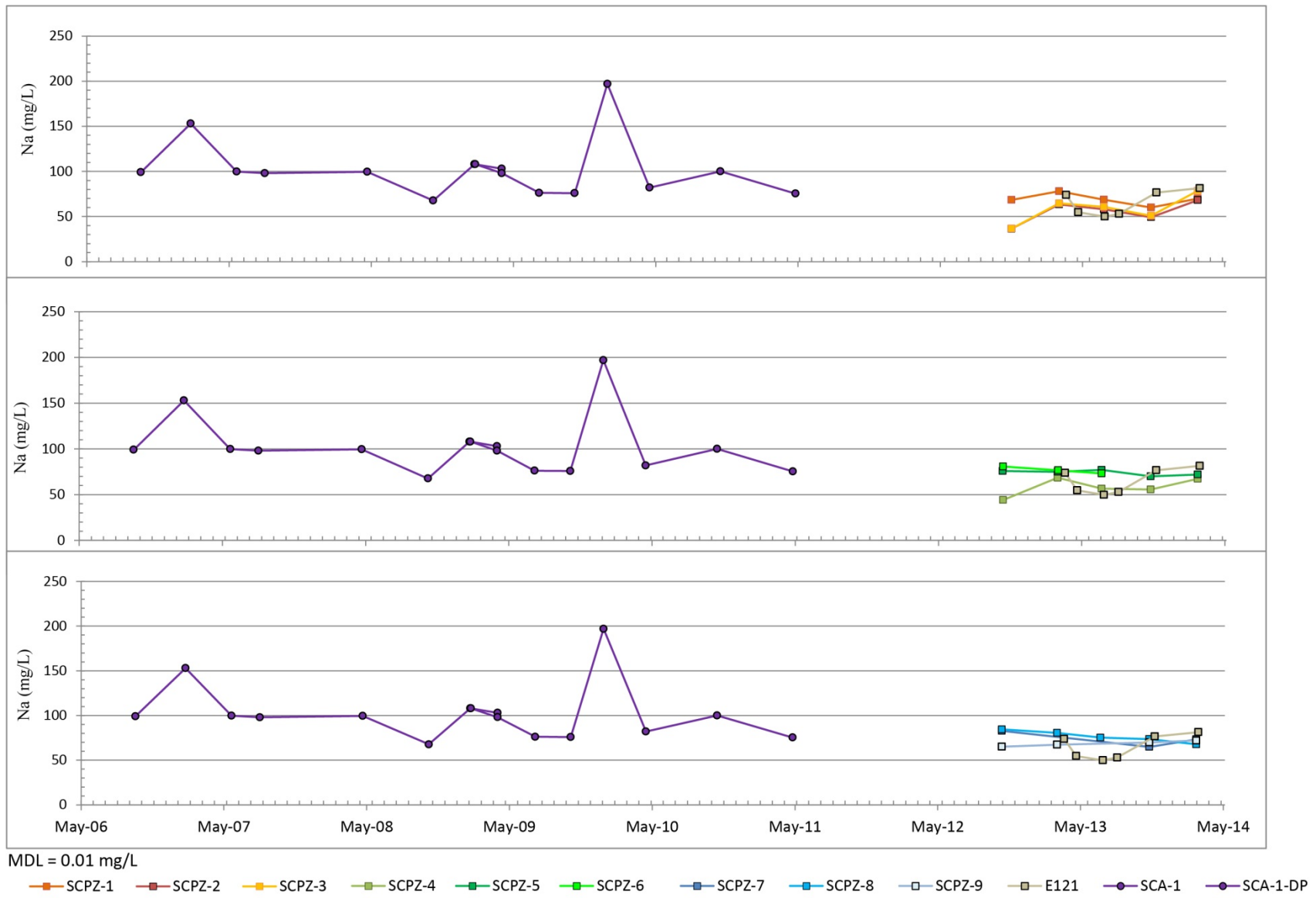


Figure C-2.0-4 Extended time-series plot showing sodium concentrations at Sandia Canyon piezometers and gaging station E121 and at alluvial wells SCA-1 and SCA-1 DP

C-18

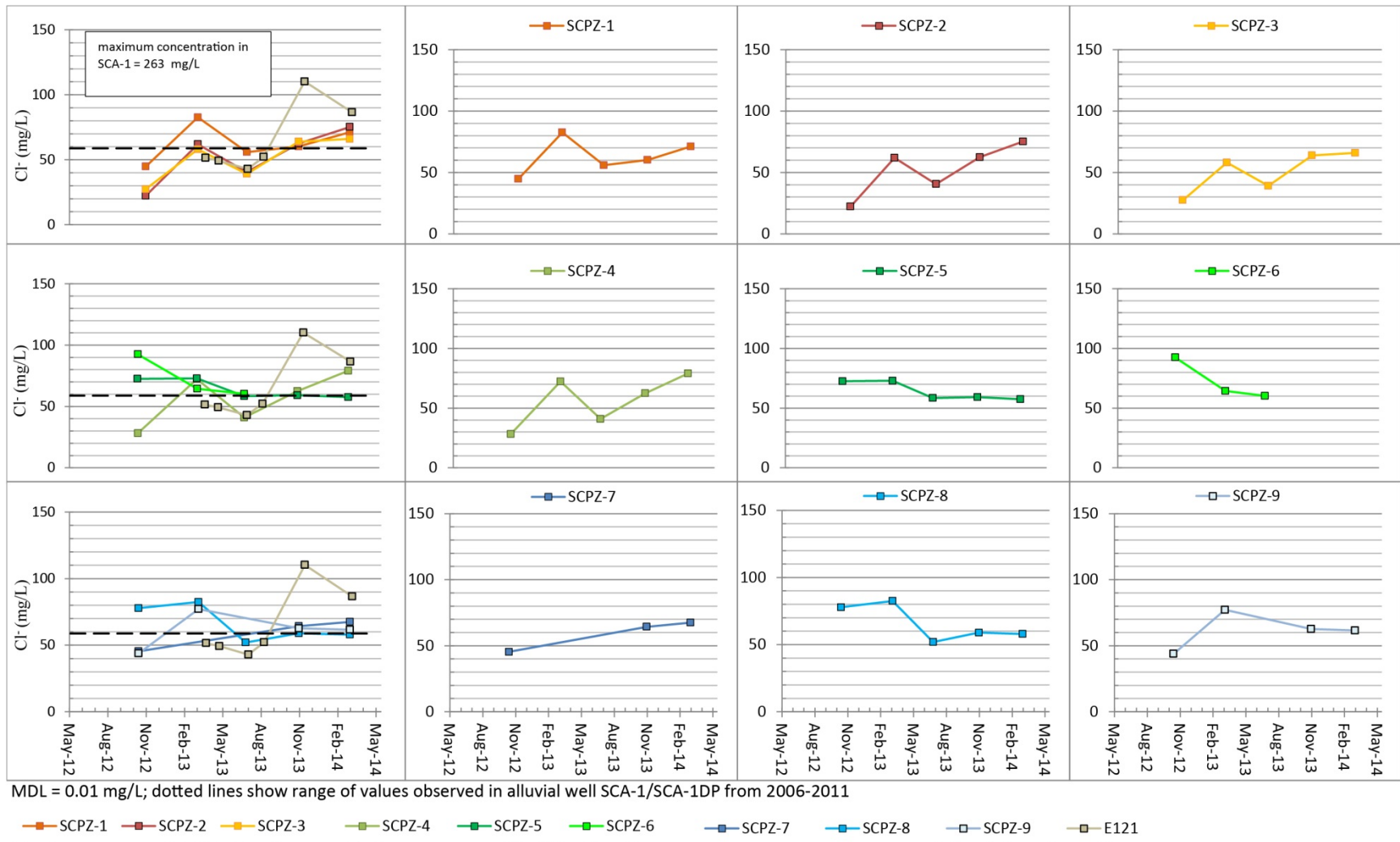
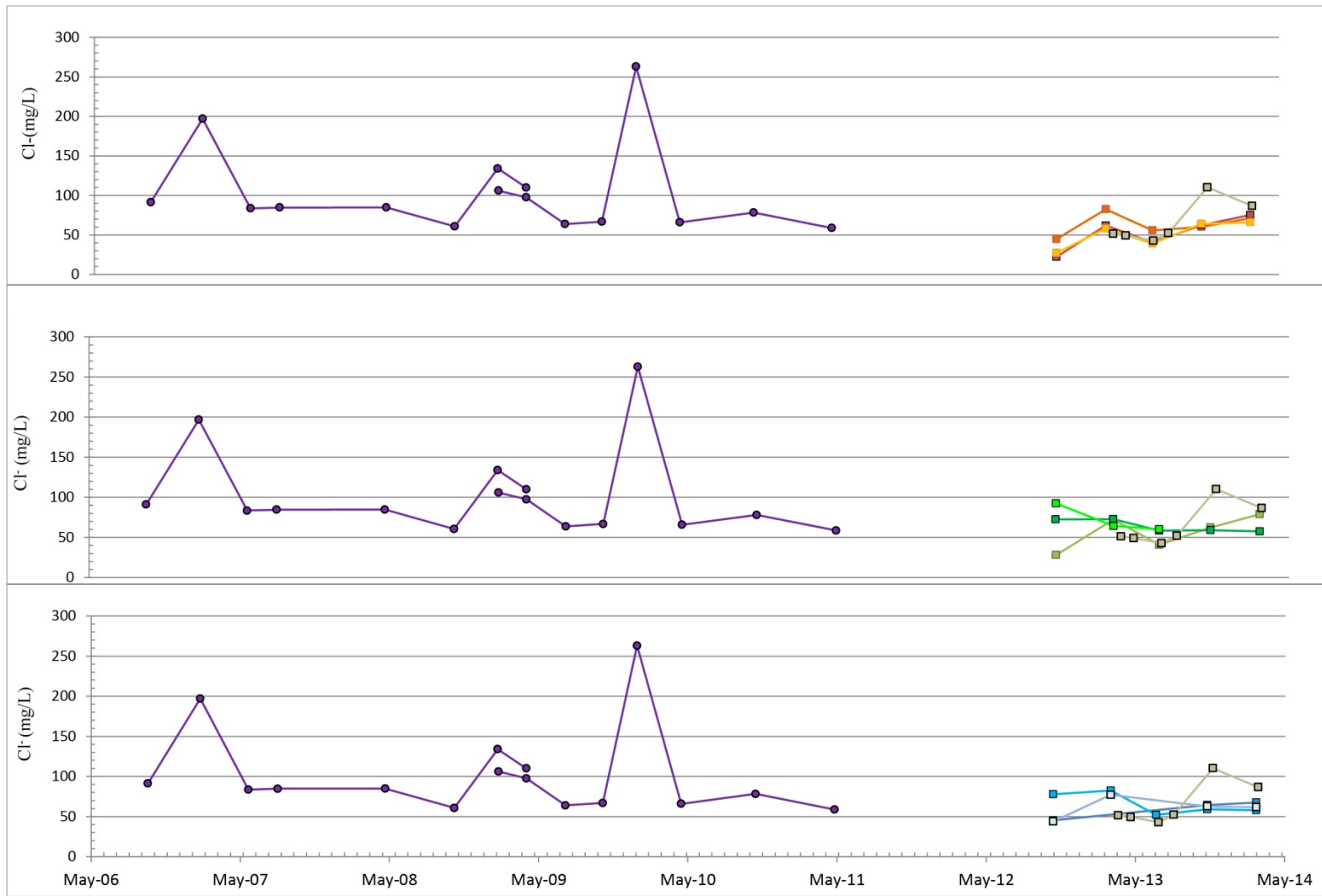


Figure C-2.0-5 Time-series plot showing chloride concentrations at Sandia Canyon piezometers and gaging station E121



MDL = 0.01 mg/L; dotted lines show range of values observed in alluvial well SCA-1/SCA-1DP from 2006-2011

SCPZ-1 SCPZ-2 SCPZ-3 SCPZ-4 SCPZ-5 SCPZ-6 SCPZ-7 SCPZ-8 SCPZ-9 E121 SCA-1 SCA-1-DP

Figure C-2.0-6 Extended time-series plot showing chloride concentrations at Sandia Canyon piezometers and gaging station E121 and at alluvial wells SCA-1 and SCA-1 DP

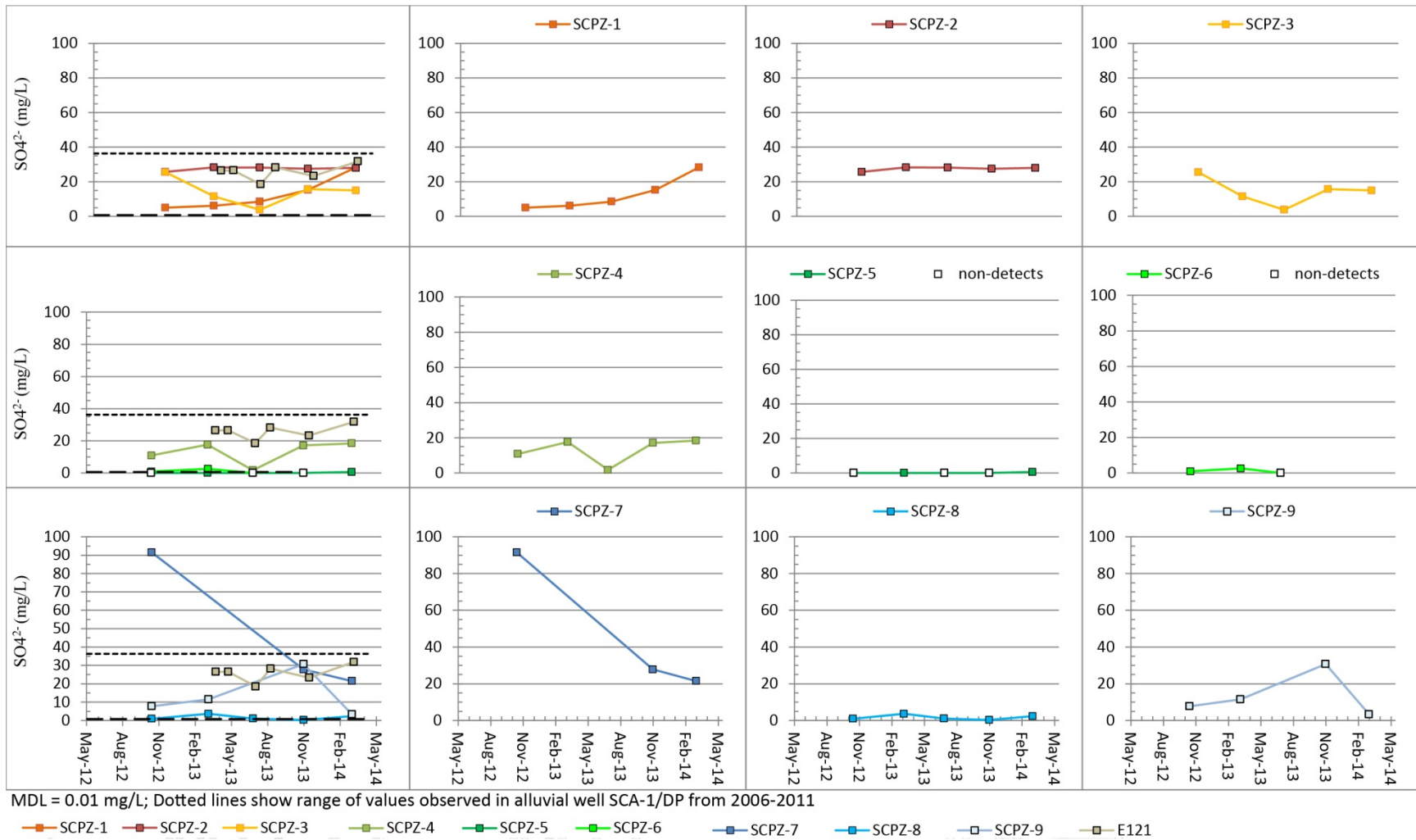


Figure C-2.0-7 Time-series plot showing sulfate concentrations at Sandia Canyon piezometers and gaging station E121

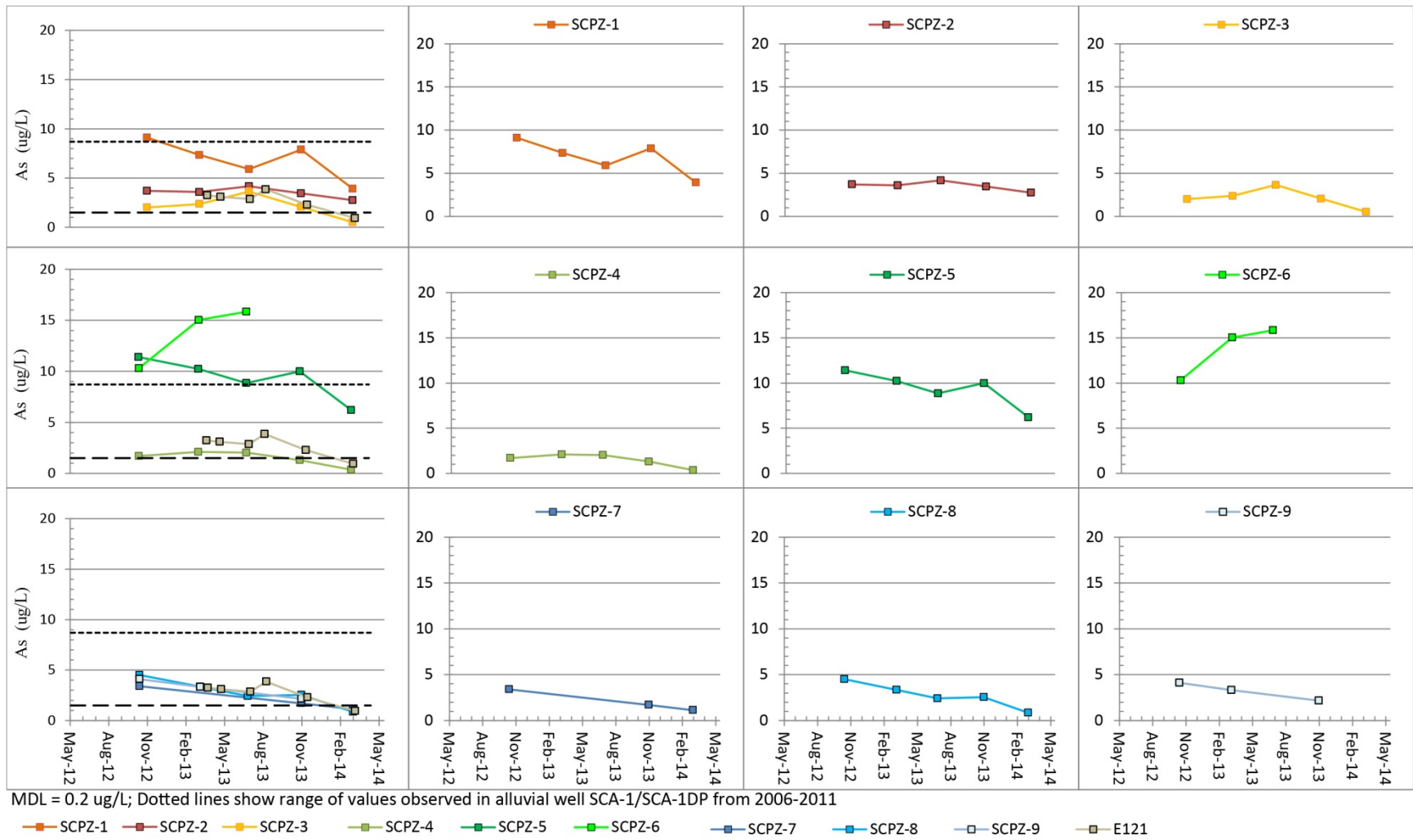


Figure C-2.0-8 Time-series plot showing arsenic concentrations at Sandia Canyon piezometers and gaging station E121

C-22

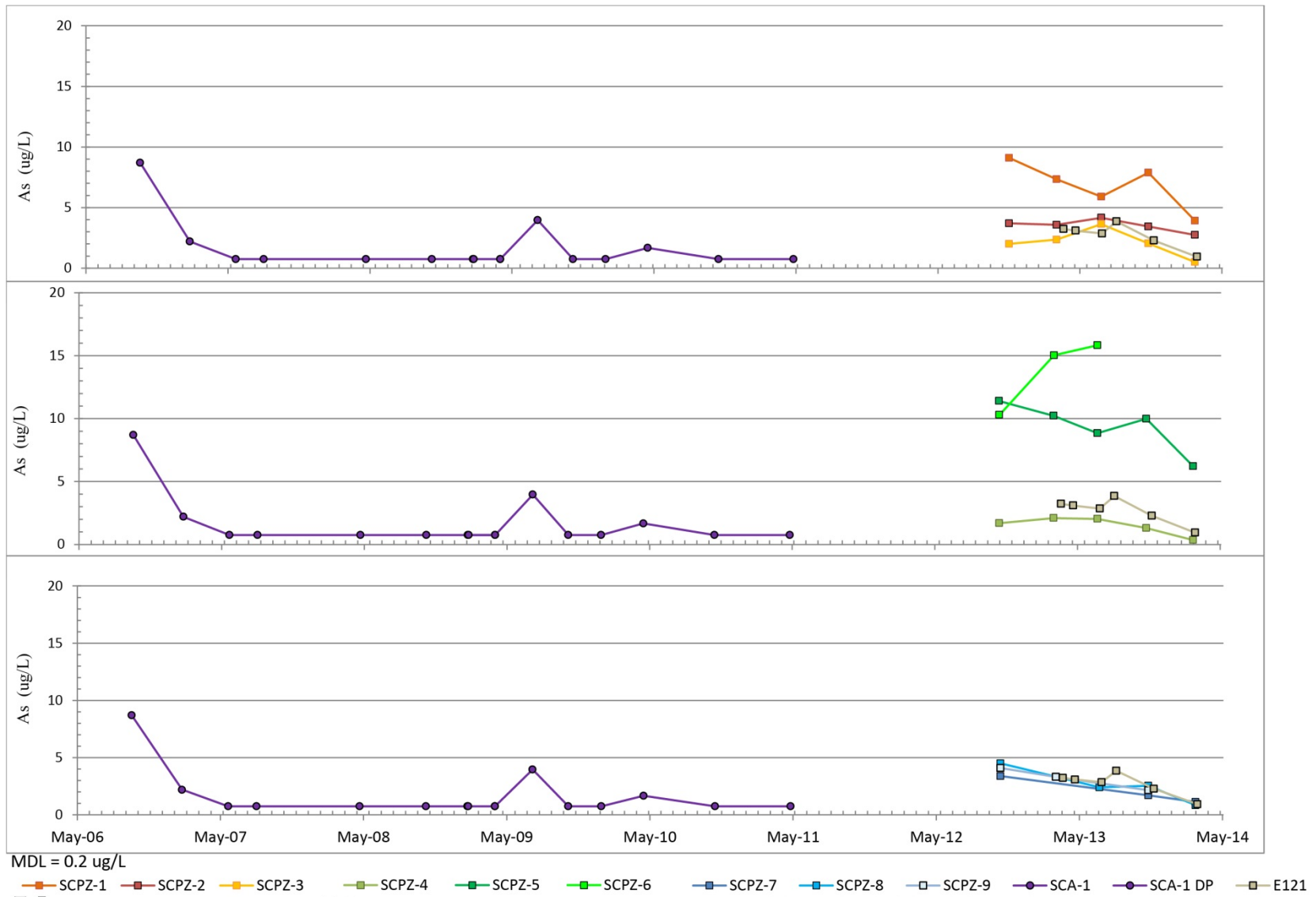


Figure C-2.0-9 Extended time-series plot showing arsenic concentrations at Sandia Canyon piezometers and gaging station E121 and at alluvial wells SCA-1 and SCA-1 DP

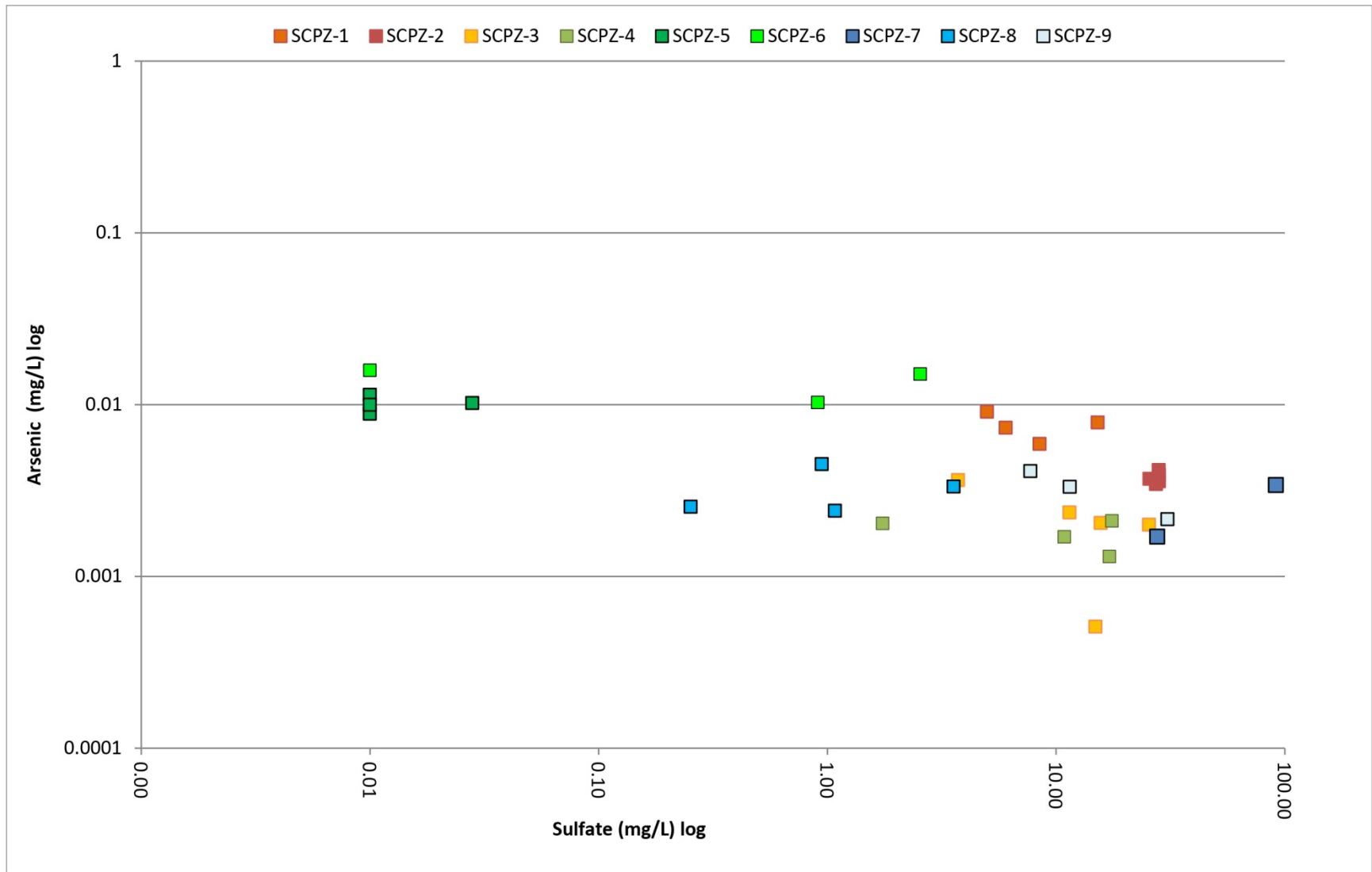
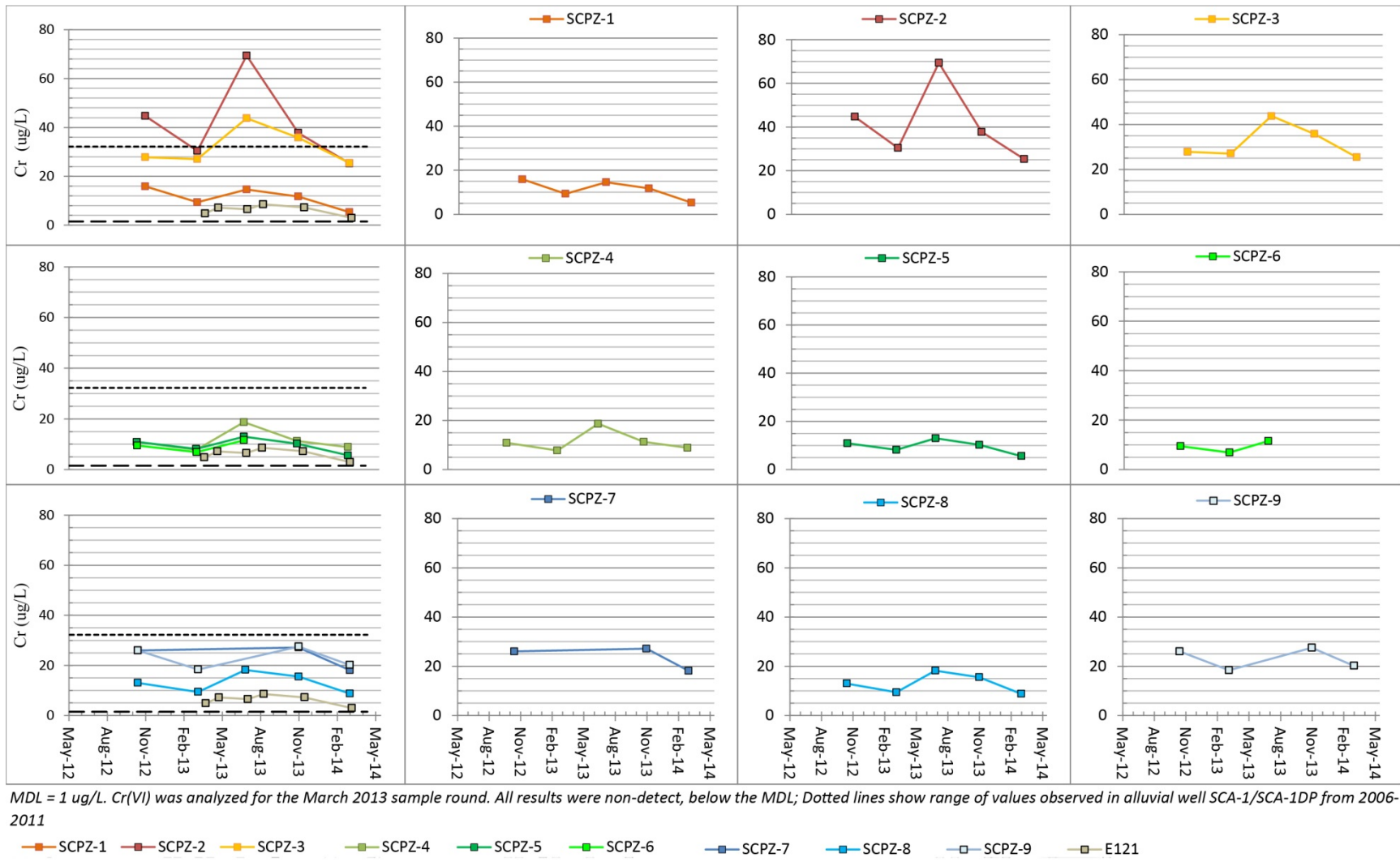


Figure C-2.0-10 Log-log cross plot of arsenic versus sulfate for Sandia Canyon piezometers



C-24

Figure C-2.0-11 Time-series plot showing chromium concentrations at Sandia Canyon piezometers and gaging station E121

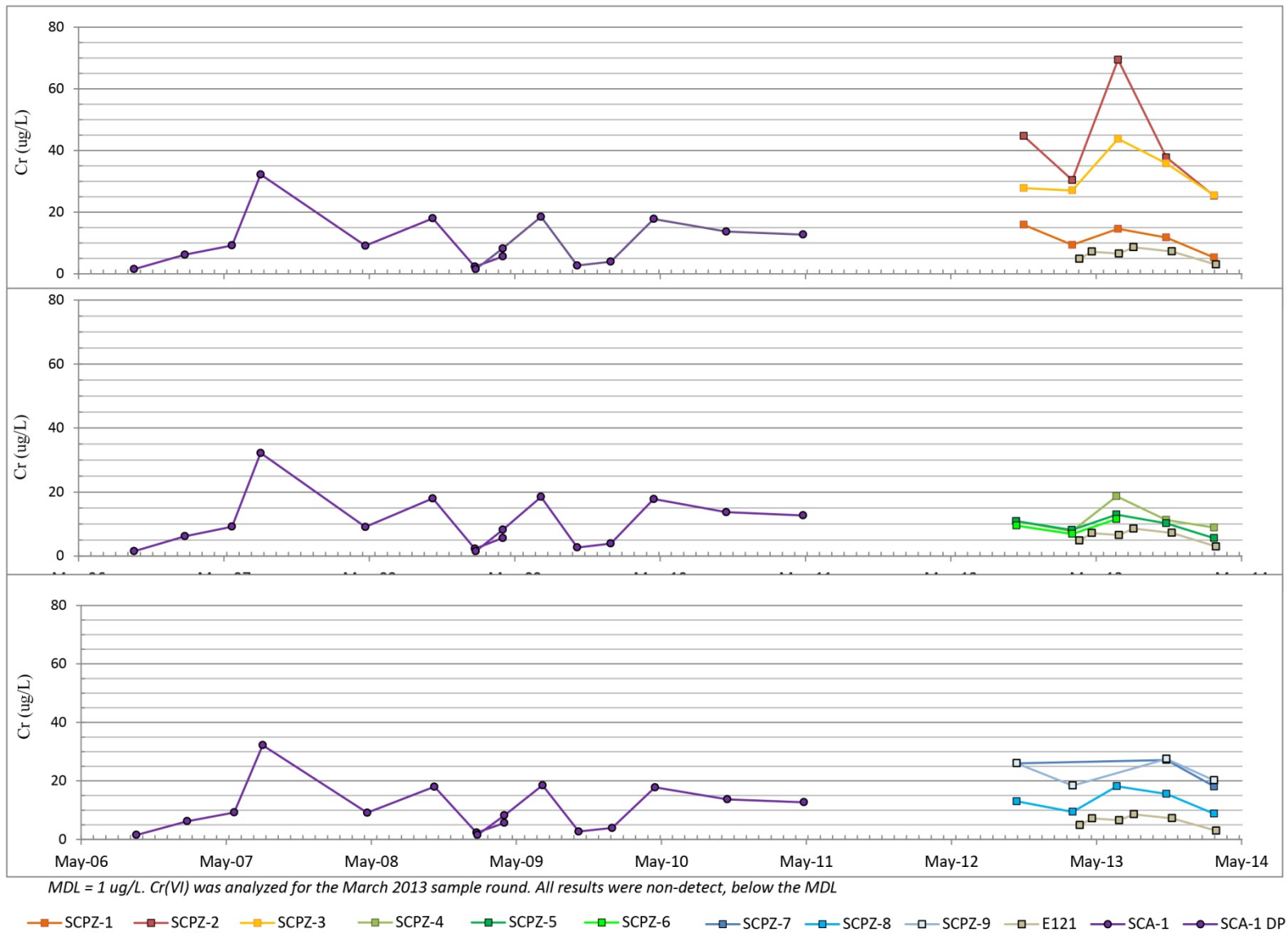


Figure C-2.0-12 Extended time-series plot showing chromium concentrations at Sandia Canyon piezometers and gaging station E121 and at alluvial wells SCA-1 and SCA-1 DP

C-26

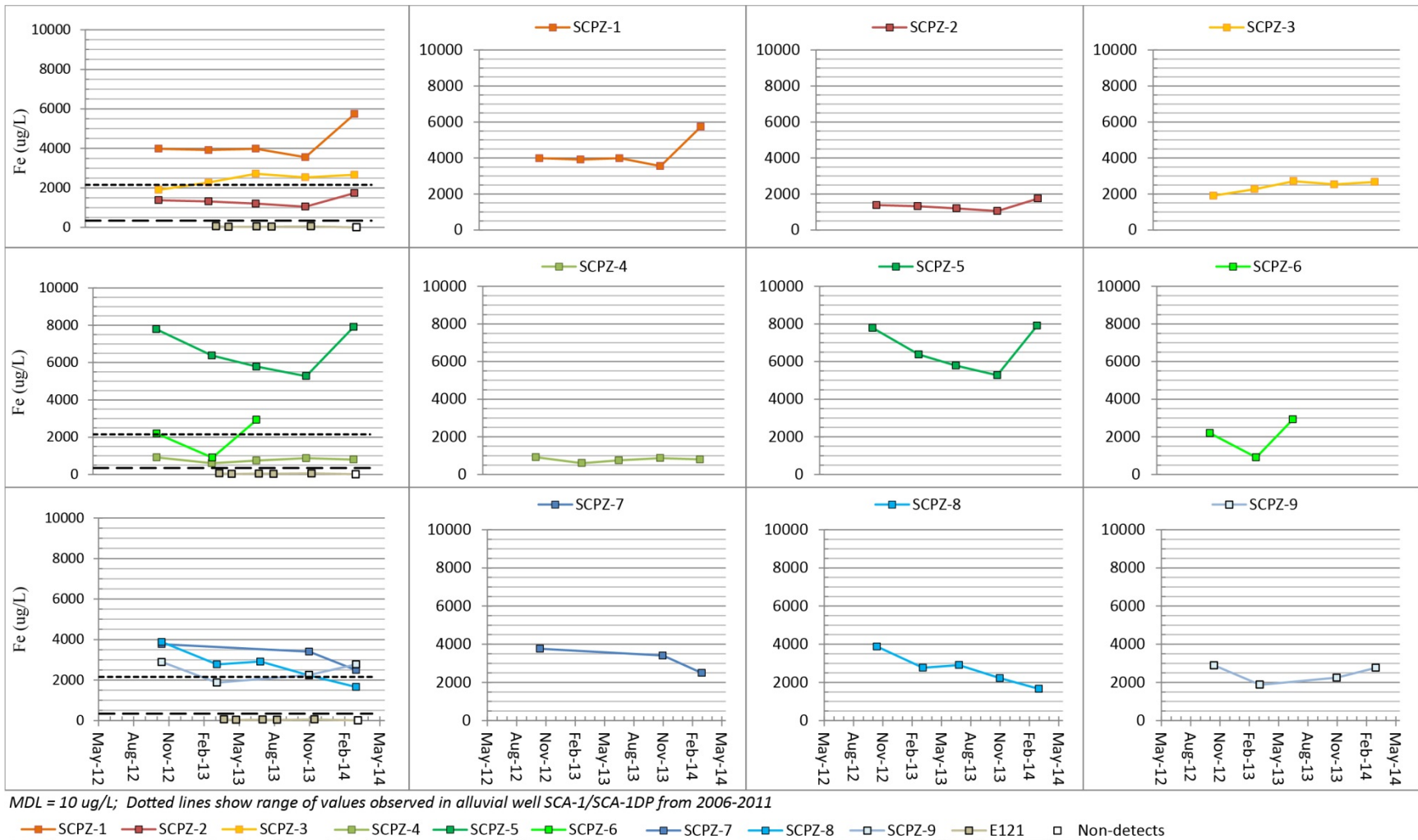


Figure C-2.0-13 Time-series plot showing iron concentrations at Sandia Canyon piezometers and gaging station E121

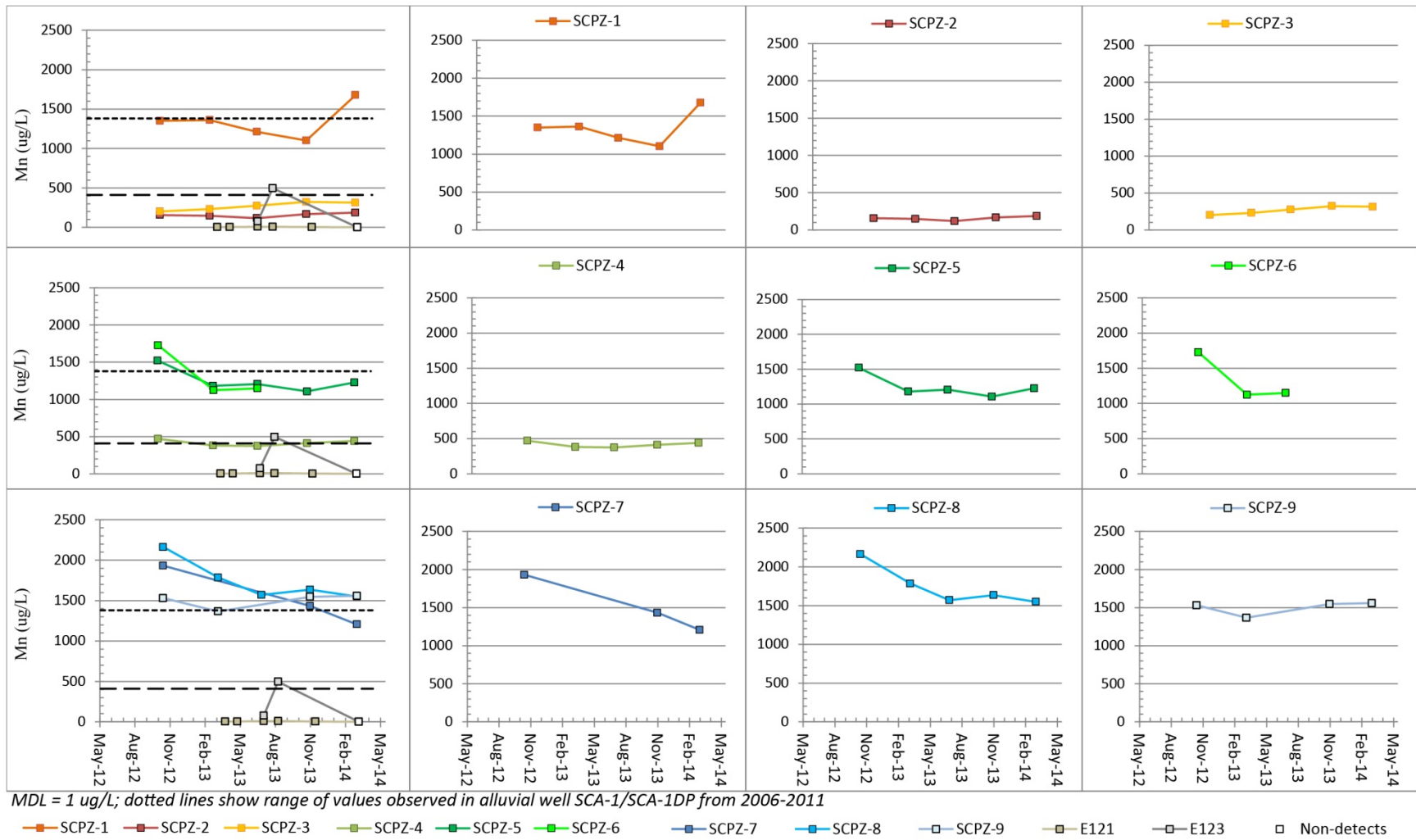


Figure C-2.0-14 Time-series plot showing manganese concentrations at Sandia Canyon piezometers and gaging stations E121 and E123

C-28

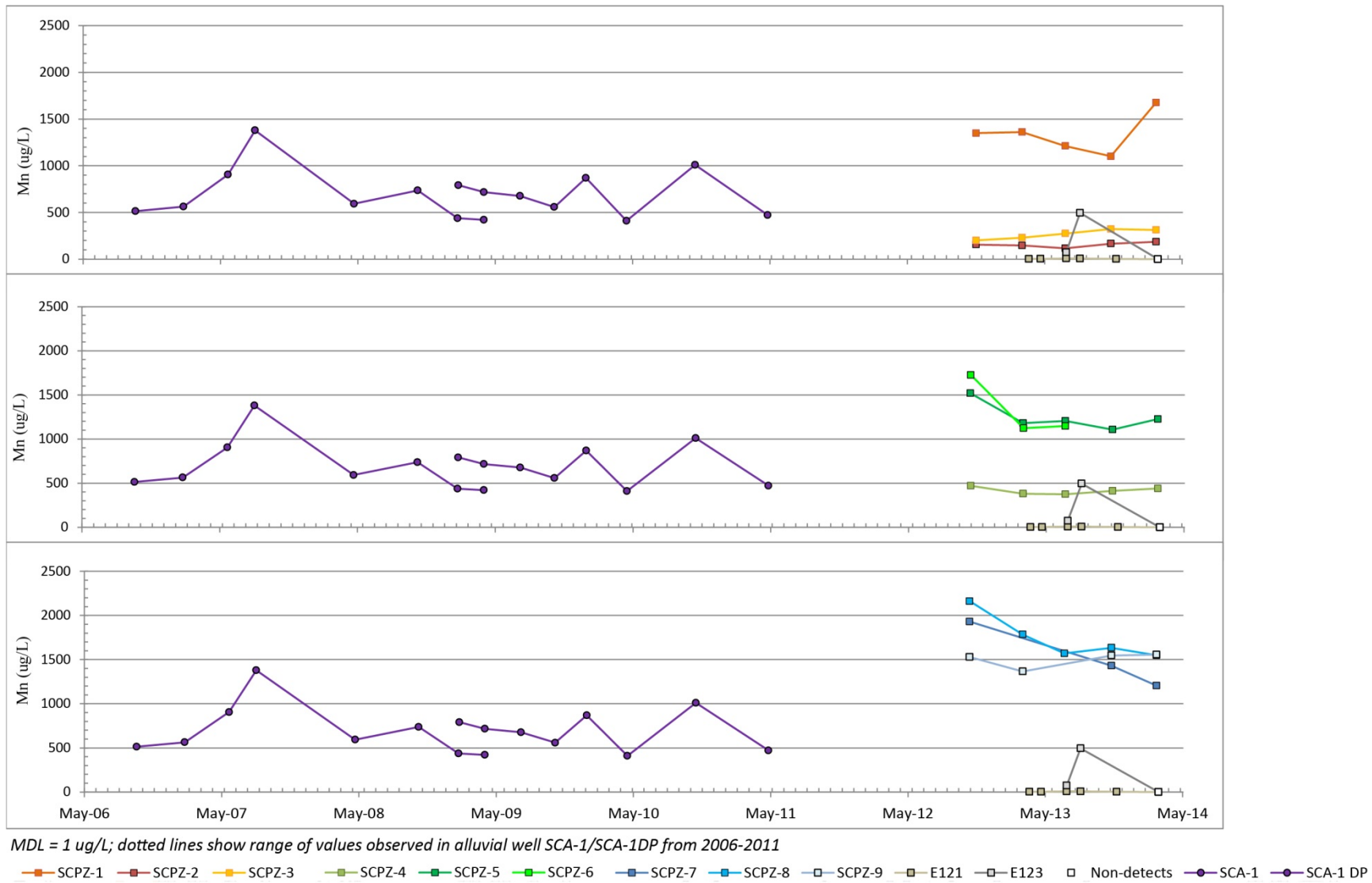


Figure C-2.0-15 Extended time-series plot showing manganese concentrations at Sandia Canyon piezometers and gaging stations E121 and E123 and at alluvial wells SCA-1 and SCA-1 DP

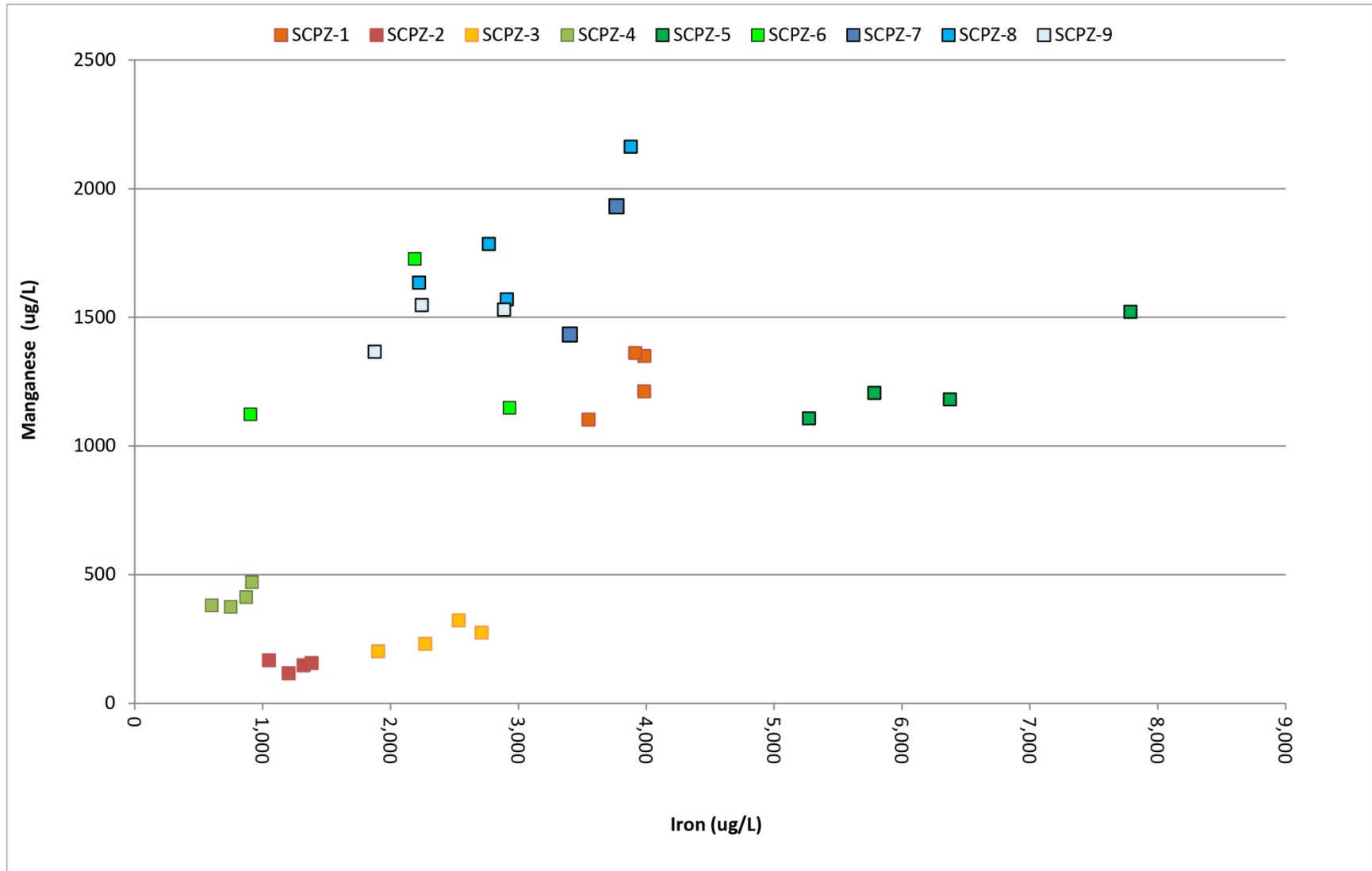


Figure C-2.0-16 Cross-plot of iron versus manganese for Sandia Canyon piezometers

C-30

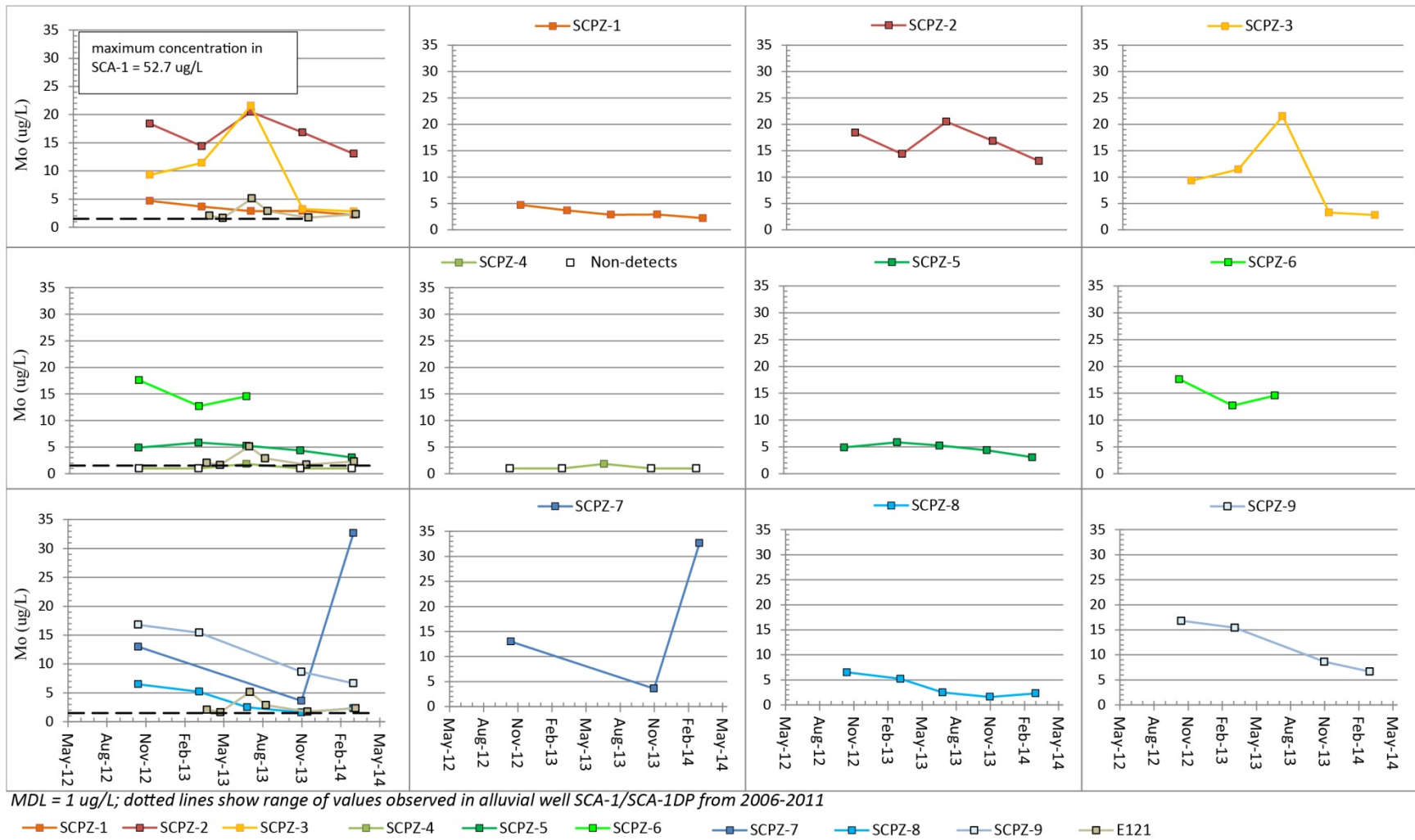


Figure C-2.0-17 Time-series plot showing molybdenum concentrations at Sandia Canyon piezometers and gaging station E121

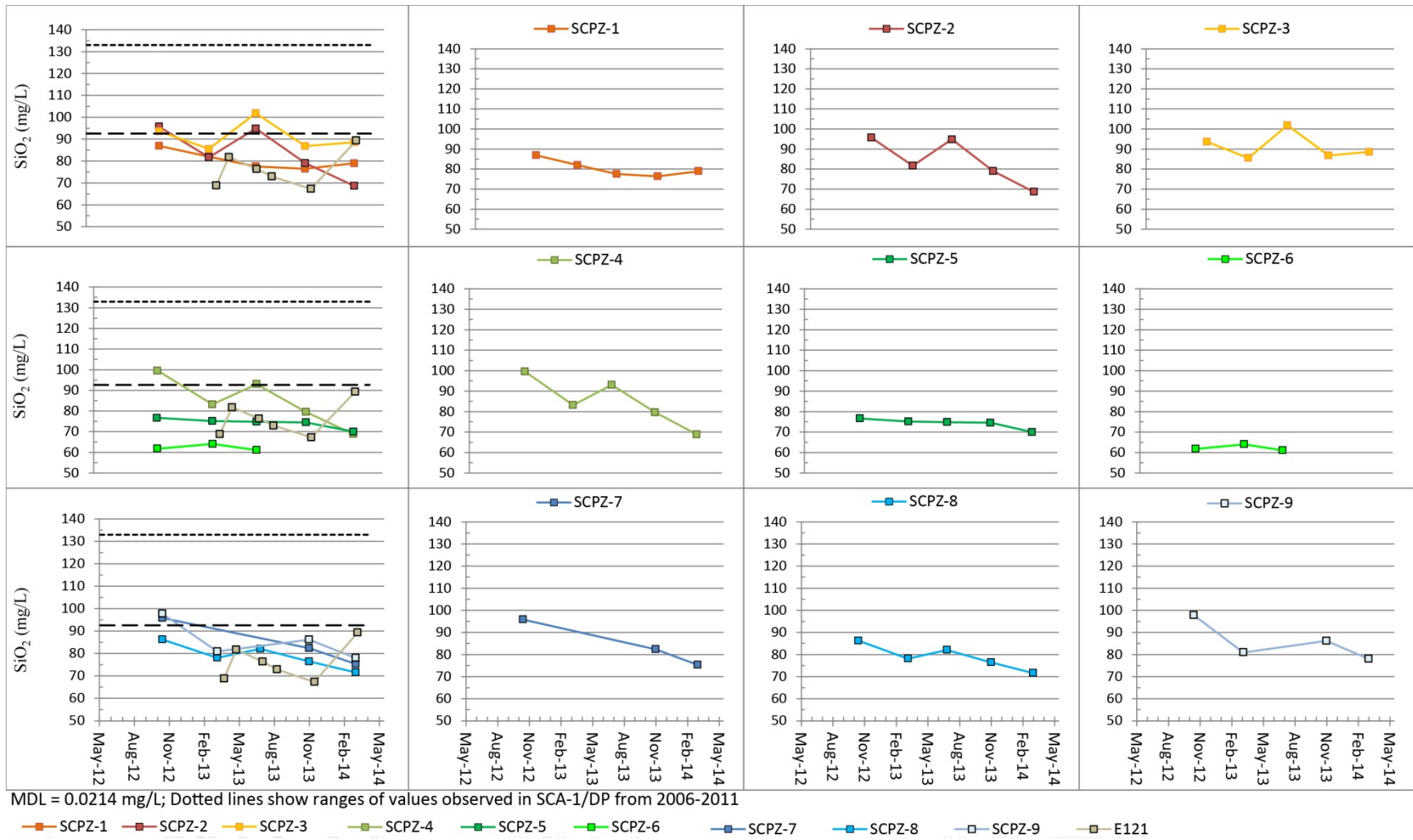


Figure C-2.0-18 Time-series plot showing silicon dioxide concentrations at Sandia Canyon piezometers and gaging station E121

C-32

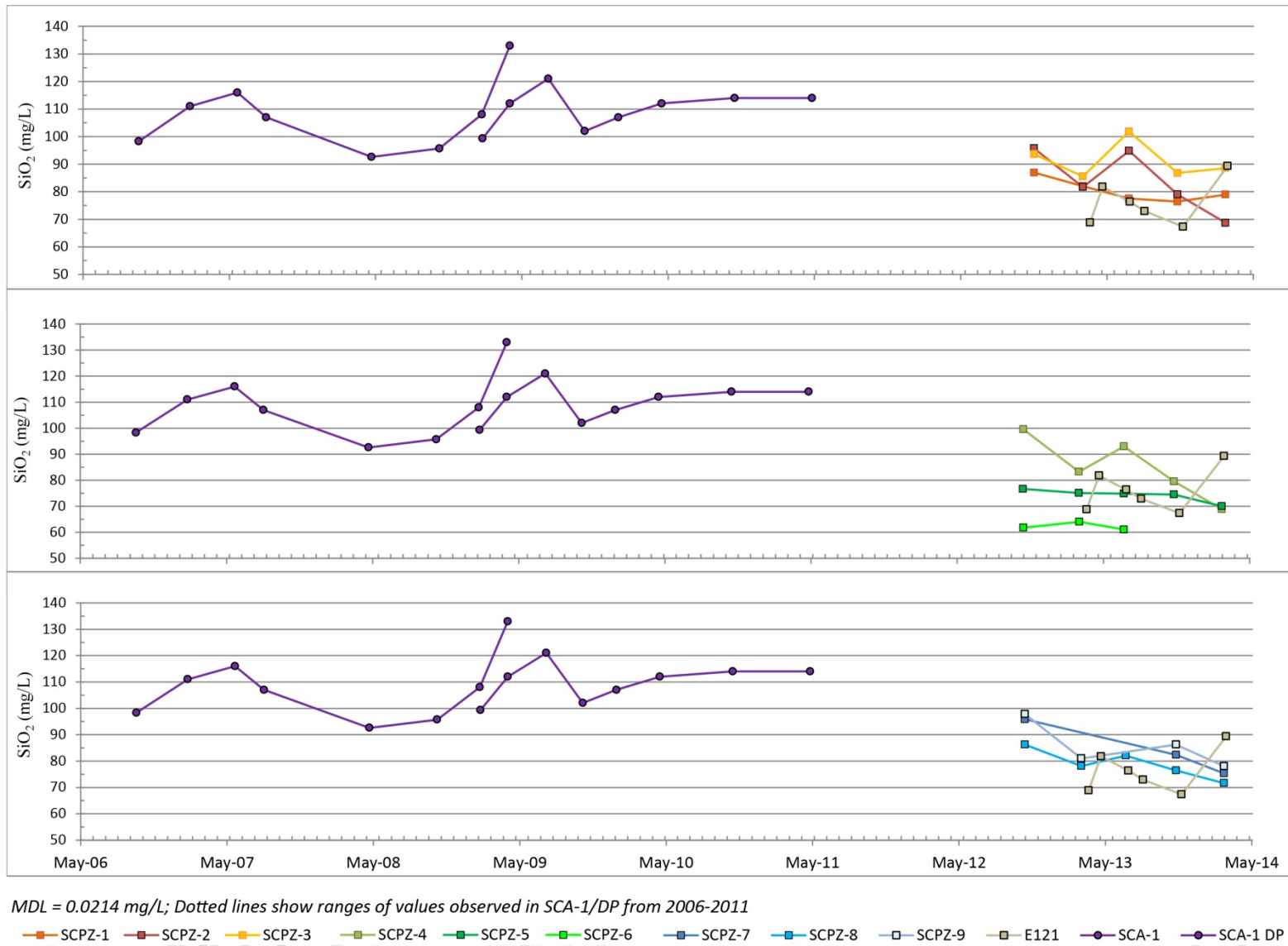


Figure C-2.0-19 Extended time-series plot showing silicon dioxide concentrations at Sandia Canyon piezometers and gaging station E121 and at alluvial wells SCA-1 and SCA-1 DP

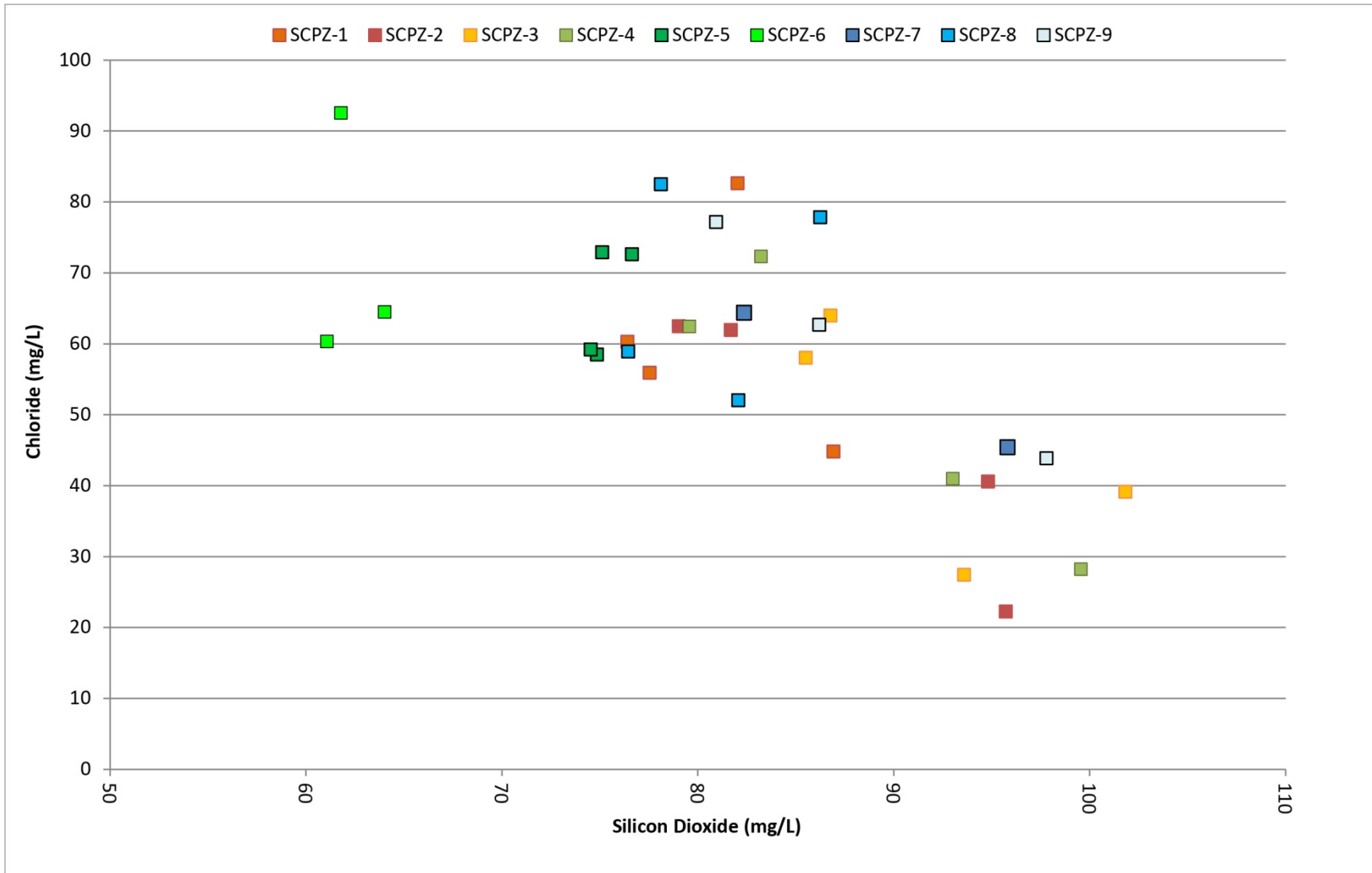


Figure C-2.0-20 Cross-plot of silicon dioxide versus chloride for Sandia Canyon piezometers

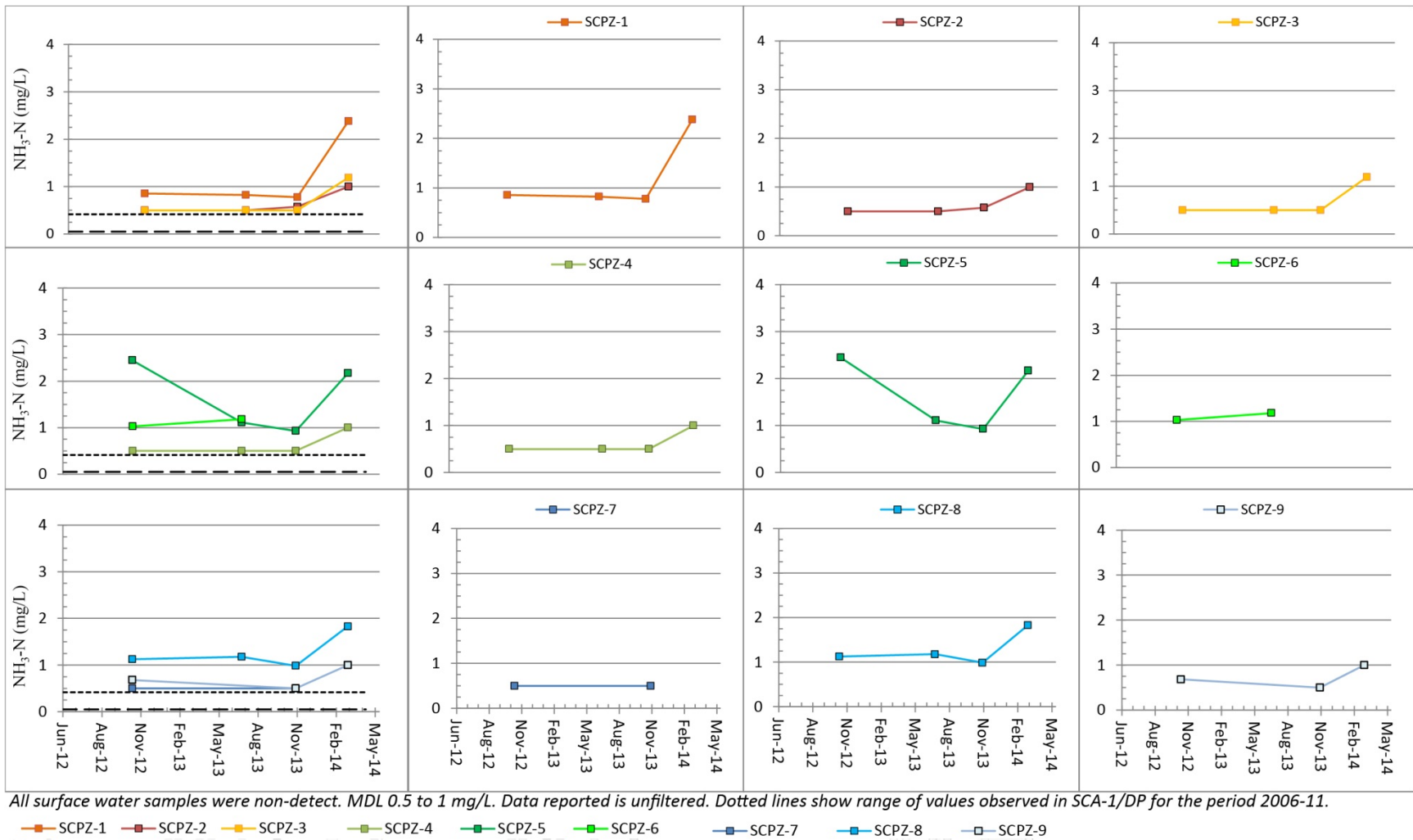


Figure C-2.0-21 Time-series plot showing ammonium concentrations at Sandia Canyon piezometers

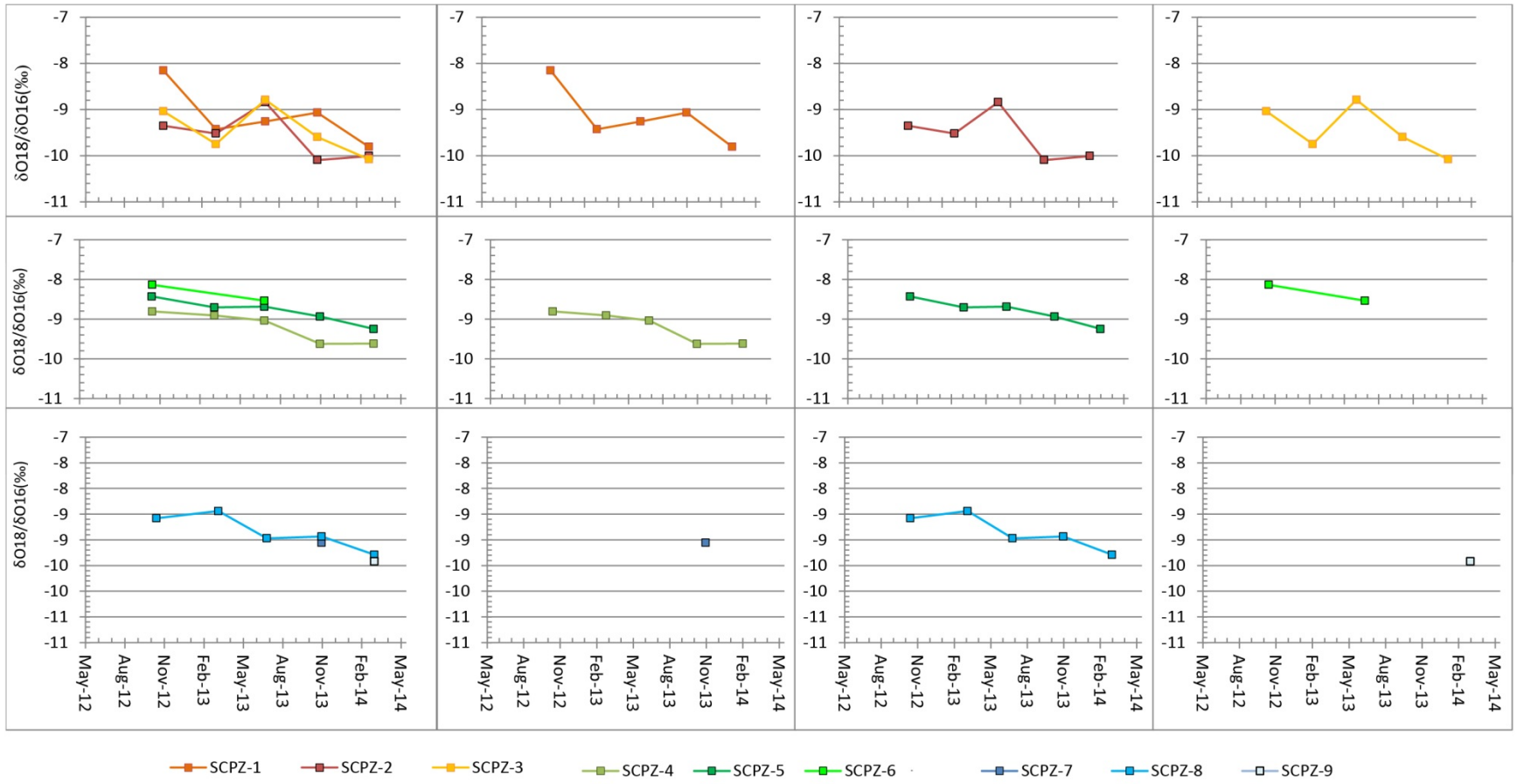


Figure C-2.0-22 Time-series plot showing oxygen isotopes at Sandia Canyon piezometers

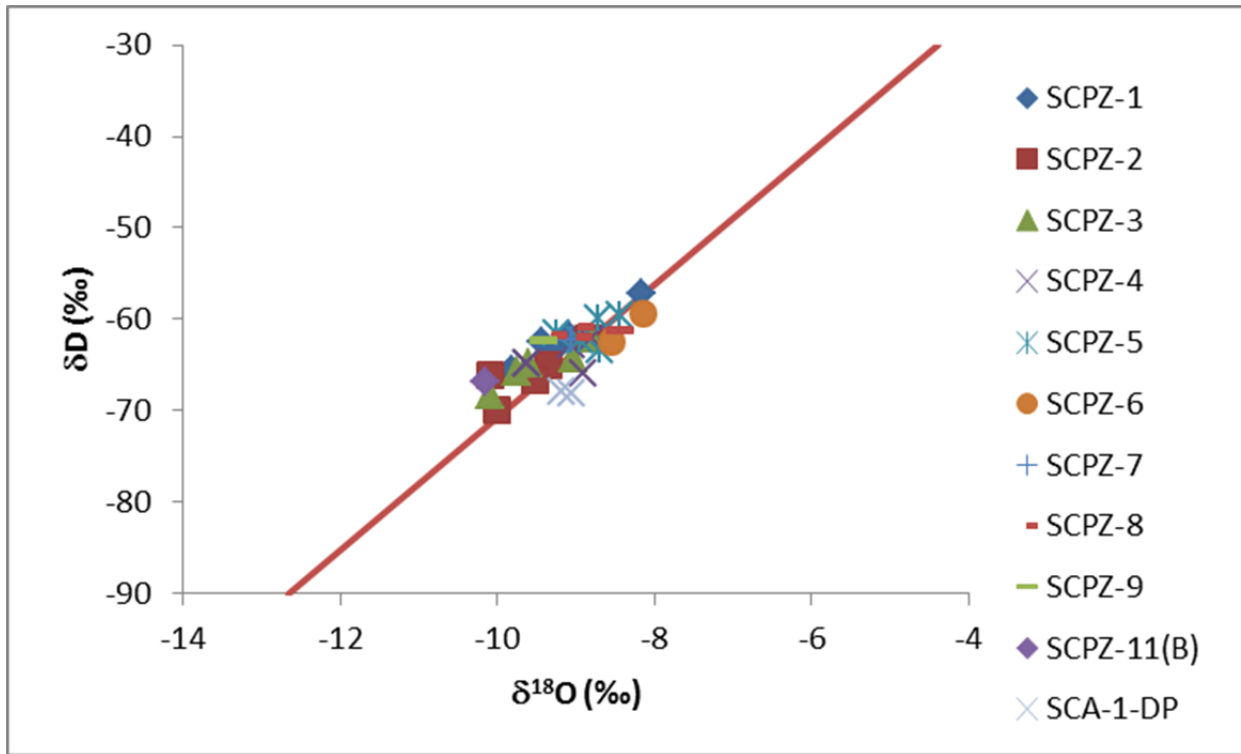


Figure C-2.0-23 Cross-plot of oxygen isotopes versus deuterium isotopes showing alluvial waters plotted on the local meteoric water line along with local rainfall and regional aquifer values

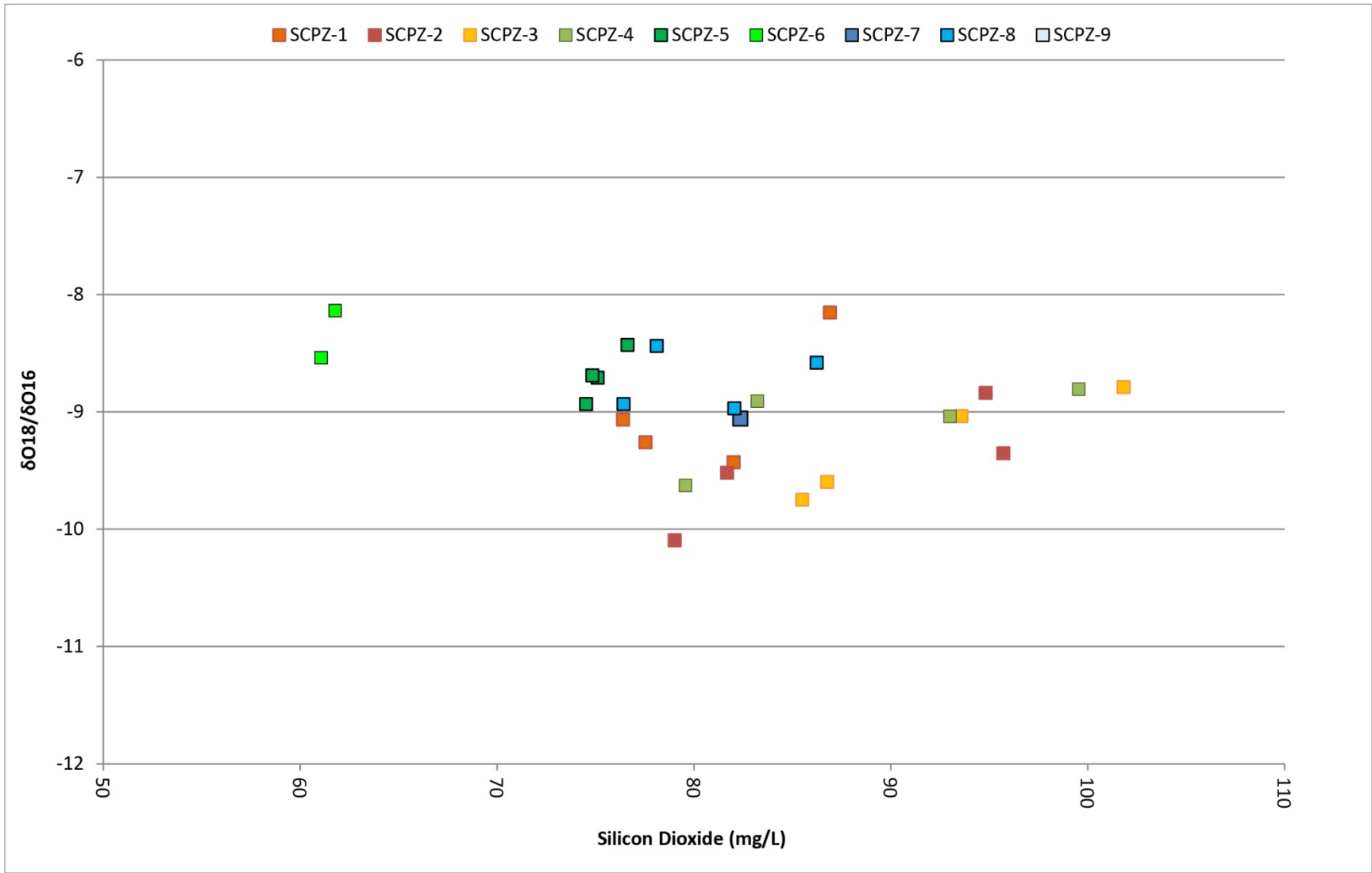
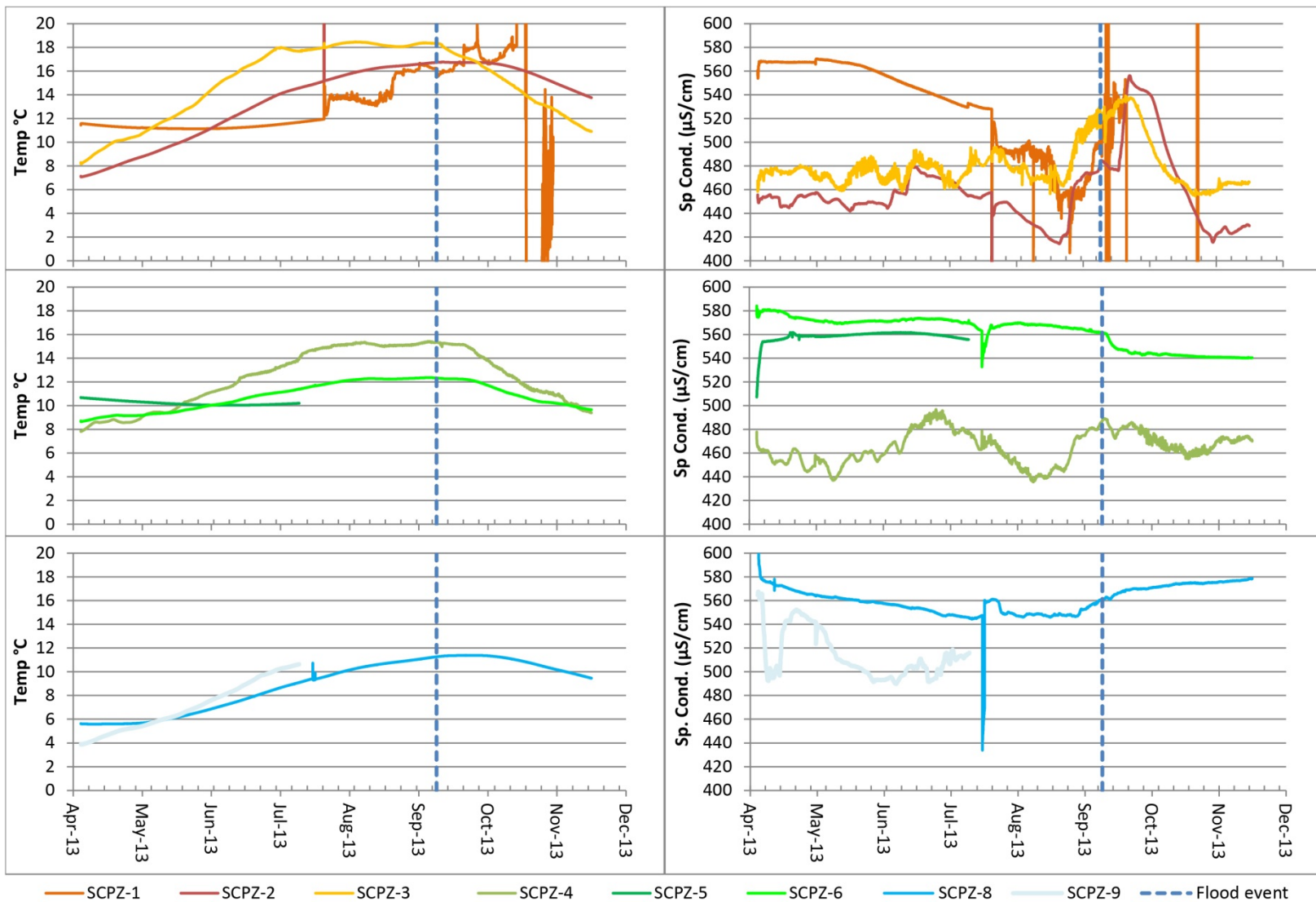


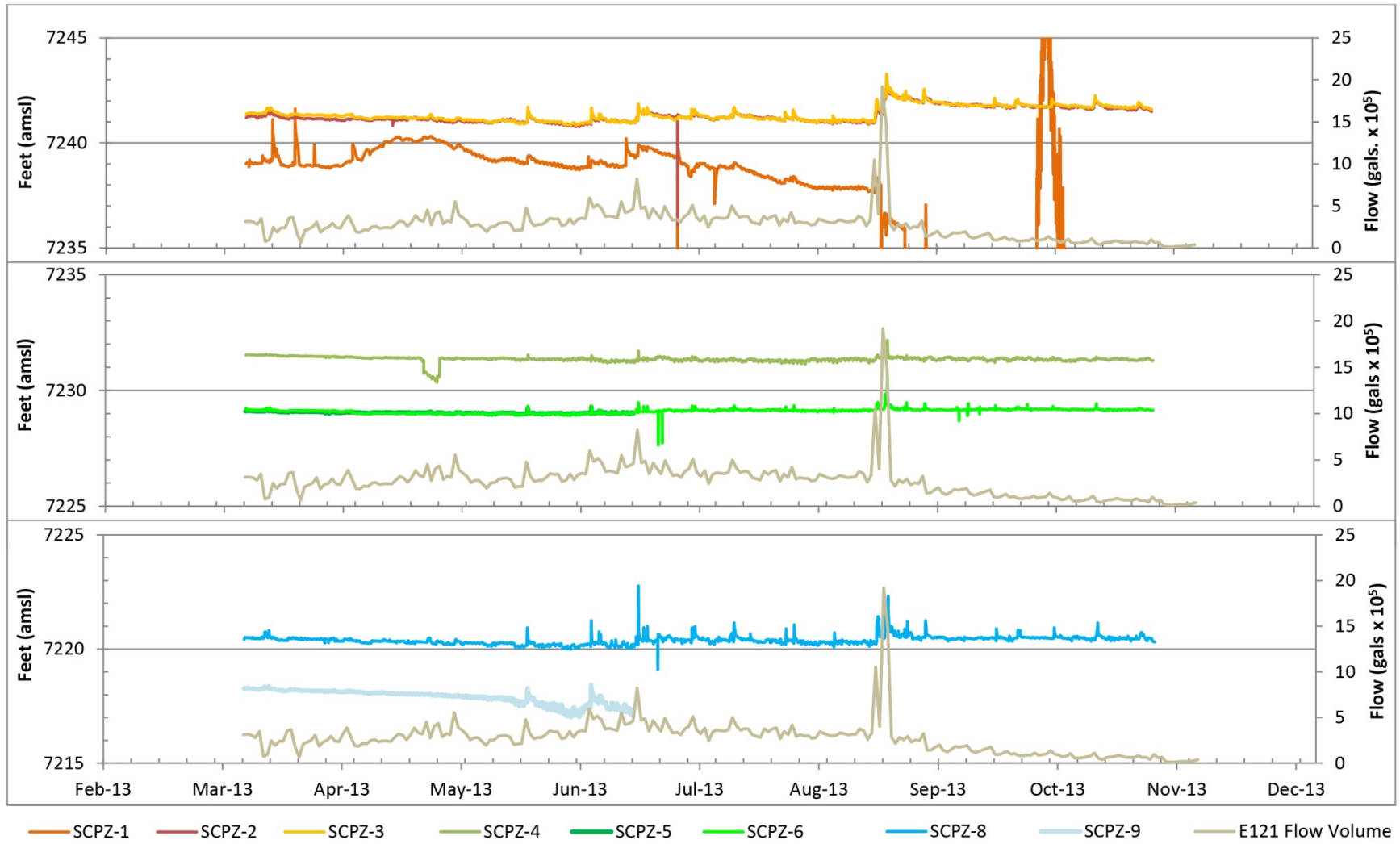
Figure C-2.0-24 Cross-plot of silicon dioxide versus $\delta^{18}O$

C-38



Notes: Sondes were not deployed in the other piezometers due to high levels of silt. Sondes located in SCPZ-5 and SCPZ-9 were lost in the September flood event so data is only available through July 2013. The sonde in SCPZ-1 appears to have malfunctioned resulting in widely variable readings.

Figure C-2.0-25 Time-series plots of temperature and specific conductance from AquaTroll sondes for piezometers SCPZ-1 to SCPZ-6 and SCPZ-8 to SCPZ-9



Note that the transducer in SCPZ-1 is believed to have malfunctioned during at least a portion of the data interval.

Figure C-3.0-1 Water-level data for Sandia Canyon piezometers plotted with daily flow at gaging station E121

Appendix D

*Analytical Data and Frequency of Detects Tables
(on CD included with this document)*

